



**Susana Teresa Antunes Martinho**

Mestrado Integrado em Engenharia Biomédica

## **Development of New Oxygen Therapeutics using Fluorinated Ionic Liquids**

Dissertação para obtenção do Grau de Mestre em  
Engenharia Biomédica

**Orientadores:** Professora Doutora Isabel Maria Delgado Jana  
Marrucho Ferreira, Investigadora Auxiliar, Laboratório de  
Termodinâmica Molecular, ITQB-UNL

Doutora Ana Belén Pereiro Estévez, Pós-Doc, Laboratório de  
Termodinâmica Molecular, ITQB-UNL

**Co-orientador:** Professor Doutor Jorge Carvalho Silva,  
Professor Assistente, FCT-UNL

Presidente: Prof. Doutora Maria Adelaide de Almeida Pedro de Jesus  
Arguente: Prof. Doutor Luís Alexandre Almeida Fernandes Cobra Branco  
Vogais: Prof. Doutora Isabel Maria Delgado Jana Marrucho Ferreira  
Prof. Doutora Ana Belém Pereiro Estévez



FACULDADE DE  
CIÊNCIAS E TECNOLOGIA  
UNIVERSIDADE NOVA DE LISBOA

**Setembro 2012**



**UNIVERSIDADE NOVA DE LISBOA**

Faculdade de Ciências e Tecnologia

Departamento de Física



**Development of New Oxygen Therapeutics using  
Fluorinated Ionic Liquids**

Susana Teresa Antunes Martinho

Dissertação apresentada na Faculdade de Ciências e Tecnologia da  
Universidade Nova de Lisboa para obtenção do grau Mestre em  
Engenharia Biomédica

**Orientadores:** Dr<sup>a</sup> Isabel Maria Delgado Jana Marrucho Ferreira

Dr<sup>a</sup> Ana Belén Pereiro Estévez

**Co-orientador:** Dr. Jorge Carvalho Silva

2012







# **Development of New Oxygen Therapeutics using Fluorinated Ionic Liquids**

**COPYRIGHT**

**Susana Teresa Antunes Martinho**

**Faculdade de Ciências e Tecnologia Universidade Nova Lisboa**

**A Faculdade de Ciências e Tecnologia e a Universidade Nova de Lisboa têm o direito, perpétuo e sem limites geográficos, de arquivar e publicar esta dissertação através de exemplares impressos reproduzidos em papel ou de forma digital, ou por qualquer outro meio conhecido ou que venha a ser inventado, e de a divulgar através de repositórios científicos e de admitir a sua cópia e distribuição com objectivos educacionais ou de investigação, não comerciais, desde que seja dado crédito ao autor e editor.**





## Agradecimentos

Este caminho que percorri teve a contribuição de várias pessoas, que fizeram com que fosse possível chegar a este dia. Queria começar por agradecer à minha orientadora Dr<sup>a</sup> Ana Belén Pereiro, que teve sempre o conselho certo para me dar e conseguiu dar-me motivação mesmo quando parecia que as coisas corriam menos bem, obrigado por sempre teres acreditado em mim e também pela paciência. Um especial obrigado à minha orientadora Dr<sup>a</sup> Isabel Marrucho por me ter dado esta oportunidade e por me ter acompanhado ao longo do trabalho, dando-me a hipótese de crescer profissionalmente e também a nível pessoal. Agradeço também ao meu co-orientador Dr. Jorge Carvalho Silva, por tão prontamente me abrir as portas para este projeto.

Agradeço a todos do laboratório de Termodinâmica Molecular que contribuíram de alguma forma para este trabalho. Agradeço especialmente à Catarina Florindo, por ter contribuído para que a integração fosse tão fácil e por todos os momentos que passámos juntas ao longo destes meses.

Agradeço à minha família, especialmente aos meus pais, por estarem sempre ao meu lado, por ouvirem todos os meus problemas e dúvidas e por terem feito com que fosse possível chegar até aqui, sem o vosso apoio nunca teria conseguido. Agradeço à minha irmã, que sabe sempre o que preciso de ouvir e por ter sempre força para me dar. Nuno muito obrigado pela paciência e por sempre acreditares em mim, foste uma grande ajuda para conseguir chegar aqui. Um obrigado aos meus avós pela preocupação e por estarem sempre presentes.

Um grande obrigado aos amigos, que foram perguntando pelo trabalho e que me foram dando força para que as coisas corressem bem, especialmente à Cláudia, Simone, Tiago N. e Tiago S., que estão comigo desde sempre.



*Aos meus pais e irmã, que estiveram comigo em todas as decisões que me fizeram chegar até aqui.*



## Palavras-chave

Líquidos Iônicos Fluorados, Perfluorocarbonetos, Caracterização Termofísica, Equilíbrio Líquido-Líquido, Substituintes Artificiais do Sangue.

## Resumo

Na última década do século XX verificaram-se progressos notáveis dos substituintes de sangue de 1ª geração. As emulsões à base de perfluorocarbonetos (PFCs) são neste momento os candidatos que apresentam maior fiabilidade e segurança como substituintes artificiais do sangue. O principal objectivo do presente trabalho é o estudo dos líquidos iónicos fluorados (FILs), de forma a que passem a substituir total ou parcialmente os PFCs atualmente usados como substituintes artificiais do sangue, de forma a desenvolver novas emulsões com propriedades avançadas.

Com este objectivo, efectuou-se a caracterização termofísica e termodinâmica de diversos FILs, de forma a seleccionar o FIL mais apropriado para a aplicação proposta. A caracterização envolve a medição experimental e análise da temperatura de decomposição e de fusão, densidade, viscosidade, índice de refração e condutividade iónica, à pressão atmosférica num intervalo de temperatura entre 298.15 e 353.15 K. Foi também estudado o equilíbrio líquido-líquido das misturas binárias PFCs e FILs, à pressão atmosférica num intervalo de temperaturas geralmente entre 293.15 e 353.15 K. O conhecimento do comportamento de fase é crucial para a reformulação das emulsões usadas atualmente como terapêuticas de oxigénio. Finalmente, foi aplicado com sucesso o modelo termodinâmico *Non-Random Two Liquid* (NRTL), de forma a poder correlacionar o comportamento das misturas binárias de PFCs e FILs.



## **Keywords**

Fluorinated Ionic Liquids, Perfluorocarbons, Thermophysical Characterization, Liquid-Liquid Equilibria, Artificial Blood Substitutes

## **Abstract**

The last decade of the 20<sup>th</sup> century has yielded a remarkable progress in the field of first generation artificial blood substitutes. Emulsions based on perfluorocarbons (PFCs) became one of the main candidates for a safe and reliable artificial blood substitute. The final objective of the present work is to study the fluorinated ionic liquids (FILs) with the purpose of replacing, partially or totally, the PFCs actually used as artificial blood substitutes, thus providing new fluids with tailored advanced properties.

With this goal in mind, the thermophysical and thermodynamic characterization of several FILs, was carried out with the aim to select the most appropriate candidate. This characterization involves the measurement and analysis of the decomposition and melting temperature, density, viscosity, refractive index, and ionic conductivity at atmospheric pressure in a temperature range from 298.15 to 353.15 K. Furthermore, the liquid-liquid equilibria of binary mixtures of PFCs and FILs were studied, at atmospheric pressure in a temperature range usually from 293.15 to 343.15 K. The knowledge of the phase behaviour is crucial to the formulation of emulsions used nowadays as suitable oxygen carriers. Finally, Non-Random Two Liquid (NRTL) thermodynamic model was successfully applied to correlate the behaviour of the binary mixtures of PFCs and FILs





# Contents

List of Abbreviations.....	XXIII
List of Symbols .....	XXV
<b>1. General Introduction .....</b>	<b>27</b>
<b>1.1 General Context.....</b>	<b>29</b>
<b>1.2 Oxygen therapeutics.....</b>	<b>29</b>
<b>1.3 Perfluorocarbons.....</b>	<b>32</b>
<b>1.4 Fluorinated Ionic Liquids.....</b>	<b>34</b>
1.4.1 Ionic Liquids.....	34
1.4.2 Ionic Liquids with fluoroalkyl-functionalized groups.....	37
<b>1.5 Objectives.....</b>	<b>41</b>
<b>2. Thermophysical Characterization of Fluorinated Ionic Liquids.....</b>	<b>43</b>
<b>2.1 Introduction .....</b>	<b>45</b>
<b>2.2 Materials and Experimental Procedure.....</b>	<b>46</b>
2.2.1 Materials.....	46
2.2.2 Experimental Procedure .....	48
2.2.2.1 Thermal properties.....	48
2.2.2.2 Viscosity and density measurements .....	49
2.2.2.3 Refractive index measurements .....	50
2.2.2.4 Ionic conductivity measurements.....	50
<b>2.3 Results and Discussion .....</b>	<b>51</b>
2.3.1 Thermal properties.....	51
2.3.2 Thermophysical and thermodynamic properties .....	53
2.3.3 Free Volume .....	58
2.3.4 Walden Plot .....	62
<b>2.4 Conclusions .....</b>	<b>64</b>
<b>3. Liquid-Liquid Equilibria of Perfluorocompounds with Fluorinated Ionic Liquids .....</b>	<b>65</b>
<b>3.1 Introduction.....</b>	<b>67</b>
<b>3.2 Materials and Experimental Procedure.....</b>	<b>68</b>
3.2.1 Materials.....	68
3.2.2 Procedure.....	69
3.2.2.1 Liquid-Liquid Equilibria.....	69
3.2.2.2 Analytical Method – Refractometry .....	71

<b>3.3</b>	<b>Results and Discussion .....</b>	<b>73</b>
3.3.1	Liquid-Liquid Equilibria of PFCs and [NBu <sub>4</sub> ][(PFOc)SO <sub>3</sub> ].....	74
3.3.2	Liquid-Liquid Equilibria of PFCs and [NBu <sub>4</sub> ][(PFBu)SO <sub>3</sub> ].....	75
3.3.3	Liquid-Liquid Equilibria diagram of PFCs and [HexMeIm][(PFBu)SO <sub>3</sub> ].....	76
3.3.4	Liquid-Liquid Equilibria of PFCs and [OcMeIm][(PFBu)SO <sub>3</sub> ].....	78
3.3.5	The Liquid-Liquid phase diagram of PFCs and [EtMepy][(PFBu)SO <sub>3</sub> ].....	79
3.3.6	Comparisons of the Liquid-Liquid Phase Diagrams of Perfluorocarbons and FILs ..	80
3.3.7	Correlation of LLE.....	81
3.3.8	Thermodynamic Functions .....	83
<b>3.4</b>	<b>Conclusions .....</b>	<b>91</b>
<b>4.</b>	<b>Final Remarks .....</b>	<b>93</b>
4.1	Conclusions .....	95
4.2	Future Work .....	95
<b>5.</b>	<b>References.....</b>	<b>97</b>
<b>Appendix A</b>	<b>.....</b>	<b>107</b>
A.1	[(EtPFHex)MeIm][PF <sub>6</sub> ] .....	109
A.2	[(EtPFHex)BuIm][PF <sub>6</sub> ] .....	110
A.3	[NBu <sub>4</sub> ][(PFOc)SO <sub>3</sub> ] .....	111
A.4	[NBu <sub>4</sub> ][(PFBu)SO <sub>3</sub> ] .....	112
A.5	[HexMeIm][(PFBu)SO <sub>3</sub> ] .....	113
A.6	[OcMeIm][(PFBu)SO <sub>3</sub> ].....	114
A.7	[EtMepy][(PFBu)SO <sub>3</sub> ].....	115
A.8	[BuMepyr][(PFBu)SO <sub>3</sub> ] .....	116
<b>Appendix B</b>	<b>.....</b>	<b>117</b>
B.1	Calibration curve for Perfluorodecalin and [NBu <sub>4</sub> ][(PFOc)SO <sub>3</sub> ].....	119
B.2	Calibration curve for Perfluorooctane and [NBu <sub>4</sub> ][(PFOc)SO <sub>3</sub> ].....	120
B.3	Calibration curve for Perfluorodecalin and [NBu <sub>4</sub> ][(PFBu)SO <sub>3</sub> ].....	121
B.4	Calibration curve for Perfluorooctane and [NBu <sub>4</sub> ][(PFBu)SO <sub>3</sub> ].....	122
B.5	Calibration curve for Perfluorodecalin and [HexMeIm][(PFBu)SO <sub>3</sub> ].....	123
B.6	Calibration curve for Perfluorooctane and [HexMeIm][(PFBu)SO <sub>3</sub> ].....	124
B.7	Calibration curve for Perfluorodecalin and [OcMeIm][(PFBu)SO <sub>3</sub> ].....	125
B.8	Calibration curve for Perfluorooctane and [OcMeIm][(PFBu)SO <sub>3</sub> ].....	126
B.9	Calibration curve for Perfluorodecalin and [EtMepy][(PFBu)SO <sub>3</sub> ].....	127

## List of figures

<b>Figure 1.1</b> – Most investigated fluorocarbons for oxygen delivery in humans:.....	<b>33</b>
<b>Figure 1.2</b> – Number of papers published from 1990 to 2011. ....	<b>34</b>
<b>Figure 1.3</b> – Most common cation structures of nitrogen-based ILs. ....	<b>35</b>
<b>Figure 1.4</b> – Most common anion structures of ILs. ....	<b>35</b>
<b>Figure 1.5</b> – Application of the IL. ....	<b>37</b>
<b>Figure 2.1</b> – Metrohm 831 Karl Fisher coulometer used. ....	<b>48</b>
<b>Figure 2.2</b> – Thermogravimetric analyses model TGA Q50 (TGA). ....	<b>49</b>
<b>Figure 2.3</b> – Differential scanning calorimeter model DSC Q200 (DSC). ....	<b>49</b>
<b>Figure 2.4</b> – SVM 3000 Anton Paar rotational Stabinger viscometer-densimeter. ....	<b>49</b>
<b>Figure 2.5</b> – Refractometer ABBEMAT 500 Anton Paar. ....	<b>50</b>
<b>Figure 2.6</b> – CDM210 Radiometer analytical conductimeter. ....	<b>51</b>
<b>Figure 2.7</b> – Melting points and decomposition temperatures of the fluorinated ionic liquids studied in this work. ....	<b>52</b>
<b>Figure 2.8</b> – Density and fitted curves as a function of temperature for the fluorinated ionic liquids.....	<b>55</b>
<b>Figure 2.9</b> – Fluidity and fitted curves as a function of temperature for the fluorinated ionic liquids. ....	<b>56</b>
<b>Figure 2.10</b> – Ionic conductivity and fitted curves as a function of temperature for the fluorinated ionic liquids. ....	<b>56</b>
<b>Figure 2.11</b> – Molar free volume as a function of temperature for the fluorinated ionic liquids. ....	<b>62</b>
<b>Figure 2.12</b> – Walden plot for the fluorinated ionic liquids. ....	<b>64</b>
<b>Figure 3.1</b> – Binary ,mixtures for liquid-liquid equilibria: (a) perfluorodecalin + [EtMepy][(PFBu)SO <sub>3</sub> ] and (b) perfluorooctane + [HexMeIm][(PFBu)SO <sub>3</sub> ]. ....	<b>70</b>
<b>Figure 3.2</b> – Experimental assembly used to measure solubility of fluorinated ionic liquid in PFC-rich. ...	<b>71</b>
<b>Figure 3.3</b> – Liquid-liquid phase diagram for water (2) and [BuMeIm] [NTf <sub>2</sub> ] (1) and comparison between values obtained and values from literature. ....	<b>73</b>
<b>Figure 3.4</b> – Liquid-liquid phase diagram for perfluorodecalin + [NBu <sub>4</sub> ][(PFOc)SO <sub>3</sub> ] and for perfluorooctane + [NBu <sub>4</sub> ][(PFOc)SO <sub>3</sub> ]. ....	<b>75</b>
<b>Figure 3.5</b> – Liquid-liquid phase diagram for perfluorodecalin + [NBu <sub>4</sub> ][(PFBu)SO <sub>3</sub> ] and for perfluorooctane + [NBu <sub>4</sub> ][(PFBu)SO <sub>3</sub> ]. ....	<b>76</b>
<b>Figure 3.6</b> – Liquid-liquid phase diagram for perfluorodecalin + [HexMeIm][(PFBu)SO <sub>3</sub> ] and for perfluorooctane + [HexMeIm][(PFBu)SO <sub>3</sub> ]. ....	<b>77</b>
<b>Figure 3.7</b> – Liquid-liquid phase diagram for perfluorodecalin + [OcMeIm][(PFBu)SO <sub>3</sub> ] and for perfluorooctane + [OcMeIm][(PFBu)SO <sub>3</sub> ]. ....	<b>79</b>
<b>Figure 3.8</b> – The liquid-liquid phase diagram of: a) perfluorodecalin and fluorinated ionic liquids and b) perfluorooctane and fluorinated ionic liquids. ....	<b>81</b>
<b>Figure A.1</b> – TGA curve for [(EtPFHex)MeIm][PF <sub>6</sub> ]. ....	<b>109</b>
<b>Figure A.2</b> – DSC curve for [(EtPFHex)MeIm][PF <sub>6</sub> ]. ....	<b>109</b>
<b>Figure A.3</b> – TGA curve for [(EtPFHex)BuIm][PF <sub>6</sub> ]. ....	<b>110</b>

<b>Figure A.4</b> – DSC curve for [(EtPFHex)BuIm][PF <sub>6</sub> ].	110
<b>Figure A.5</b> – TGA curve for [NBu <sub>4</sub> ][(PFOc)SO <sub>3</sub> ].	111
<b>Figure A.6</b> – DSC curve for [NBu <sub>4</sub> ][(PFOc)SO <sub>3</sub> ].	111
<b>Figure A.7</b> – TGA curve for [NBu <sub>4</sub> ][(PFBu)SO <sub>3</sub> ].	112
<b>Figure A.8</b> – DSC curve for [NBu <sub>4</sub> ][(PFBu)SO <sub>3</sub> ].	112
<b>Figure A.9</b> – TGA curve for [HexMeIm][(PFBu)SO <sub>3</sub> ].	113
<b>Figure A.10</b> – DSC curve for [HexMeIm][(PFBu)SO <sub>3</sub> ].	113
<b>Figure A.11</b> – TGA curve for [OcMeIm][(PFBu)SO <sub>3</sub> ].	114
<b>Figure A.12</b> – DSC curve for [OcMeIm][(PFBu)SO <sub>3</sub> ].	114
<b>Figure A.13</b> – TGA curve for [EtMepy][(PFBu)SO <sub>3</sub> ].	115
<b>Figure A.14</b> – DSC curve for [EtMepy][(PFBu)SO <sub>3</sub> ].	115
<b>Figure A.15</b> – TGA curve for [BuMepyr][(PFBu)SO <sub>3</sub> ].	116
<b>Figure A.16</b> – DSC curve for [BuMepyr][(PFBu)SO <sub>3</sub> ].	116
<b>Figure B.1</b> – Calibration curve for perfluorodecalin and [NBu <sub>4</sub> ][(PFOc)SO <sub>3</sub> ].	119
<b>Figure B.2</b> – Calibration curve for perfluorooctane and [NBu <sub>4</sub> ][(PFOc)SO <sub>3</sub> ].	120
<b>Figure B.3</b> – Calibration curve for perfluorodecalin and [NBu <sub>4</sub> ][(PFBu)SO <sub>3</sub> ].	121
<b>Figure B.4</b> – Calibration curve for perfluorooctane and [NBu <sub>4</sub> ][(PFBu)SO <sub>3</sub> ].	122
<b>Figure B.5</b> – Calibration curve for perfluorodecalin and [HexMeIm][(PFBu)SO <sub>3</sub> ].	123
<b>Figure B.6</b> – Calibration curve for perfluorooctane and [HexMeIm][(PFBu)SO <sub>3</sub> ].	124
<b>Figure B.7</b> – Calibration curve for perfluorodecalin and [OcMeIm][(PFBu)SO <sub>3</sub> ].	125

## List of Tables

<b>Table 1.1</b> – Composition and characteristics of injectable PFC emulsion oxygen carriers .....	<b>31</b>
<b>Table 1.2</b> – Physicochemical properties of liquid perfluoroalkanes.....	<b>32</b>
<b>Table 1.3</b> – Structure and family of fluorinated ionic liquids.....	<b>38</b>
<b>Table 2.1</b> – Chemical structure and respective abbreviation of fluorinated ionic liquids. ....	<b>47</b>
<b>Table 2.2</b> – Thermal properties of fluorinated ionic liquids: start temperature, onset temperature, decomposition temperature, melting temperature, and glass transition temperature. ....	<b>52</b>
<b>Table 2.3</b> – Density, dynamic viscosity, refractive index, and ionic conductivity, of the pure fluorinated ionic liquids as a function of temperature. ....	<b>53</b>
<b>Table 2.4</b> – Fitting parameters for the density, refractive index, fluidity and ionic conductivity as a function of temperature for the studied fluorinated ionic liquids. Standard deviations are also shown.....	<b>57</b>
<b>Table 2.5</b> – Values of calculated molar volume, molar refraction and free volume as a function of temperature for the studied fluorinated ionic liquids. ....	<b>60</b>
<b>Table 3.1</b> – Chemical structure and respective abbreviation of perfluorocarbon.....	<b>69</b>
<b>Table 3.2</b> – Experimental liquid-liquid equilibria data for binary mixture [BuMeIm] [NTf <sub>2</sub> ] + water as function of temperature and comparison with the values from the literature. ....	<b>73</b>
<b>Table 3.3</b> – Experimental liquid-liquid equilibria data for binary mixture perfluorocarbon with [NBu <sub>4</sub> ][(PFOc)SO <sub>3</sub> ]. ....	<b>74</b>
<b>Table 3.4</b> – Experimental liquid-liquid equilibria data for binary mixture perfluorocarbon with [NBu <sub>4</sub> ][(PFBu)SO <sub>3</sub> ]. ....	<b>75</b>
<b>Table 3.5</b> – Experimental liquid-liquid equilibria data for binary mixture perfluorocarbon with [HexMeIm][(PFBu)SO <sub>3</sub> ]. ....	<b>77</b>
<b>Table 3.6</b> – Experimental liquid-liquid equilibria data for binary mixture perfluorocarbon with [OcMeIm][(PFBu)SO <sub>3</sub> ]. ....	<b>78</b>
<b>Table 3.7</b> – Experimental liquid-liquid equilibria data for binary mixture perfluorocarbon with [EtMepy][(PFBu)SO <sub>3</sub> ]. ....	<b>79</b>
<b>Table 3.8</b> – Parameters of the NRTL equations for the binary mixture. ....	<b>83</b>
<b>Table 3.9</b> – Thermodynamic conventional properties of solution of PFCs in FILs studied.....	<b>85</b>
<b>Table 3.10</b> – Thermodynamic conventional properties of solvation of PFCs in FILs studied at 298.15 K..	<b>89</b>
<b>Table 3.11</b> – Thermodynamic local standard properties of the solvation of PFCs in the FILs studied at 298.15 K. ....	<b>90</b>
<b>Table B.1</b> – Refractive index as function of [NBu <sub>4</sub> ][(PFOc)SO <sub>3</sub> ] molar fraction for binary mixture [NBu <sub>4</sub> ][(PFOc)SO <sub>3</sub> ] + perfluorodecalin. ....	<b>119</b>
<b>Table B.2</b> – Refractive index as function of [NBu <sub>4</sub> ][(PFOc)SO <sub>3</sub> ] molar fraction for binary mixture [NBu <sub>4</sub> ][(PFOc)SO <sub>3</sub> ] + perfluorooctane. ....	<b>120</b>
<b>Table B.3</b> – Refractive index as function of [NBu <sub>4</sub> ][(PFBu)SO <sub>3</sub> ] molar fraction for binary mixture [NBu <sub>4</sub> ][(PFBu)SO <sub>3</sub> ] + perfluorodecalin. ....	<b>121</b>

<b>Table B.4</b> – Refractive index as function of [NBu <sub>4</sub> ][(PFBu)SO <sub>3</sub> ] molar fraction for binary mixture [NBu <sub>4</sub> ][(PFBu)SO <sub>3</sub> ] + perfluorooctane. ....	<b>122</b>
<b>Table B.5</b> – Refractive index as function of [HexMeIm][(PFBu)SO <sub>3</sub> ] molar fraction for binary mixture [HexMeIm][(PFBu)SO <sub>3</sub> ] + perfluorodecalin. ....	<b>123</b>
<b>Table B.6</b> – Refractive index as function of [HexMeIm][(PFBu)SO <sub>3</sub> ] molar fraction for binary mixture [HexMeIm][(PFBu)SO <sub>3</sub> ] + perfluorooctane. ....	<b>124</b>
<b>Table B.7</b> – Refractive index as function of [OcMeIm][(PFBu)SO <sub>3</sub> ] molar fraction for binary mixture [OcMeIm][(PFBu)SO <sub>3</sub> ] + perfluorodecalin. ....	<b>125</b>
<b>Table B.8</b> – Refractive index as function of [OcMeIm][(PFBu)SO <sub>3</sub> ] molar fraction for binary mixture [OcMeIm][(PFBu)SO <sub>3</sub> ] + perfluorooctane. ....	<b>126</b>
<b>Table B.9</b> – Refractive index as function of [EtMepy][(PFBu)SO <sub>3</sub> ] molar fraction for binary mixture [EtMepy][(PFBu)SO <sub>3</sub> ] + perfluorodecalin. ....	<b>127</b>

## List of Abbreviations

<b>D</b>	Demal (1 g equivalent of solute dissolved in 1 dm <sup>3</sup> solvent)
<b>DSC</b>	Differential Scanning Calorimeter Model
<b>EYP</b>	Egg yolk phospholipids
<b>FDA</b>	American food and drug administration
<b>FIL</b>	Fluorinated ionic liquids
<b>HBPO</b>	High boiling point oil
<b>HPLC</b>	High performance liquid chromatography
<b>IL</b>	Ionic liquid
<b>LLE</b>	Liquid-liquid Equilibria
<b>MRI</b>	Magnetic resonance imaging
<b>NMR</b>	Nuclear magnetic resonance
<b>NRTL</b>	Non Random Two-Liquid Model
<b>Perflubron</b>	bromoperfluoro-n-octane
<b>PFC</b>	Perfluorocarbon
<b>RSD</b>	Relative standard deviation
<b>TGA</b>	Thermogravimetric analyses
<b>[OcMeIm][(PFBu)SO<sub>3</sub>]</b>	1-Mehtyl-3-octylimidazolium perfluorobutanesulfonate
<b>[NBu<sub>4</sub>][(PFOc)SO<sub>3</sub>]</b>	Tetrabutylammonium heptadecafluorooctanesulfonate
<b>[NBu<sub>4</sub>][(PFBu)SO<sub>3</sub>]</b>	Tetrabutylammonium perfluorobutanesulfonate
<b>[HexMeIm][(PFBu)SO<sub>3</sub>]</b>	1-Hexyl-3-methylimidazolium perfluorobutanesulfonate
<b>[EtMepy][(PFBu)SO<sub>3</sub>]</b>	1-Ethyl-3-methylpyridinium perfluobutanesulfonate
<b>[BuMepyr][(PFBu)SO<sub>3</sub>]</b>	1-Butyl-1-methylpyrrolidinum perfluorobutanesulfonate
<b>[BuMeIm][NTf<sub>2</sub>]</b>	1-butyl-3-methylimidazolium bis(trifluoromethylsulfonyl) imide
<b>[(EtPFHex)MeIm][PF<sub>6</sub>]</b>	1-Methyl-3-(3,3,4,4,5,5,6,6,7,7,8,8,8-tridecafluorooctyl)imidazolium hexafluophosphate
<b>[(EtPFHex)BuIm][PF<sub>6</sub>]</b>	1-Butyl-3-(3,3,4,4,5,5,6,6,7,7,8,8,8-tridecafluorooctyl)imidazolium hexafluorophosphate





## List of Symbols

$N_A$	Avogadro's constant
$T_{dec}$	Decomposition temperature
$f$	Degrees of freedom
$\rho$	Density
$\eta$	Dynamic viscosity
$\epsilon_0$	Electric constant
$\alpha_e$	Electronic polarizability
$\phi$	Fluidity
$f_m$	Free volume
$G$	Gibbs energy
$R$	Ideal gas constant
$\tau_{ij}$	Interaction parameters
$k$	Ionic conductivity
$\alpha_j$	Isobaric thermal expansibility
$\Delta_{svt}G_m^*(T)$	Local standard Gibbs energy of solvation
$x$	Molar fraction
$\Delta_{svt}H_m^*(T)$	Molar local standard enthalpy of solvation
$\Delta_{svt}S_m^*(T)$	Molar local standard entropy of solvation
$R_m$	Molar refraction
$V_m$	Molar volume
$V_{j,m}$	Molar volume of the solvent $j$
$M_w$	Molecular weight
$a$	Non randomness parameter
$T_{onset}$	Onset temperature
$n_D$	Refractive index
$\sigma$	Standard deviation
$\Delta_{sol}H_m^0$	Standard molar enthalpy of solution
$\Delta_{svt}H_m^0(T)$	Standard molar enthalpy of solvation
$\Delta_1^gH_m^0$	Standard molar enthalpy of vaporization of the solute
$\Delta_{sol}S_m^0$	Standard molar entropy of solution
$\Delta_{sol}S_m^0(T)$	Standard molar entropy of solvation
$\Delta_{sol}G_m^0$	Standard molar Gibbs energy of solution

$\Delta_{\text{svt}}G_m^0(T)$	Standard molar Gibbs free of solvation
$T_{\text{start}}$	Start temperature
$T$	Temperature
$p(\text{s},T)$	Vapor pressure of the solute

# **1. General Introduction**

---



## 1.1 General Context

The transport and delivery of oxygen *in vivo* by other means than the red blood cells has become one of the most challenging research topics of the last 25 years [1]. Considering its undeniable value in procedures that imply blood loss, different substitutes have been developed so far. The first generation of artificial oxygen carriers, often referred as *oxygen therapeutics*, is now reaching the critical phase of trials. Taking into account its reliability, emulsions based on perfluorocarbons (PFCs) are currently among the preferred artificial blood candidates.

The final goal of this thesis is to give the first step into the development of a new and improved generation of oxygen therapeutics using fluorinated ionic liquids (FILs). In particular, the partial or total replacement of the PFCs currently used in the emulsions for oxygen therapeutics by FILs will be addressed since several advantages, such as enhancement of respiratory gas solubility and emulsion stability and lowering of vapour pressure, are envisaged. The feasibility of this proposal will be evaluated through the study of the thermodynamic properties and phase equilibria of pure FILs and mixtures with FIL.

The benefits for the society of a safe blood substitute that could be administered disregarding the recipient's blood type are enormous, not to mention the prolonged shelf life under a wide range of temperatures. Everyday there is a large demand for blood to replace acute blood loss in accident victims and surgical patients needing short term replenishment of blood's oxygen carrying capacity.

The innovative results of this thesis are expected to raise new relevant questions in the ionic liquids community. Furthermore, the nearly null volatility of ionic liquids, its easy recovery and therefore, recyclability completely justify the development of this research work, particularly given the undeniably important objective of improving the available *oxygen therapeutics*.

## 1.2 Oxygen therapeutics

Oxygen carriers are responsible for the transport of the respiratory gases (oxygen and carbon dioxide) for a limited period of time during clinical applications [2] such as in the management of operative blood loss, trauma, acute normovolemic hemodilution, traumatic brain injury, and blood requirements in patients who refuse or have contraindications to transfusions of red blood cells. Although the designation of "blood substitutes" is frequently used, it can be misleading [1] since it implies that these products can totally replace all the functions of blood

(such as immunity, coagulation etc), which is not the case. These fluids only have the function to transport oxygen to the cells and carbon dioxide from the cells to the lungs.

There are two classes of *oxygen therapeutics* based on the transport mechanism: perfluorocarbon-based, where oxygen is physically dissolved in the carrier, and hemoglobin-based, where oxygen is chemically bounded to the carrier. The use of the hemoglobin-based as oxygen therapeutic emerged over a century ago [3] and since the first results were disappointing, PFC-emulsions were proposed as an alternative to deliver oxygen *in vivo*.

Then, Hemoglobin-based oxygen therapeutics have been derived from human, animal, or recombinant hemoglobin and have involved an impressive diversity of structural modifications and formulations. The modifications are made accordingly to physiological characteristics and are most important to the indication pursued [3]. The final products are eventually formulated as solutions, capsules or suspensions of liposome. The hemoglobin concentration ranges have limitations due to colloidal osmotic pressure, viscosity or encapsulation efficiency. Each product has its own unique oxygen delivery characteristics and physiological responses [3].

Due to their immiscibility in water, the PFCs are formulated as emulsions for intravascular administration. In these emulsions, the PFCs are coated with a thin layer of a surfactant that serves as an emulsifier and a stabilizer [4]. The emulsifier most used in the PFC emulsions is egg yolk phospholipids (EYP) and typically, fluorocarbon emulsion droplet sizes [4] are in the 0.1-0.2  $\mu\text{m}$  range (30-70 times smaller than the red blood cells). These droplets will fill the gaps present in the plasma between red cells that are found in microcirculation. The PFC particles provide a strong driving force for diffusion of oxygen to the tissues [5]. Therefore, a great effectiveness of PFC-based emulsions in capillary bed and at low hematocrits is expected.

Afterwards, it was discovered that perfluorodecalin is excreted from the body much more rapidly than previously investigated [6-8], allowing for the first commercial emulsion, *Fluosol* [8], which became the first injectable oxygen carrier to be approved by the American Food and Drug Administration (FDA). The emulsion received regulatory approval in the USA and Europe in the period 1989-1990 for clinical use as an oxygen-carrier [9-11]. However, the cardiologists did not adopt *Fluosol* because improvements in angioplasty technology made its use redundant and its manufacture was terminated in 1994. The principal limitations of this first PFC-based emulsion were: the need to store frozen, the need to defrost and re-constitute before use and the main disadvantage, its poor efficacy as an oxygen carrier [10, 11]. Other PFC-emulsions of first generation include *Perftotran* [12] and *Oxypherol* [11].

The objectives of the second generation of PFC emulsions were to use highly purified PFCs with biocompatibility and excretion properties acceptable for *in vivo* use, to improve stability characteristics and hence shelf-life and to develop concentrated emulsions having significantly increased PFC content and thus conferring superior oxygen-carrying capacity [11]. However, one

of the biggest problems found for concentrated PFC emulsions with increased oxygen-carrying potential, was their high viscosities which prevented their use in vasculature. The second-generation emulsions were essentially based on perflubron (bromoperfluoro-n-octane) or perfluorodecalin and have been stabilized avoiding molecular diffusion using small quantities of an appropriate high boiling point oil (HBPO) [3]. The second generation of perfluorocarbon emulsions (*Oxygent*, *Oxyfluor*, *TherOx*, among others) was less sensitive to processing parameters, easier to sterilize and also displayed better resistance to mechanical stress. *Oxygent* presented a shelf-life of at least 24 months, when stored at 278-283 K, and had a viscosity close to that of the blood, contributing to the maintenance of normal hemodynamics. However, *TherOx* [13] had a shelf-life of 1 year at 277 K. Sustained efforts have subsequently led to more advanced second generation products that are now in clinical trials [4]. The composition and characteristics of injectable PFC emulsion are shown in **Table 1.1**.

**Table 1.1** – Composition and characteristics of injectable PFC emulsion oxygen carriers [4].

Emulsion	Perfluorocarbon(s)	Perfluorocarbon concentration (%weight/volume)	Surfactant(s)/ stabilizer(s)	Typical storage conditions
<b>1. 'First-Generation' emulsions</b>				
<i>Fluosol</i>	Perfluorodecalin	14	Pluronic F-68	Frozen
	Perfluorotripropylamine	6	EYP Potassium oleate	
<i>Perftoran</i>	Perfluorodecalin	14	Proxanol	Frozen
	Perfluoromethylcycloperidine	6		
<i>Oxypherol</i>	Perfluorotributylamine	20	Pluronic F-68	Refrigeration
<b>2. 'Second-Generation' emulsions</b>				
<i>Oxygent</i>	Perflurobron	58	EYP	Refrigeration
	Perfluorodecyl bromide	2		
<i>Oxyfluor</i>	Perfluorodichlorooctane	76	Safflower oil EYP	Refrigeration
<i>TherOx</i>	Bis(perfluorobutyl)ethene	83	EYP	Refrigeration

Fluorocarbon emulsions offer a simple, elegant and cost-effective vehicle for delivering oxygen to tissues. Further efforts will be focused in extending the range of therapeutic indications of such products.

### 1.3 Perfluorocarbons

The Fluorine (F) atom is characterized by a high electronegativity, relatively small size, very low polarizability, tightly bound with three non-bonding electron pairs, excellent overlap between F 2s and 2p orbitals with corresponding orbitals of other second period elements [14]. Fluorine has an electronegativity of 4.0 on the Pauling scale, which is the highest of all the elements. The incorporation of fluorine atoms into organic materials imparts dramatic changes in physical properties as well as chemical reactivities of the molecules. Actually, depending upon the site and level of fluorination, organofluorine compounds have solvent properties ranging from extreme non-polar perfluoroalkanes to the extraordinary polar solvent, hexafluoroisopropanol [14]. Physicochemical properties of perfluoroalkane are shown in **Table 1.2**.

**Table 1.2** – Physicochemical properties of liquid perfluoroalkanes [15].

Property	Range	Units
<b>Gas Solubility</b> (310.15 K, 1 atm)		
Oxygen	33 – 66	mL/100 mL PFC
Carbon Dioxide	140 – 210	mL/100 mL PFC
<b>Diffusion Coefficient</b> (310.15 K, 1 atm)		
Oxygen	$2 - 5.8 \cdot 10^{-5}$	cm <sup>2</sup> /sec
Carbon Dioxide	$1.1 - 1.3 \cdot 10^{-5}$	cm <sup>2</sup> /sec
<b>Vapor Pressure</b> (310.15 K, 1 atm)		
	0.2 – 400	mm Hg
<b>Surface Tension</b> (298.15 K, 1 atm)		
	13.6 – 18	dynes/cm
<b>Spreading Coefficient</b>		
	-0.2 to +4.5	dynes/cm
<b>Density</b> (298.15 K, 1 atm)		
	1.58 – 2.02	g/mL
<b>Kinematic Viscosity</b> (298.15 K, 1 atm)		
	0.8 – 8	cS
<b>Log P</b>		
	6.1 – 9.7	–
<b>Lipid Solubility</b> (310.15 K)		
	0.14 – 1.70	µgm PFC/mglipid/mmHg

Data based on a survey of 18 liquid perfluoroalkanes

From the standpoint of the molecular structure, fluorocarbons have little similarity with the complex metal porphyrin-centered hemoglobin proteins. PFCs are synthetic, considerably smaller



and exceedingly simple molecules, with no structural requirements. Typical examples of fluorocarbons most investigated for oxygen delivery are shown in **Figure 1.1**

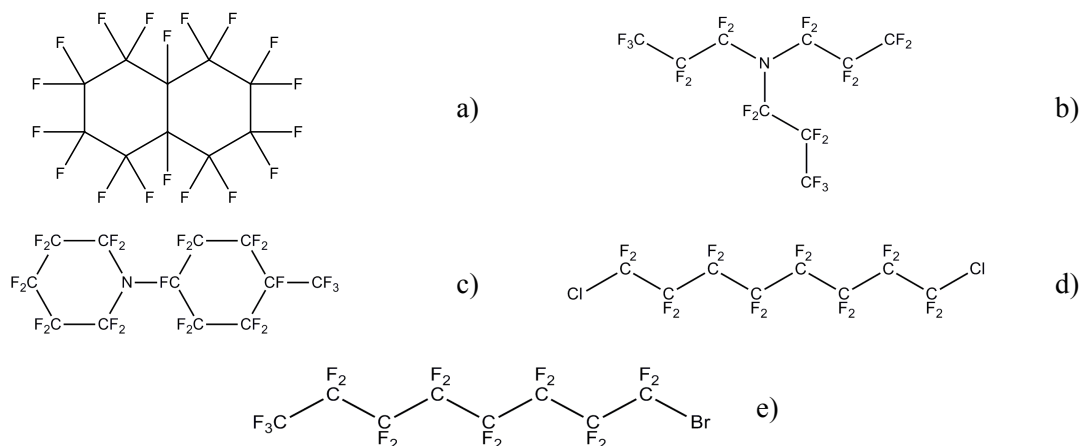


**Figure 1.1** – Most investigated fluorocarbons for oxygen delivery in humans: a) perfluorodecalin; b) perfluorotripropylamine; c) perfluoromethylcyclohexypiperidine; d)  $\alpha,\omega$ - dichloroperfluorooctane; e) perfluorooctyl bromide (perfluorobron).

Perfluorocarbons have numerous applications for biomedical purposes, such as using them pure as liquids for liquid ventilation or in the emulsified form for respiratory failure treatment [16]. They are also used as high-density intraoperative fluids for eye surgery [17], and as red cell blood substitutes, including all the situations of surgical anemia, some haemolytic anemia, ischemic disease, angioplasty, extracorporeal organ perfusion, cardioplegia [18], radiotherapy of tumours [19], and as an ultrasound contrast agent to detect myocardial perfusion abnormalities [20]. Furthermore, PFCs are used in oral use as a bowel marker during magnetic resonance imaging (MRI) [21]; in external application on patient's body to improve magnetic homogeneity when fat saturation techniques are employed during magnetic resonance imaging (MRI) [22]; in ultrasound imaging [23] and a range of other applications of fluorocarbons in medicine are being explored [24].

In industry, there are a large number of documented applications of PFCs: as co-solvents in supercritical extraction improving the solubility of hydrophilic substances in supercritical reaction or extraction media [25]; as medium in two-phase reaction mixture, in separation and purification technique [26]; as refrigerants, aerosol propellants and foam blowing agents [27] and in cell culture aeration [28]. Besides, due to the exceptional solubility of carbon dioxide in perfluoroalkanes these compounds are being studied for industrial and environmental applications as the removal of carbon from gaseous effluents [29].

However, the perfluorocarbons present clear limitations such as high vapor pressures and poor solvating capacity for organic compounds, which might compromise their use as oxygen carriers.

## 1.4 Fluorinated Ionic Liquids

### 1.4.1 Ionic Liquids

The first ionic liquid (IL) was synthesized by Paul Walden in 1914, when he was testing new explosives for the substitution of nitroglycerin, the ethylammonium nitrate, with a melting point of 12 °C [30]. However, the first patent regarding an industrial application of ILs was filed in the preparation of cellulose solutions, being registered only in 1934 by Charles Graenacher [31]. A few more patents were registered during the 2<sup>nd</sup> World War [32, 33].

However, in the last two decades, with the appearance of air and water stable ILs, the research and development of novel ILs and their possible applications increased significantly. The number of articles concerning ILs published between 1990 and 2011 are shown in **Figure 1.2**.

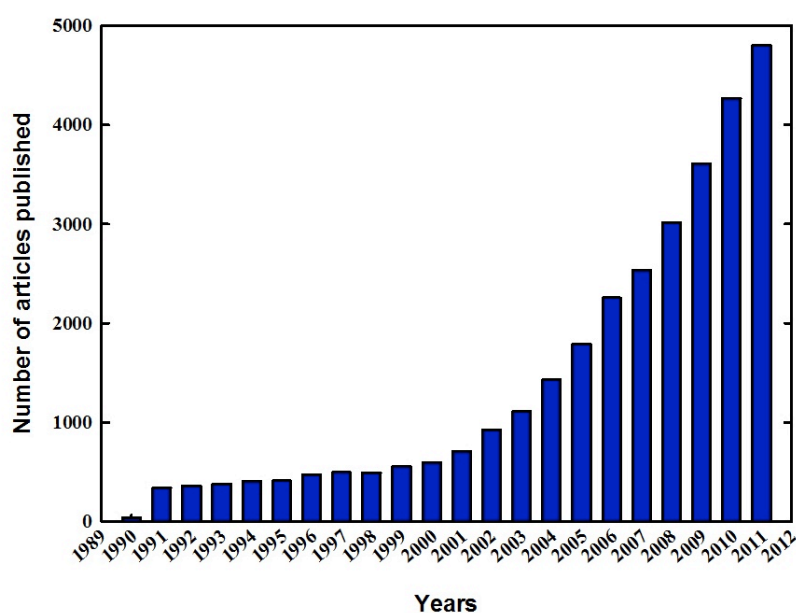


**Figure 1.2** – Number of papers published from 1990 to 2011. Values taken from ISI Web of Knowledge.

Ionic liquids are salts, thus ionic compounds, that are liquid below a conventional temperature of 373 K [34]. This is due to their low symmetry [35, 36], ions with a high distribution of charge [37] low intermolecular interactions [38, 39] and dispersion caused by the large organic cation and organic or inorganic anion [40]. Among other unique thermophysical



hydrophobicity, solution behaviour, thermophysical properties, biodegradation or toxicological [43, 44]. These properties made them improved alternatives to volatile organic compounds in the most diverse applications, such as in biphasic catalysis, in organic synthesis [45], in polymerization, in separation and extraction processes [46] and in the dissolution of biomaterials [47].

Ionic liquids applications started to be devoted to electrolytes in batteries [48]. The area of electrochemical processes is still very significant, and important work is carried out toward integration of ILs into lithium-ion batteries, fuel cells or solar cells, as well as electrochemical syntheses and electrodeposition of metals [49]. Later, ILs were suggested as solvents and catalysts in reactions [36] and have been successfully tested for a wide variety of reactions: hydrogenations and hydroformylations, polymerizations, isomerizations, alkylations, acylations, Diels-Alder reactions, Heck and Suzuki coupling reactions, among others.

Ionic liquids may be the basis of new technologies in liquid extraction [45] and gas separations [50]. Some other innovative solutions, related to the extraordinary ability of ILs as solvents, are currently studied, for instance the storage and delivery of hazardous gases absorbed in ILs [51]

Due to the active work of research groups, as well as the interest of companies, often in mutual collaboration, a lot of applications currently in development will become real processes in the near future, thus increasing the portfolio of industrial applications based on ILs technology. The applications of the ILs are summarized in **Figure 1.5**.

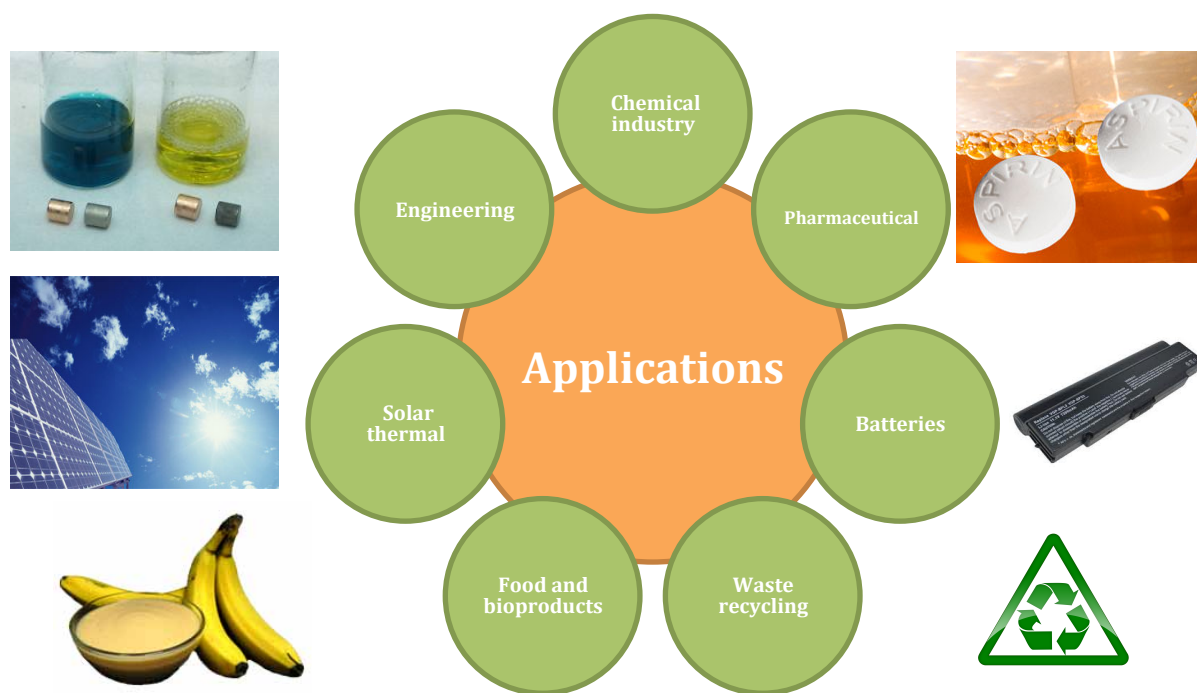


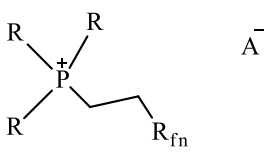
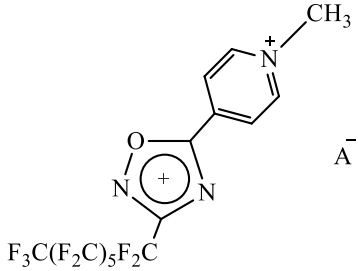
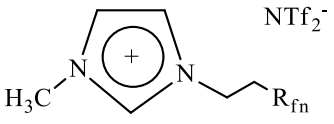
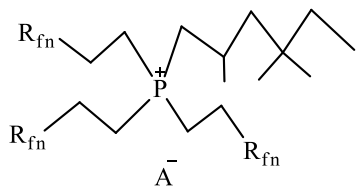
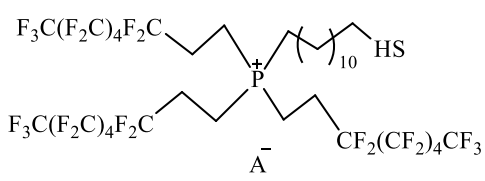
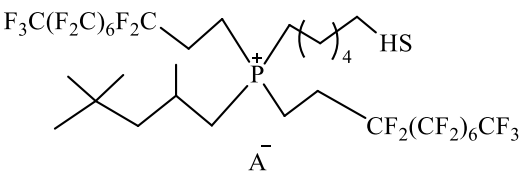
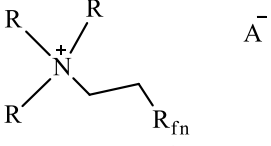
Figure 1.5 – Application of ILs.

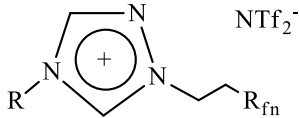
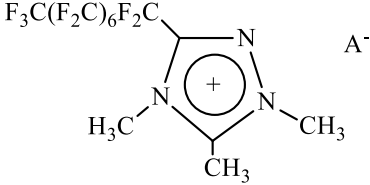
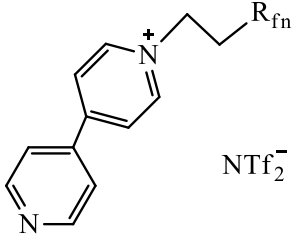
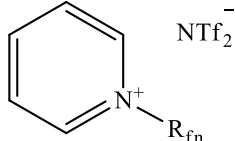
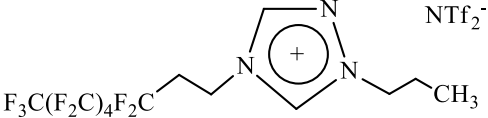
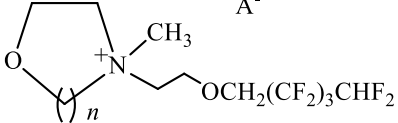
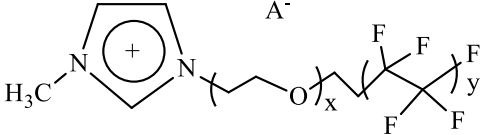
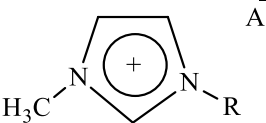
## 1.4.2 Ionic Liquids with fluoroalkyl-functionalized groups

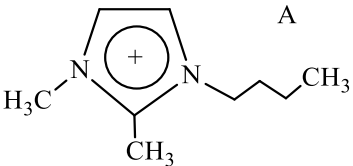
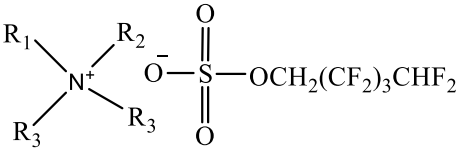
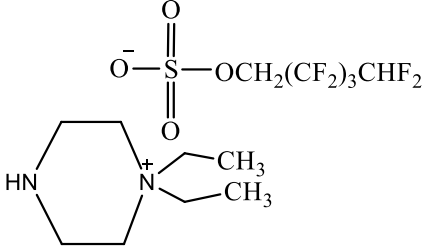
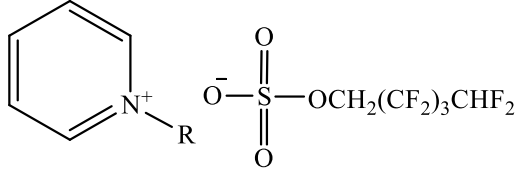
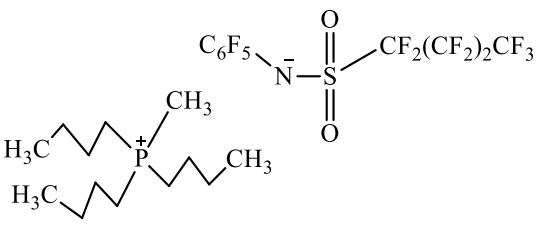
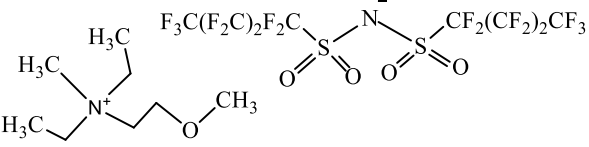
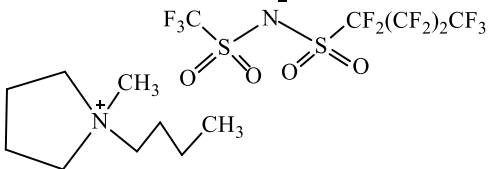
Although the number of publications in ionic liquids has recently exponentially increased, there are unexploited subjects, namely the fluorinated ionic liquids (FILs) family, which are used in this work. The solvation in fully or partially fluorinated ionic liquids has particular interest in areas where PFCs are of relevant biomedical application, such as their use as *in vivo* gas carriers in liquid ventilation or artificial blood substitute formulation. This is viable due to the unique properties of fluorocarbons, namely high capacity for dissolving gases, low surface tension and outstanding chemical and biological inertness [3].

The majority of articles published are only focused on the synthesis and characterization of FILs and their application as reaction media [52-60]. However, there are works where new fluorinated ionic liquids have been synthesized and studied for several applications, such as potential role in “green” chemical synthesis, catalysis, batteries and as electrolytes for fuel [53] as solar cells and as even telescope construction [61]; and as liquid crystals for optoelectronic applications [62]. The families and structure of some fluorinated ionic liquids from literature review are shown in **Table 1.3**.

**Table 1.3** – Structure and family of fluorinated ionic liquids.

Structure	Family	Reference
 <p>R = Me, Bu, Oc; R<sub>fn</sub> = PFBu, PFHex, PFDe; A = I, BF<sub>4</sub>, PF<sub>6</sub>, OTs, OTf</p>	Phosphonium ionic liquids containing perfluoroalkyl substituent	[63]
 <p>A = I, OTf</p>	1,2,4-oxadiazolopyridinium ionic liquids containing perfluoroheptyl substituent	[62]
 <p>R<sub>fn</sub> = PFBu, PFHex, PFOc, SF<sub>5</sub>PFBu</p>	Imidazolium ionic liquids containing perfluoroalkyl substituent with bis(trifluoromethylsulfonyl)imide anion	[52, 54, 60, 64]
 <p>R<sub>fn</sub> = PFHex, PFOc; A = I, BF<sub>4</sub>, PF<sub>6</sub>, NTf<sub>2</sub>, OTs, OTf</p>	Phosphonium ionic liquids containing tri-perfluoroalkyl and 2,4,4-trimethylpentyl substituents	[59, 65]
 <p>A = Br, NTf<sub>2</sub></p>	Phosphonium ionic liquids containing tri-perfluoroalkyl and dodecanethiol substituents	[65]
 <p>A = Br, PF<sub>6</sub>, NTf<sub>2</sub></p>	Phosphonium ionic liquids containing bis-perfluoroalkyl, 2,4,4-trimethylpentyl and hexanethiol substituents	[58]
 <p>R = Bu, Oc; R<sub>fn</sub> = PFBu, PFOc, PFDe; A = I, NTf<sub>2</sub>, C<sub>3</sub>F<sub>7</sub>CO<sub>2</sub>H</p>	Ammonium ionic liquids containing perfluoroalkyl substituent	[60]

Structure	Family	Reference
 <p>R = Me, Bu, Hep, De; R<sub>fn</sub> = PFBu, PFHex</p>	Triazolium ionic liquids containing perfluoroalkyl substituent with bis(trifluoromethylsulfonyl)imide anion	[60]
 <p>A = NTf<sub>2</sub>, ClO<sub>4</sub>, BF<sub>4</sub></p>	Triazolium ionic liquids containing perfluoroalkyl substituent	[60]
 <p>R<sub>fn</sub> = PFHex, PFOc</p>	Bipyridinium ionic liquids containing perfluoroalkyl substituent with bis(trifluoromethylsulfonyl)imide anion	[60]
 <p>R<sub>fn</sub> = EtSF<sub>5</sub>PFBu, EtPFHex</p>	Pyridinium ionic liquids containing perfluoroalkyl substituent with bis(trifluoromethylsulfonyl)imide anion	[60]
	1-Methyl-4-(3,3,4,4,5,5,6,6,7,7,8,8,8-tridecafluorooctyl)1,2,4-triazolium bis(trifluoromethylsulfonyl)imide	[60]
 <p>n = 2; A = NTf<sub>2</sub>, PF<sub>6</sub></p>	Oxazolidinium ionic liquids containing perfluoroalkyl substituent	[60]
 <p>x = 6.5; y = 3.5; A = NTf<sub>2</sub>, I</p>	Imidazolium ionic liquids containing perfluoroalkyl PEG functionalized substituent	[66]
 <p>R = Et, Bu</p> <p>A = CHF<sub>2</sub>(CF<sub>2</sub>)<sub>3</sub>CH<sub>2</sub>SO<sub>4</sub>, (PFPh)NSO<sub>2</sub>(PFBu), CF<sub>3</sub>CHFO(CF<sub>2</sub>)<sub>2</sub>SO<sub>3</sub>, CF<sub>3</sub>CF<sub>2</sub>OCHFCF<sub>2</sub>SO<sub>3</sub></p>	Imidazolium ionic liquids with anion containing perfluoroalkyl functionalized substituent	[56, 59, 67]

Structure	Family	Reference
 <p>A<sup>-</sup></p> <p>A = CHF<sub>2</sub>(CF<sub>2</sub>)<sub>3</sub>CH<sub>2</sub>SO<sub>4</sub>, (PFPh)NSO<sub>2</sub>(PFBu)</p>	1-Butyl-2,3-dimethylimidazolium with anion containing perfluoroalkyl functionalized substituent	[56, 59, 67]
 <p>R<sub>1</sub> = Me, Et, Bu; R<sub>2</sub> = Et, Bu, Oc; R<sub>3</sub> = Et, Bu</p>	Ammonium ionic liquids with 2,2,3,3,4,4,5,5-octafluoropentanesulfate anion	[59]
	Diethylpiperazinium 2,2,3,3,4,4,5,5-octafluoropentanesulfate	[59]
 <p>R = Et, Bu</p>	Pyridinium ionic liquids with 2,2,3,3,4,4,5,5-octafluoropentanesulfate anion	[59]
	Tributylmethylphosphonium 2,3,4,5,6-pentafluorophenyl-nonafluorobutylsulfonamide	[56]
	Diethylmethyl(2-methoxyethyl)ammonium bis(perfluorobutanesulfonyl)imide	[68]
	1-Butyl-1-methylpyrrolidinium (perfluorobutanesulfonyl) (trifluoromethylsulfonyl)imide	[69]

The high solubility of gases, especially carbon dioxide [52, 70] in FILs has already been demonstrated. A comparison between values for the CO<sub>2</sub> solubility in [C<sub>8</sub>H<sub>4</sub>F<sub>13</sub>MIM][NTF<sub>2</sub>] FIL (mole fraction = 0.18 at 298.15 K and ≈ 5 bar) [70] and in perfluoro-n-octane (mole fraction =



0.104 at 293.15 K and 5.29 bar) [71] at similar conditions indicate that the new FILs have greater solubilisation capacities for this gas than the traditional PFCs. The transport properties of CO<sub>2</sub>, CH<sub>4</sub>, O<sub>2</sub> and N<sub>2</sub> in FILs using supported liquid membranes have been also tested [54]. The diffusivities and permeability presents the following general trends: O<sub>2</sub> ≈ N<sub>2</sub> > CH<sub>4</sub> ≈ CO<sub>2</sub> [54].

Fluorinated surfactants are commonly used to promote high stability of various colloidal systems, including different types of emulsions or vesicles, and FILs have also shown a good behaviour as surfactant, remarkably facilitating the formation and stabilization of dispersions of perfluorocarbons in a conventional IL ([C<sub>6</sub>MIM][PF<sub>6</sub>]) [72]. FILs can display several behaviours common to surfactants: smaller surface tensions than those of conventional ILs; higher viscosity of the studied emulsions with the addition of FILs; and still, the most dramatic surfactant behaviour is their capacity to act as agents to promote and stabilize dispersion of PFCs in conventional ILs. In the absence of FILs, the emulsion aged in five minutes and when the experiment is repeated using FIL, the dispersion persist for week without visible change [72].

All the above mentioned properties of the neat FILs are essential to apply the FILs-water and FIL+PFC-water emulsions as oxygen carriers in blood substitutes. Apart from a few examples [52, 55, 59, 60, 73], FILs thermophysical properties have never been evaluated, while the toxicity and biocompatibility of the new FILs have never been studied. Besides, solubility data, properties or phase behaviour or FILs+PFC have not been found in the literature.

## 1.5 Objectives

This work is a part of a broader project focused on the development of a new and improved generation of artificial blood substitutes containing fluorinated ionic liquids. The overall objective of this work is to evaluate the thermophysical properties of some FILs and their liquid-liquid phase equilibria with PFCs, in order to conclude about the feasibility of partially replacing PFCs in PFCs emulsions used as suitable oxygen carriers. The first part of this thesis includes the study of thermophysical properties of the FILs in order to compare with those of the PFC used as oxygen therapeutics. This thermophysical and thermodynamic characterization is centred on:

- Melting and decomposition temperatures, because they determine the liquid range of these fluids and their range of application;
- Viscosity, because the viscosity of oxygen carrier emulsions have to be within a very strict range so that they can be used *in vivo*;
- Density, because the density of FILs should be similar to that of PFCs so that one single phase is easily obtained;

- Refractive index, which allows the free volume's calculation that gives information about the capacity of fluorinated ionic liquids to solubilise respiratory gases;
- Conductivity, that is directly related with ionicity and allowing us to compare FILs with other conventional ionic liquids and evaluate which compound is closest to ideal electrolyte.

The second part of this thesis, addresses the phase behaviour of the FILs with PFC. The feasibility of using FIL for replacing, totally or in part, the PFC present in the emulsions will be evaluated through the liquid-liquid equilibria of binary mixtures of five fluorinated ionic liquids with perfluorodecalin and perfluorooctane. The experimental data will be correlated through non-random two liquid model (NRTL).

## **2. Thermophysical Characterization of Fluorinated Ionic Liquids**

---



## **2.1 Introduction**

The knowledge of thermophysical and transport properties of ILs, such as density, viscosity, ionic conductivity and refractive index, is crucial from an engineering point of view. This information is also vital for process scale up, since it decisively affects technological operations like mixing, pumping, and stirring, and plays a crucial role in other properties like diffusion [74]. A few examples of physical properties and thermal characterisation are reported for fluorinated ionic liquids [52, 54-56, 58-60, 63-69], and measurements of these properties have been performed for specific temperatures only. Therefore, there is a clear need for reliable systematic thermodynamic and thermophysical properties for these ionic liquids to point out their availability for use at the industrial processes level.

The physicochemical properties of ILs in general and thus these FILs in particular can be fine-tuned through an adequate combination of the cation and the anion leading to the optimal physicochemical properties for each application. Nevertheless, this process would require wide collection of accurate physicochemical properties data for different families of FILs and the understanding of the relationships between each property and the ionic liquid intermolecular forces. This work provides a critical analyze of the thermodynamic and thermophysical properties of novel, non-volatile, recyclable fluorinated ionic liquids for the establishment of guidelines for selecting the most suitable FILs for development of new and improved generation of artificial blood substitute. This characterization involves analysis of decomposition temperature, melting point, density, dynamic viscosity, refractive index and ionic conductivity at atmospheric pressure in a large temperature interval.

Melting and decomposition temperatures are important properties of ionic liquids, especially for their application as alternative solvents, because they determine the liquid range of the fluids and thus their range of application. For example, the upper operating temperature of an ionic liquid is usually determined by the temperature at which it decomposes.

Viscosity and density are the most relevant properties for any fluid phase; viscosity is a measure of the resistance of a fluid which is being deformed by either shear stress or tensile stress. The less viscous the fluid is, the greater its ease of movement (fluidity). All fluorinated ionic liquids have a viscosity higher than water [52, 55, 59, 60, 68] or PFCs [75, 76]. Therefore, the viscosity will increase with the addition of FILs to emulsions used as artificial blood substitutes. However, FILs with high viscosity should not be selected because might present problems in promoting the dispersion of fluorinated compound in water. On the other hand, PFCs used in artificial blood substitute have a density around 1.5 [77] and FILs with similar densities are good candidates to increase the fluorinated domains of the emulsion. Additional transport

properties, such as ionic conductivity and its relation with viscosity, known as ionicity, are also important for the characterization of pure fluorinated ionic liquids.

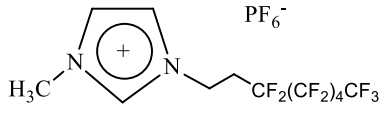
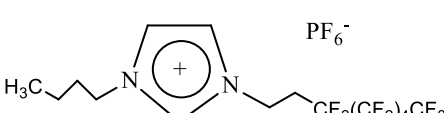
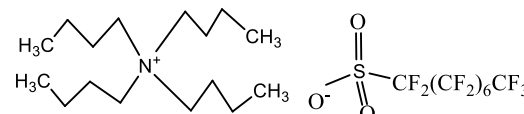
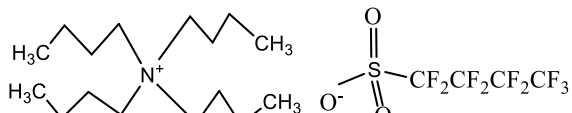
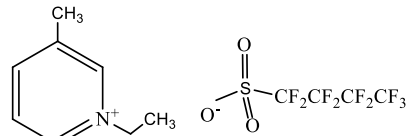
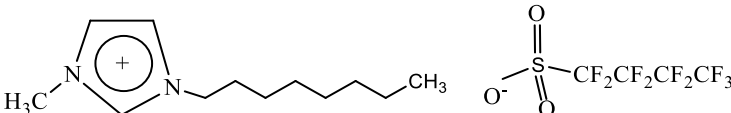
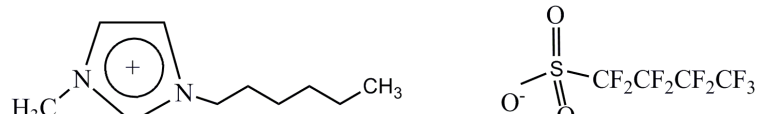
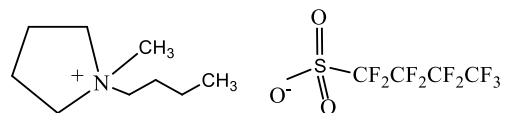
Density, refractive index and related properties such as the molar free volumes can be related with the solubility of different species in mixtures containing ionic liquid, especially low molecular weight solutes that are gaseous at normal conditions [78]. Refractive index can also provide important insights of the electric polarizability of a molecule and can provide useful information when studying the forces between molecules or their behaviour in solution. The first refractive index data of this new class of ionic liquids are determined in this work. These data will allow the evaluation of these fluorinated ionic liquids to solubilise respiratory gases.

## **2.2 Materials and Experimental Procedure**

### **2.2.1 Materials**

1-Methyl-3-(3,3,4,4,5,5,6,6,7,7,8,8,8-tridecafluorooctyl)imidazolium hexafluorophosphate, >97% mass fraction purity; 1-butyl-3-(3,3,4,4,5,5,6,6,7,7,8,8,8-tridecafluorooctyl)imidazolium hexafluorophosphate, >97% mass fraction purity; tetrabutylammonium heptadecafluorooctanesulfonate, >97% mass fraction purity; tetrabutylammonium perfluorobutanesulfonate, >97% mass fraction purity; 1-ethyl-3-methylpyridinium perfluorobutanesulfonate, >97% mass fraction purity; 1-methyl-3-octylimidazolium perfluorobutanesulfonate, >99%; 1-hexyl-3-methylimidazolium perfluorobutanesulfonate, >99% mass fraction purity and 1-butyl-1-methylpyrrolidinium perfluorobutanesulfonate, 98% mass fraction purity, were acquired at IoLitec and are shown in **Table 2.1**. All fluorinated ionic liquids were dried under vacuum ( $3 \cdot 10^{-2}$  Torr) and vigorously stirred at 323.15K for at least 2 days, immediately prior to their use. This step is crucial in order to reduce volatile impurities, as well, as water, which can influence the ionic liquids properties. The water content, determined by Karl Fisher titration (Metrohm 831 Karl Fisher coulometer, shown in **Figure 2.1**), was less than 100 ppm for all the studied ionic liquids. No further purification was carried out. The purity of the final products was checked by  $^1\text{H-NMR}$ .

**Table 2.1** - Chemical structure and respective abbreviation of fluorinated ionic liquids.

FIL Designation	Chemical Structure
1-Methyl-3-(3,3,4,4,5,5,6,6,7,7,8,8,8-tridecafluorooctyl)imidazolium hexafluorophosphate <b>[(EtPFHex)MeIm][PF<sub>6</sub>]</b>	
1-Butyl-3-(3,3,4,4,5,5,6,6,7,7,8,8,8-tridecafluorooctyl)imidazolium hexafluorophosphate <b>[(EtPFHex)BuIm][PF<sub>6</sub>]</b>	
Tetrabutylammonium heptadecafluorooctanesulfonate <b>[NBu<sub>4</sub>][(PFOc)SO<sub>3</sub>]</b>	
Tetrabutylammonium perfluorobutanesulfonate <b>[NBu<sub>4</sub>][(PFBu)SO<sub>3</sub>]</b>	
1-Ethyl-3-methylpyridinium perfluorobutanesulfonate <b>[EtMepy][(PFBu)SO<sub>3</sub>]</b>	
1-Methyl-3-octylimidazolium perfluorobutanesulfonate <b>[OcMeIm][(PFBu)SO<sub>3</sub>]</b>	
1-Hexyl-3-methylimidazolium perfluorobutanesulfonate <b>[HexMeIm][(PFBu)SO<sub>3</sub>]</b>	
1-Butyl-1-methylpyrrolidinium perfluorobutanesulfonate <b>[BuMepyr][(PFBu)SO<sub>3</sub>]</b>	



**Figure 2.1** - Metrohm 831 Karl Fisher coulometer used.

## 2.2.2 Experimental Procedure

Each fluorinated ionic liquid was taken from the respective schlenk flask with a syringe under a nitrogen flow to prevent humidity and was immediately placed in the apparatus.

### 2.2.2.1 Thermal properties

Thermogravimetric analyses (TGA) were carried out with a TA instrument model TGA Q50, shown in **Figure 2.2**, and the thermal stabilities and decomposition temperatures of the fluorinated ionic liquids were measured. Nitrogen was used for the TGA measurements at a flow rate of  $60 \text{ mL min}^{-1}$ . Samples were placed inside aluminium pans and heated to 873 K at a rate of  $1 \text{ K min}^{-1}$  until complete thermal degradation was achieved. Universal Analysis, version 4.4 software, was used to determine the onset ( $T_{onset}$ ), the starting ( $T_{start}$ ) and the decomposition ( $T_{dec}$ ) temperatures corresponding to the temperature at which the baseline slope changed during heating, the weight loss was less than 1 % and the weight loss was 50 %, respectively. A Differential Scanning Calorimeter TA Instrument model DSC Q200 (DSC), shown in **Figure 2.3**, was used to measure the thermal properties of the fluorinated ionic liquids. The sample was continuously purged with  $50 \text{ mL min}^{-1}$  dinitrogen. About 5 to 10 mg of fluorinated IL was crimped in an aluminum standard sample pan. Indium (melting point  $T = 429.76 \text{ K}$ ) was used as standard compound for the calibration of the DSC.





**Figure 2.2** – Thermogravimetric analyses model TGA Q50 (TGA).



**Figure 2.3** – Differential scanning calorimeter model DSC Q200 (DSC).

### 2.2.2.2 Viscosity and density measurements

Measurements of viscosity and density were performed in the temperature range between 283.15 and 353.15 K at atmospheric pressure using an automated SVM 3000 Anton Paar rotational Stabinger viscometer-densimeter (**Figure 2.4**). The SVM 3000 uses Peltier elements for fast and 49epresent thermostability. The temperature uncertainty is  $\pm 0.02$  K. The precision of the dynamic viscosity measurements is  $\pm 0.5\%$  and the absolute uncertainty of the density is  $\pm 0.0005$  g cm<sup>-3</sup>. For each fluorinated ionic liquid, triplicates were measured and the reported result is the average value with a maximum relative standard deviation (RSD) of 0.51%.



**Figure 2.4** – SVM 3000 Anton Paar rotational Stabinger viscometer-densimeter.

### 2.2.2.3 Refractive index measurements

The refractive index of the ionic liquids were determined using the automatic refractometer ABBEMAT 500 Anton Paar (**Figure 2.5**) with a resolution of  $\pm 10^{-6}$  and the uncertainty in the experimental measurements of  $\pm 4 \cdot 10^{-5}$ . The apparatus was calibrated by measuring the refractive index of Millipore quality water and tetrachloroethylene (provided by the supplier) before each series of measurements.



**Figure 2.5** – Refractometer ABBEMAT 500 Anton Paar.

### 2.2.2.4 Ionic conductivity measurements

A CDM210 Radiometer Analytical conductimeter (**Figure 2.6**) was used to measure the ionic conductivities in a jacketed glass cell containing a magnetic stirrer. A water bath controlled to  $\pm 0.01$  K was used to thermostate the cell. Cell temperature was measured by means of a platinum resistance thermometer coupled to a Keithly 199 System DMM/Scanner. The thermometer was calibrated against high accuracy reference thermometers (0.01 K). For the electrical conductivity measurements, 1.5 mL of the sample was added to the thermostatic cell and vigorously stirred. The cell was closed with screw caps to ensure a secure seal and flushed with dry nitrogen to prevent humidity. Each measurement was performed as quickly as possible to minimize undesired effects, such as self-heating of the samples or ionization in the electrodes [79, 80] that might modify the measured conductivity values. This conductimeter uses an alternating current of 12 V and a frequency of 2.93 kHz (4.00 mS range) in the range of conductivities measured. The use of high frequency alternating current (greater than 600 Hz) and the fact that the electrodes are platinized avoids polarization phenomena at the reference of the cell electrodes [80, 81]. The conductimeter was previously calibrated at each temperature with certified 0.01 D and 0.1 D KCl standard solutions supplied by Radiometer Analytical. This technique was validated using the pure ionic liquids 1-ethyl-3-methylimidazolium bis(trifluoromethylsulfonyl)imide and 1-hexyl-3-

methylimidazolium bis(trifluoromethylsulfonyl)imide. The obtained results were compared with the published data using the impedance method [82, 83] showing maximum relative deviations of 2%. Every conductivity value was determined at least three times and the uncertainty of the measurements is estimated to be 1% in absolute value.

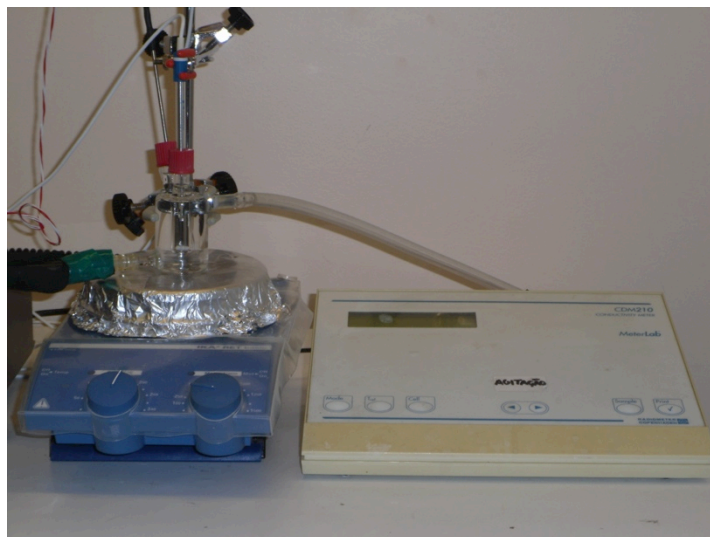


**Figure 2.6** – CDM210 Radiometer analytical conductimeter.

## **2.3 Results and Discussion**

### **2.3.1 Thermal properties**

Melting and decomposition temperatures, are one of the most remarkable properties for ionic liquids, especially for their application as alternative 51epresent, because they determine the liquid range of the fluids and their range of application, which make them the most studied properties. The 51epres properties (51epres stabilities, decomposition temperatures, melting points and glass transition temperatures see Appendix A) of the fluorinated ionic liquids studied in this work are summarized in **Table 2.2**. The melting points and decomposition temperatures for these fluorinated ionic liquids are illustrated in **Figure 2.7**.

**Table 2.2** – Thermal properties of fluorinated ionic liquids: start temperature,  $T_{start}$ , onset temperature,  $T_{onset}$ , decomposition temperature,  $T_{dec}$ , melting temperature,  $T_m$ , and glass transition temperature,  $T_g$ .

	$T_{start}^a / K$	$T_{onset}^a / K$	$T_{dec}^a / K$	$T_m / K$	$T_g / K$
[(EtPFHex)MeIm][PF <sub>6</sub> ]	429.93	535.20	544.39	338.94	236.18
[(EtPFHex)BuIm][PF <sub>6</sub> ]	420.52	519.75	557.73	362.57	–
[Nbu <sub>4</sub> ][(PFOc)SO <sub>3</sub> ]	373.67	385.08	402.61	255.14	225.72
[Nbu <sub>4</sub> ][(PFBu)SO <sub>3</sub> ]	545.07	587.04	619.21	327.13	234.45
[HexMeIm][(PFBu)SO <sub>3</sub> ]	565.56	627.00	666.18	296.78	264.07
[OcMeIm][(PFBu)SO <sub>3</sub> ]	581.98	621.41	655.78	308.13	–
[EtMepy][(PFBu)SO <sub>3</sub> ]	574.13	629.10	651.89	277.85	–
[BuMepyr][(PFBu)SO <sub>3</sub> ]	588.99	632.25	650.62	632.08	–

<sup>a</sup> Note that these values are from scanning TGA, and do not represent isothermal stabilities.

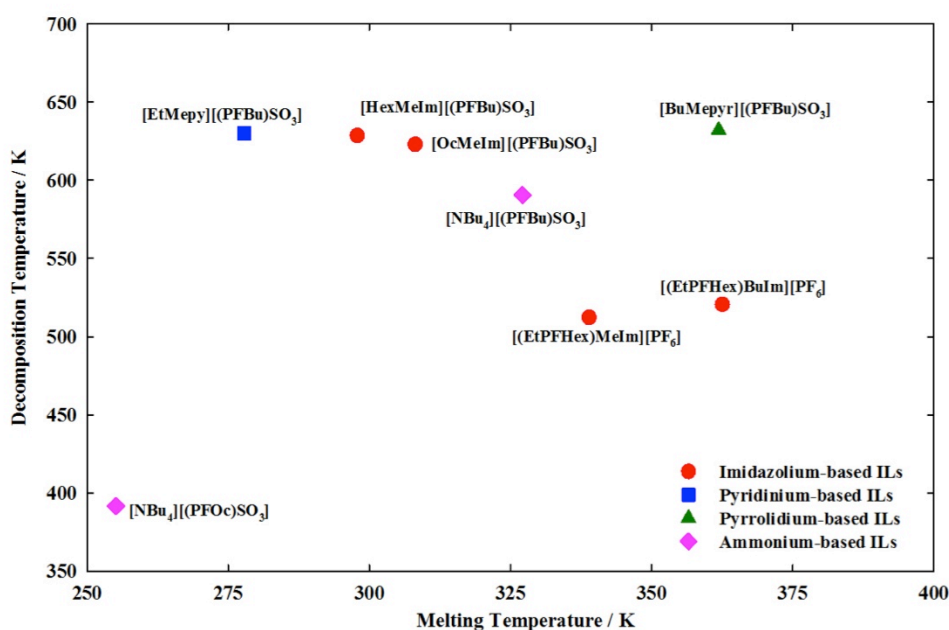


**Figure 2.7** – Melting points and decomposition temperatures of the fluorinated ionic liquids studied in this work.

In order to explore the application of fluorinated ionic liquids for artificial gas carriers and blood substitutes the most relevant temperature is 310.15 K since it is accepted as the average temperature of human body. From **Figure 2.7** [EtMepy][(PFBu)SO<sub>3</sub>] is the ionic liquid that has the highest thermal stability and the lowest melting point, constituting thus the most promising candidate in terms of thermal properties. The results also indicate that the melting points of FILs based on perfluorobutanesulfonate anion ([BuMepyr][(PFBu)SO<sub>3</sub>], [Nbu<sub>4</sub>][(PFBu)SO<sub>3</sub>], [HexMeIm][(PFBu)SO<sub>3</sub>], [OcMeIm][(PFBu)SO<sub>3</sub>] and [EtMepy][(PFBu)SO<sub>3</sub>]) decrease in the

following order: pyrrolidiums > ammonium > imidazoliums > pyridiniums. In ammonium-based ionic liquids, the increment of fluorinated chain decreases the decomposition and the melting temperatures ( $[\text{NBu}_4][(\text{PFOc})\text{SO}_3] < [\text{NBu}_4][(\text{PFBu})\text{SO}_3]$ ).

### 2.3.2 Thermophysical and thermodynamic properties

The experimental density, dynamic viscosity, refractive index and ionic conductivities of fluorinated ionic liquids as a function of temperature are listed in **Table 2.3**.

**Table 2.3** – Density,  $\rho$ , dynamic viscosity,  $\eta$ , refractive index,  $n_D$ , and ionic conductivity,  $k$ , of the pure fluorinated ionic liquids as a function of temperature.

T/K	$\rho/\text{g}\cdot\text{cm}^{-3}$	$\eta/\text{mPa}\cdot\text{s}$	$n_D$	$k/\text{mS}\cdot\text{cm}^{-1}$
[NBu <sub>4</sub> ][(PFOc)SO <sub>3</sub> ]				
283.15	–	–	1.40102	$1.28 \cdot 10^{-3}$
288.13	–	–	1.39946	$2.44 \cdot 10^{-3}$
293.15	1.3215	12159	1.39788	$4.41 \cdot 10^{-3}$
298.15	1.3173	6690	1.39625	$7.39 \cdot 10^{-3}$
303.15	1.3129	3879	1.39478	$1.22 \cdot 10^{-2}$
308.15	1.3083	2340	1.39321	$1.89 \cdot 10^{-2}$
313.15	1.3034	1464	1.39165	$2.86 \cdot 10^{-2}$
318.15	1.2984	947.2	1.39006	$4.19 \cdot 10^{-2}$
323.15	1.2934	631.9	1.38849	$5.95 \cdot 10^{-2}$
328.15	1.2882	433.5	1.38692	–
333.15	1.2833	305.1	1.38535	–
338.15	1.2783	219.9	1.38373	–
343.15	1.2735	161.9	1.38205	–
348.15	1.2686	121.6	–	–
353.15	1.2638	92.94	–	–
[NBu <sub>4</sub> ][(PFBu)SO <sub>3</sub> ]				
293.15	1.2371	28508	1.41696	–
298.15	1.2335	15319	1.41547	–
303.15	1.2301	8622	1.41400	–
308.15	1.2266	5059	1.41249	–
313.15	1.2230	3081	1.41101	–

T/K	$\rho/\text{g}\cdot\text{cm}^{-3}$	$\eta/\text{mPa}\cdot\text{s}$	$n_D$	$k/\text{mS}\cdot\text{cm}^{-1}$
318.15	1.2192	1946	1.40954	–
323.15	1.2152	1265	1.40814	–
328.15	1.2111	846.5	1.40669	–
333.15	1.2069	581.3	1.40522	–
338.15	1.2028	409.1	1.40364	–
343.15	1.1987	294.4	1.40231	–
348.15	1.1944	216.2	–	–
353.15	1.1899	161.8	–	–
[HexMeIm][(PFBu)SO <sub>3</sub> ]				
293.15	1.3967	570.0	1.40987	0.218
298.15	1.3918	401.7	1.40847	0.299
303.15	1.3871	290.2	1.40704	0.401
308.15	1.3824	214.4	1.40562	0.527
313.15	1.3778	161.6	1.40421	0.678
318.15	1.3732	124.1	1.40281	0.857
323.15	1.3686	96.98	1.40130	1.07
328.15	1.3639	76.95	1.40005	–
333.15	1.3593	61.92	1.39867	–
338.15	1.3546	50.49	1.39731	–
343.15	1.3499	41.66	1.39595	–
348.15	1.3450	34.76	–	–
353.15	1.3401	29.31	–	–
[OcMeIm][(PFBu)SO <sub>3</sub> ]				
298.15	1.3381	374.6	1.412790	–
303.15	1.3332	344.9	1.41134	–
308.15	1.3287	252.9	1.40990	0.355
313.15	1.3242	189.2	1.40848	0.461
318.15	1.3197	144.3	1.40710	0.588
323.15	1.3153	111.9	1.40568	0.732
328.15	1.3109	88.21	1.40430	–
333.15	1.3065	70.53	1.40289	–
338.15	1.3020	57.15	1.40152	–
343.15	1.2976	46.88	1.40008	–
348.15	1.2931	38.89	–	–
353.15	1.2885	32.61	–	–

T/K	$\rho/\text{g}\cdot\text{cm}^{-3}$	$\eta/\text{mPa}\cdot\text{s}$	$n_D$	$k/\text{mS}\cdot\text{cm}^{-1}$
[EtMepy][(PFBu)SO <sub>3</sub> ]				
283.15	1.5306	578.9	1.42439	0.405
288.13	1.5252	394.8	1.42290	0.565
293.15	1.5199	278.2	1.42142	0.765
298.15	1.5148	201.8	1.41997	1.01
303.15	1.5098	150.3	1.41850	1.30
308.15	1.5048	114.4	1.41703	1.64
313.15	1.4998	88.98	1.41554	2.03
318.15	1.4949	70.46	1.41405	2.48
323.15	1.4899	56.72	1.4899	2.97
328.15	1.4850	46.34	1.4850	–
333.15	1.4802	38.39	1.4802	–
338.15	1.4753	32.18	1.4753	–
343.15	1.4704	27.26	1.4704	–
348.15	1.4655	23.33	1.4655	–
353.15	1.4607	20.15	1.4607	–

The densities, fluidities (1 / dynamic viscosity) and ionic conductivities of the fluorinated ionic liquids are shown in **Figure 2.8**, **Figure 2.9** and **Figure 2.10**, respectively, as function of the temperature.

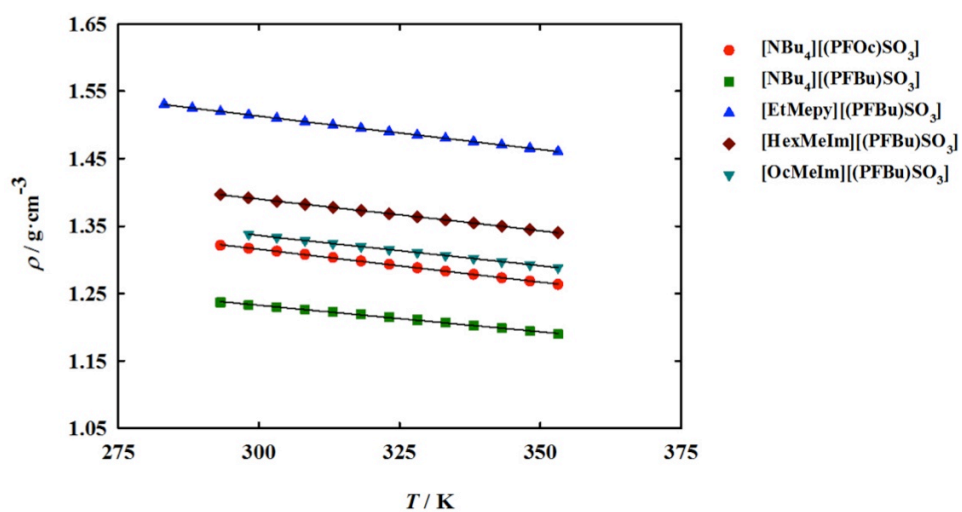


**Figure 2.8** – Density and fitted curves as a function of temperature for the fluorinated ionic liquids.

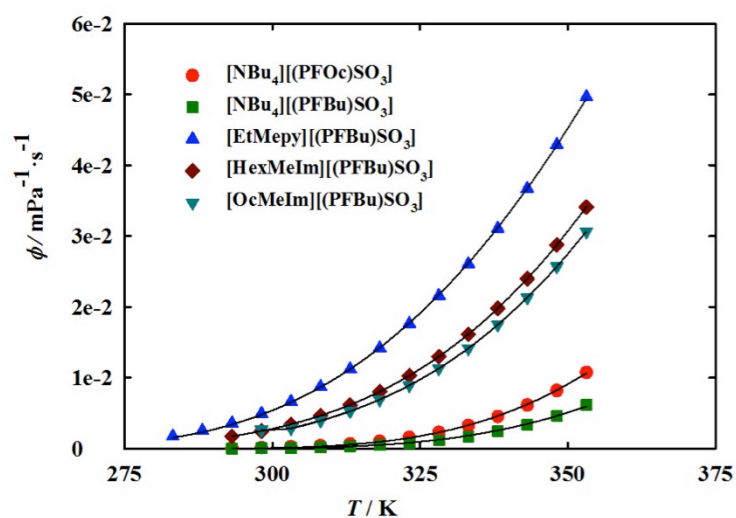


**Figure 2.9** – Fluidity (1/viscosity) and fitted curves as a function of temperature for the fluorinated ionic liquids.

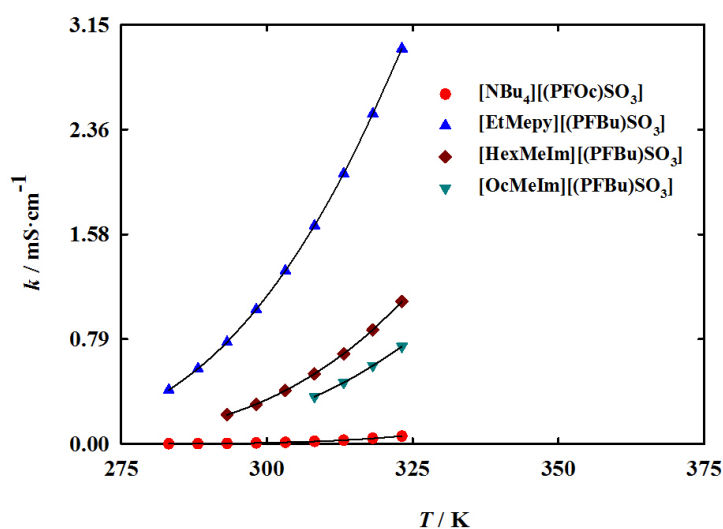


**Figure 2.10** – Ionic conductivity and fitted curves as a function of temperature for the fluorinated ionic liquids.

The temperature dependence of the density and the refractive index was studied by applying the following expression:

$$\ln \rho = A_0 + A_1 T \quad (2.1)$$

$$n_D = A_0 + A_1 T \quad (2.2)$$

where  $T$  is the absolute temperature and  $A_0$ , and  $A_1$  are adjustable parameters. The correlation parameters are given in **Table 2.4** together with the standard deviations (S.D.). These deviations were calculated by applying the following expression:



$$\text{S.D.} = \left( \frac{\sum_i^{n_{\text{DAT}}} (z_{\text{exp}} - z_{\text{adjust}})^2}{n_{\text{DAT}}} \right)^{1/2} \quad (2.3)$$

where property values and the number of experimental and adjustable data are represented by  $z$  and  $n_{\text{DAT}}$ , respectively.

Arrhenius fitting for fluidity,  $\phi$ , and of the ionic conductivity,  $k$ , was well carried out using Vogel-Fulcher-Tammann (VFT) equation:

$$P = P_0 \exp\left(\frac{-B}{T - T_0}\right) \quad (2.4)$$

where  $P$  designates the thermophysical property (fluidity,  $\phi$ , or ionic conductivity,  $k$ ) and  $P_0$  corresponds to  $\phi_0$  or  $k_0$ .  $B$  and  $T_0$  are constants. The fitting parameters of the fluidity and ionic conductivity are also summarized in **Table 2.4**. This equation is used to show temperature dependence of ionic conductivity and fluidity.

Density and fluidity (inverse of dynamic viscosity) are relevant characteristics, when it comes to blood substitutes, since they are crucial for  $\text{O}_2$  and  $\text{CO}_2$  transport and delivery [84]. Both these properties show similar behaviour: the denser and less viscous FIL is the [EtMepy][[(PFBu)SO<sub>3</sub>]<sup>-</sup>], followed by imidazolium based on [(PFBu)SO<sub>3</sub>]<sup>-</sup> anion.

**Table 2.4** - Fitting parameters for the density (equation 2.1), refractive index (equation 2.2), fluidity (equation 2.4) and ionic conductivity (equation 2.4) as a function of temperature for the studied fluorinated ionic liquids. Standard deviations (S.D.) (equation 2.3) are also shown.

<b>[NBu<sub>4</sub>][(PFOc)SO<sub>3</sub>]</b>				
$\ln \rho / \text{g} \cdot \text{cm}^{-3}$	$A_0 = 0.5008$	$A_1 = -7.547 \cdot 10^{-4}$	–	S.D. = $3.4 \cdot 10^{-4}$
$n_D$	$A_0 = 1.4902$	$A_1 = -3.150 \cdot 10^{-4}$	–	S.D. = $5.0 \cdot 10^{-5}$
$\phi / \text{mPa}^{-1} \cdot \text{s}^{-1}$	$\phi_0 = 3.75$	$B = 707.29$	$T_0 = 232.5$	S.D. = $7.7 \cdot 10^{-5}$
$k / \text{mS} \cdot \text{cm}^{-1}$	$k_0 = 1334.6$	$B = 1349.7$	$T_0 = 186.4$	S.D. = $4.5 \cdot 10^{-4}$
<b>[NBu<sub>4</sub>][(PFBu)SO<sub>3</sub>]</b>				
$\ln \rho / \text{g} \cdot \text{cm}^{-3}$	$A_0 = 0.4037$	$A_1 = -6.482 \cdot 10^{-4}$	–	S.D. = $5.5 \cdot 10^{-4}$
$n_D$	$A_0 = 1.5029$	$A_1 = -2.934 \cdot 10^{-4}$	–	S.D. = $4.3 \cdot 10^{-5}$

$\phi / \text{mPa}^{-1} \cdot \text{s}^{-1}$	$\phi_0 = 2.14$	$B = 707.34$	$T_0 = 232.8$	S.D. = $9.0 \cdot 10^{-5}$
<b>[HexMeIm][(PFBu)SO<sub>3</sub>]</b>				
$\ln \rho / \text{g} \cdot \text{cm}^{-3}$	$A_0 = 0.5346$	$A_1 = -6.840 \cdot 10^{-4}$	–	S.D. = $1.5 \cdot 10^{-4}$
$n_D$	$A_0 = 1.4920$	$A_1 = -2.801 \cdot 10^{-4}$	–	S.D. = $6.1 \cdot 10^{-5}$
$\phi / \text{mPa}^{-1} \cdot \text{s}^{-1}$	$\phi_0 = 3.75$	$B = 705.46$	$T_0 = 203.34$	S.D. = $2.0 \cdot 10^{-4}$
$k / \text{mS} \cdot \text{cm}^{-1}$	$k_0 = 1376.8$	$B = 1186.9$	$T_0 = 157.4$	S.D. = $1.4 \cdot 10^{-3}$
<b>[OcMeIm][(PFBu)SO<sub>3</sub>]</b>				
$\ln \rho / \text{g} \cdot \text{cm}^{-3}$	$A_0 = 0.5006$	$A_1 = -6.802 \cdot 10^{-4}$	–	S.D. = $3.4 \cdot 10^{-4}$
$n_D$	$A_0 = 1.4967$	$A_1 = -7.008 \cdot 10^{-4}$	–	S.D. = $2.7 \cdot 10^{-5}$
$\phi / \text{mPa}^{-1} \cdot \text{s}^{-1}$	$\phi_0 = 3.56$	$B = 706.04$	$T_0 = 205.01$	S.D. = $3.2 \cdot 10^{-4}$
$k / \text{mS} \cdot \text{cm}^{-1}$	$k_0 = 1381.1$	$B = 1295.0$	$T_0 = 151.4$	S.D. = $1.8 \cdot 10^{-3}$
<b>[EtMepy][(PFBu)SO<sub>3</sub>]</b>				
$\ln \rho / \text{g} \cdot \text{cm}^{-3}$	$A_0 = 0.6136$	$A_1 = -6.648 \cdot 10^{-4}$	–	S.D. = $1.1 \cdot 10^{-4}$
$n_D$	$A_0 = 1.5094$	$A_1 = -3.001 \cdot 10^{-4}$	–	S.D. = $7.4 \cdot 10^{-5}$
$\phi / \text{mPa}^{-1} \cdot \text{s}^{-1}$	$\phi_0 = 4.12$	$B = 704.89$	$T_0 = 193.8$	S.D. = $1.3 \cdot 10^{-4}$
$k / \text{mS} \cdot \text{cm}^{-1}$	$k_0 = 1430.0$	$B = 1028.1$	$T_0 = 156.5$	S.D. = $1.4 \cdot 10^{-2}$

### 2.3.3 Free Volume

The refractive index can be used as a measure of the electric polarizability of a molecule and can provide useful information when studying the forces between molecules or their behaviour in solution [78]. Polarizability is the measure of the change in a molecule's electron distribution in response to an applied electric field, which can also be induced by electric interactions with solvents or ionic solvents. Polarizabilities determine the dynamical response of a bound system to external fields, and provide insight into a molecule's internal structure [85]. The Lorenz-Lorentz equation relates the electronic polarizability,  $\alpha_e$ , with the refractive index,  $n_D$ , and can also be expressed in terms of the molar refraction, or molar polarizability [86],  $R_m$ , using the expression:

$$R_m = \frac{N_A \alpha_e}{3\epsilon_0} = \left( \frac{n_D^2 - 1}{n_D^2 + 2} \right) V_m \quad (2.5)$$

where the  $N_A$  is the Avogadro's constant and  $V_m$  the molar volume.

The relation between the polarizability and the refractive index shown above can provide important information about the behaviour of a liquid as a solvent medium and constitutes a

measure of the importance of the dispersion forces to the cohesion of the liquid. Therefore, solvents with a large index of refraction, and consequently large polarizability, should be capable of enjoying particularly strong dispersion forces [87], being also good solvents for species possessing high polarizabilities. Molar refractions can be considered as a measure of the hard-core molecular volumes because the electronic polarizability can be related to a spherical molecular radius [78],  $a$ , as follows:

$$\alpha_e = 4\pi\epsilon_0 a^3 \quad (2.6)$$

and the equation 2.5 can be expressed in the following form:

$$n_D^2 - 1 = 3 \left( \frac{V_m}{R_m - 1} \right)^{-1} = 3 \left( \frac{R_m}{f_m} \right) \quad (2.7)$$

where  $f_m$  is the free volume defined as:

$$f_m = (V_m - R_m) \quad (2.8)$$

which means that  $(n_D^2 - 1)$  is directly proportional to the occupied part of the molar volume,  $R_m$  being then considered as the hard-core molecular volume [88, 89].

The molar free volumes can be related to the solubility of low molecular weight solutes that are gaseous at normal conditions [78]. The values for the calculated molar refractions (from equation 2.5) and free volumes (from equation 2.8), from Lorentz-Lorenz equation, of all the studied fluorinated ionic liquids were calculated and are listed in **Table 2.5** together with the values for molar volume.

**Table 2.5** – Values of calculated molar volume,  $V_m$ , molar refraction,  $R_m$ , and free volume,  $f_m$ , as a function of temperature for the studied fluorinated ionic liquids.

$T/K$	$V_m/\text{cm}^3 \cdot \text{mol}^{-1}$	$R_m/\text{cm}^3 \cdot \text{mol}^{-1}$	$f_m/\text{cm}^3 \cdot \text{mol}^{-1}$
<b>[NBu<sub>4</sub>][(PFOc)SO<sub>3</sub>]</b>			
293.15	561.12	135.39	425.73
298.15	562.93	135.33	427.60
303.15	564.82	135.34	429.47
308.15	566.80	135.34	431.46
313.15	568.93	135.37	433.56
318.15	571.12	135.40	435.72
323.15	573.33	135.44	437.89
328.15	575.62	135.49	440.13
333.15	577.85	135.52	442.32
338.15	580.08	135.54	444.54
343.15	582.29	135.53	446.77
<b>[NBu<sub>4</sub>][(PFBu)SO<sub>3</sub>]</b>			
293.15	437.73	110.07	327.66
298.15	439.01	110.04	328.97
303.15	440.22	110.01	330.22
308.15	441.48	109.97	331.51
313.15	442.78	109.94	332.84
318.15	444.16	109.94	334.22
323.15	445.62	109.97	335.66
328.15	447.13	109.99	337.14
333.15	448.69	110.03	338.66
338.15	450.22	110.02	340.20
343.15	451.76	110.08	341.68
<b>[HexMeIm][(PFBu)SO<sub>3</sub>]</b>			
293.15	333.87	82.70	251.17
298.15	335.06	82.74	252.32
303.15	336.19	82.77	253.43
308.15	337.33	82.79	254.54
313.15	338.46	82.81	255.65
318.15	339.59	82.84	256.76
323.15	340.74	82.84	257.90
328.15	341.89	82.89	259.00

$T/K$	$V_m/\text{cm}^3 \cdot \text{mol}^{-1}$	$R_m/\text{cm}^3 \cdot \text{mol}^{-1}$	$f_m/\text{cm}^3 \cdot \text{mol}^{-1}$
333.15	343.06	82.92	260.14
338.15	344.25	82.96	261.29
343.15	345.46	83.00	262.46
<b>[OcMelm][(PFBu)SO<sub>3</sub>]</b>			
298.15	369.49	92.09	277.40
303.15	370.85	92.15	278.70
308.15	372.10	92.17	279.93
313.15	373.37	92.20	281.17
318.15	374.63	92.24	282.39
323.15	375.90	92.27	283.63
328.15	377.17	92.30	284.87
333.15	378.44	92.33	286.11
338.15	379.73	92.36	287.36
343.15	381.03	92.39	288.65
<b>[EtMepy][(PFBu)SO<sub>3</sub>]</b>			
283.15	275.21	70.28	204.92
288.15	276.19	70.32	205.88
293.15	277.14	70.34	206.80
298.15	278.08	70.37	207.71
303.15	279.01	70.39	208.62
308.15	279.93	70.40	209.53
313.15	280.86	70.41	210.45
318.15	281.78	70.42	211.36
323.15	282.73	70.43	212.30
328.15	283.66	70.40	213.25
333.15	284.59	70.41	214.18
338.15	285.52	70.42	215.10
343.15	286.48	70.45	216.03

The molar free volumes of fluorinated ionic liquids are plotted in **Figure 2.11**. The analysis of molar free volume indicates that the increment of alkyl and fluorinated chain increases the molar free volume, which might be beneficial for the use of these fluids as gases carriers. It has been shown that the oxygen and the carbon dioxide solubility in fluorinated compounds is largely governed by entropic contributions, meaning that the creation of free cavities which can better accommodate the gas molecules might enhance the gas solubility of these.

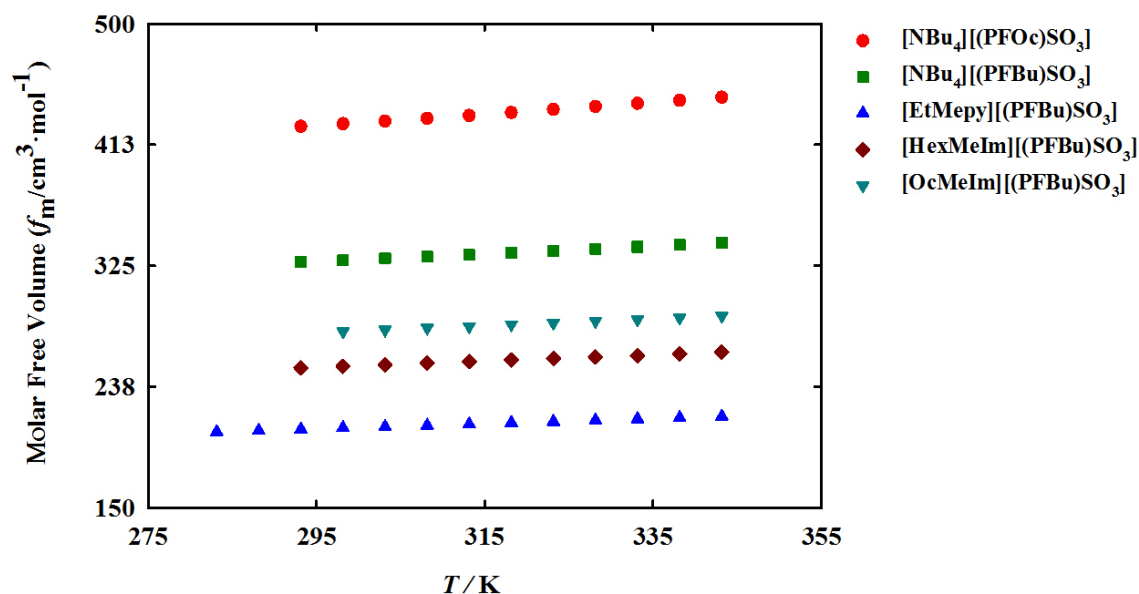


**Figure 2.11** – Molar free volume as a function of temperature for the fluorinated ionic liquids.

A combined analysis of the results obtained so far from **Figure 2.8** to **Figure 2.11**, shows that [EtMepy][(PFBu)SO<sub>3</sub>] can be a good election because can increase viscosity of PFC-based emulsions and has a similar density to PFCs (PFCs used in artificial blood substitute have a density around 1.5 [90]) favouring the easy preparation of solutions. However, this fluorinated ionic liquid presents the lowest value of molar free volume (calculated from density and refractive index), which can be attributed to the small perfluorinated chain present in this anion combined with short alkyl chains in the cation. The highest free volume is obtained for the [NBu<sub>4</sub>][(PFOc)SO<sub>3</sub>] FIL which has a octylperfluorooctyl chain in the anion combined with tetrabutylammonium cation.

### 2.3.4 Walden Plot

The Walden plot is a convenient and versatile tool to measure the ionicity of ionic liquids [91, 92] since it establishes a relationship between the molar conductivity and the viscosity of a fluid. A way to determine the efficiency of an ionic liquid as an electrolyte, solvent, or reaction medium [93], has been proposed by Walden rule [94]. The Walden rule gives information on the relationship between ion mobility and viscosity. In the case of an ideal ionic liquid conductor, conductivity is only influenced by the viscosity [95] in the form:

$$\text{Molar conductivity} = \frac{C}{\eta} \quad (2.9)$$

where the molar conductivity is expressed in  $\text{S cm}^2 \text{ mol}^{-1}$  and the viscosity ( $\eta$ ) is expressed in Poise, and  $C$  is a constant. “The fractional” Walden model added an exponent  $\alpha$  [96].

$$\text{Molar conductivity} \propto \left(\frac{1}{\eta}\right)^\alpha \quad (2.10)$$

For ionic liquids, it has been shown that the molar conductivity can be calculated by [95]:

$$\text{Molar conductivity} = \frac{k}{\rho M_w} \quad (2.11)$$

with the  $k$  conductivity in  $\text{S cm}^{-1}$ , the  $\rho$  the density in  $\text{g cm}^{-3}$  and  $M_w$  the molecular weight in  $\text{g mol}^{-1}$ . The eq. (2.11) can be also expressed by:

$$\log(\text{Molar conductivity}) = \alpha \log\left(\frac{1}{\eta}\right) + \log C \quad (2.12)$$

The Walden-plot is usually represented by the  $\log(\text{Molar conductivity})$  as a function of  $\log(1/\eta)$  [96] and is a good and versatile tool to measure ionicity of inorganic salts solutions and ionic solvents. The straight line of **Figure 2.12** fixes the position of the “ideal” electrolyte, where the system is known to be fully dissociated and to have ions of equal mobility. Usually, the behaviour of diluted aqueous potassium chloride solutions are taken as the behaviour of an ideal electrolyte [97]. For the unit chosen, the ideal line runs from corner to corner of a square diagram [98]. **Figure 2.12** shows the classification proposed by Angell and co-workers [91, 98] for “good” and “poor” ionic liquids.

Experimental information on ionicity of fluorinated ionic liquids is extremely scarce in literature review and experimental data are available for only two FILs [91, 92]. The data obtained for the four fluorinated ionic liquids studied in this work are represented in **Figure 2.12** together with the classification proposed by Angell and co-workers [92, 99]. For each fluorinated ionic liquid, the Walden plot has a linear behaviour with the temperature. The behaviour of  $[\text{EtMepy}][(\text{PFBu})\text{SO}_3]$  is the closest to ideal electrolyte (straight black line) and the ionicity decreases in the following order:  $[\text{EtMepy}][(\text{PFBu})\text{SO}_3] > [\text{HexMeIm}][(\text{PFBu})\text{SO}_3] > [\text{OcMeIm}][(\text{PFBu})\text{SO}_3] > [\text{NBu}_4][(\text{PFOc})\text{SO}_3]$ .

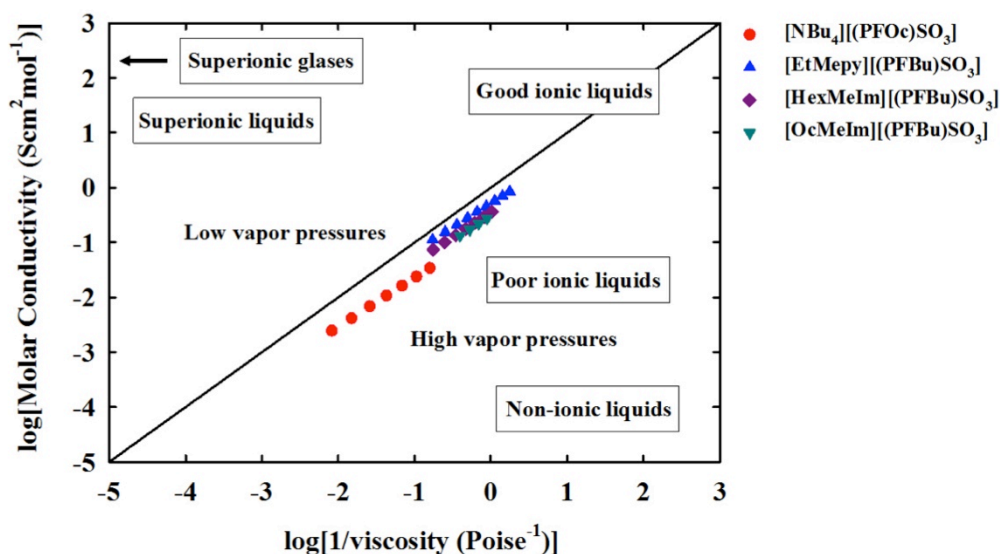


Figure 2.12 – Walden plot for the fluorinated ionic liquids.

## 2.4 Conclusions

The goal of this chapter was to report the measurement of the thermodynamic and thermophysical properties of 8 FILs in order to understand its behaviour as pure fluid so that they can be used in oxygen therapeutics based on PFCs-emulsions.

The viscosity of PFC-based emulsions should increase when a good surfactant is added with the aim to enhance the stability of emulsions. All the fluorinated ionic liquids have higher viscosity than the PFCs and can increase the stability of actual oxygen therapeutics. However, the FILs with higher viscosity should not be selected because they can present problems to promote dispersion of fluorinated compounds in the water.

By the behaviour of thermodynamic and thermophysical properties, it may be concluded that  $[\text{EtMepy}][(\text{PFBu})\text{SO}_3]$  is a good election because it has the lowest viscosity and a density similar to that of PFC-based emulsions and thus would not present any problems in the preparation or stability of the emulsion. However,  $[\text{EtMepy}][(\text{PFBu})\text{SO}_3]$  presents the lowest value of molar free volume, which may hinder the solubility of respiratory gases.



### **3. Liquid-Liquid Equilibria of Perfluorocompounds with Fluorinated Ionic Liquids**

---



### 3.1 Introduction

In system at equilibrium [100], the number of variables is called the number of degrees of freedom ( $f$ ) and is related to the number of components ( $c$ ) and number of phases ( $n$ ) as follows, at constant pressure:

$$f=c+1-n \quad (3.1)$$

This is a key rule in the study of phase equilibria, and has influences in the way in which the liquid-liquid equilibrium (LLE) data are represented [101]. The word “equilibrium” denotes the absence of change and the absence of any tendency towards change on a macroscopic scale. The phase diagrams are a useful graphical representation of phase equilibria, guided by application of the phase rule, where data are easy to apply and read. For a binary liquid system, the most common phase diagram is the so-called temperature-composition diagram, at constant pressure, whereas temperature is represented in the y-axis and composition in the x-axis. Therefore, the number of degree of freedom available will be  $f=2$  if there is homogeneity in the system, but only  $f=1$  if the system presents two immiscible phases.

From the first law of thermodynamic, (which says although energy assumes many forms, the total quantity of energy is constant, and when energy disappears in one form it appears simultaneously in other forms), and the second law, (which says that it is impossible by a cyclic process to convert the heat absorbed by a system completely into work done by the system and that no process is possible which consist solely in the transfer of heat from one temperature level to a higher one), can be demonstrable [102] that the equilibrium state of a closed system at a constant temperature and pressure is the state for which the total Gibbs energy ( $G$ ) is at a minimum with respect to all possible changes at the given temperature and pressure, and can be expressed as:

$$(dG)_{T,P} = 0 \quad (3.2)$$

which is valid regardless of the number of phases and components in the system.

The experimental methods for determining phase equilibria can be classified in two main categories: the synthetic and the analytical. The synthetic method involves the preparation, usually by mass, of a mixture of known composition, followed by a measurement of the temperature at which the phase separation is formed or disappears. Traditionally visual

observation of the clear and/or cloud points of the mixtures is used [103]. The advantages of the synthetic method are essentially applicability and the simplicity while the two major disadvantages is that both components and their mixtures must be stable at the microscopic timescale up to the maximum temperature of interest [103]. The analytical method requires that the different phases are in equilibrium, allowing for the separation. Then, samples of both phases are analysed by some appropriate method (measuring the refractive index, titration, spectrophotometry, chromatography, etc.). This method is usually the method of choice, because of its accuracy, speed, simplicity and lack of requirement for specialized apparatus [44]. However, this method can be more time consuming in systems that require large equilibration times and large phase separation periods. In order to obtain accurate measurements, a complete separation of the phases must be achieved before sampling.

In this work, the liquid-liquid phase equilibria behaviour of perfluorocarbons and fluorinated ionic liquids will be measured. The aim of this study is to evaluate the possible replacement totally or partially of the perfluorocarbons used in artificial blood substitutes by fluorine ionic liquids, in order to provide a more stable product. Two perfluorocarbons were chosen, perfluorodecalin and perfluorooctane, since these compounds, or compounds derived from them, have been the most studied for this application.

The experimentally obtained liquid-liquid equilibrium data are correlated using Non Random Two-Liquid Model (NRTL) equation, which is a semi-empirical model [104] that takes account of the non-random nature of liquid mixtures by using the concept of a local composition. This model, although simplistic, can attest the thermodynamic consistency of the measured data.

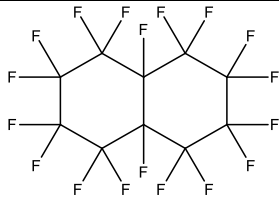
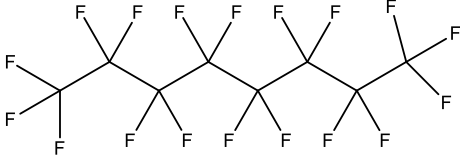
## **3.2 Materials and Experimental Procedure**

### **3.2.1 Materials**

1-Methyl-3-(3,3,4,4,5,5,6,6,7,7,8,8,8-tridecafluorooctyl)imidazolium hexafluorophosphate, >97% mass fraction purity; 1-butyl-3-(3,3,4,4,5,5,6,6,7,7,8,8,8-tridecafluorooctyl)imidazolium hexafluorophosphate, >97% mass fraction purity; tetrabutylammonium heptadecafluorooctanesulfonate, >97% mass fraction purity; tetrabutylammonium perfluorobutanesulfonate, >97% mass fraction purity; 1-ethyl-3-methylpyridinium perfluorobutanesulfonate, >97% mass fraction purity; 1-methyl-3-octylimidazolium perfluorobutanesulfonate, >99%; 1-hexyl-3-methylimidazolium perfluorobutanesulfonate, >99%

mass fraction purity and 1-butyl-1-methylpyrrolidinium perfluorobutanesulfonate, 98% mass fraction purity, were acquired at IoLitec, and are shown in **Table 2.1**. The ionic liquid 1-butyl-3-methylimidazolium bis(trifluoromethylsulfonyl) imide, 99% mass fraction purity from IoLitec, were used for the method validation. Ionic liquids were dried under constant agitation in vacuum ( $3 \cdot 10^{-2}$  Torr) and at 323.15 K, for a minimum of 48 h immediately prior to their use. Perfluorodecalin, 96% mass fraction purity and perfluorooctane, >99% mass fraction purity were supplied by Apollo Scientific and are shown in **Table 3.1**.

**Table 3.1** - Chemical structure and respective abbreviation of perfluorocarbon.

PFC Designation	Chemical Structure
Perfluorodecalin	
Perfluorooctane	

## 3.2.2 Procedure

### 3.2.2.1 Liquid-Liquid Equilibria

Liquid-liquid equilibria was studied for the 9 binary mixtures perfluorocarbons + fluorinated ionic liquids in the temperature range from  $T = 293.15$  to  $343.15$  K and at atmospheric pressure.

Preliminary studies indicated in the studied systems, the solubility of the selected FILs in the two chosen PFC are very small, almost close to zero. On the other hand, the solubilities of the PFCs in the FILs were found to be larger, around 0.8 of FIL in molar fraction. These facts dictated the choices of the different experimental methodologies (synthetic and the analytical) adopted for determination of both PFC-rich and FIL-rich sides of the phase diagram.

The solubility of each perfluorocarbon in FIL-rich phase was determined by the analytical method, using refratometry. The measurements were started with an addition of 3 ml of an

immiscible binary mixture (**Figure 3.1**) of known composition inside of a glass cell. The temperature was set and the mixture was vigorously stirred for 1 h, which was found to be the adequate period of time to reach the equilibrium. Then, a needle was inserted through the septum of the cell in FIL-rich phase, in order to not disturb the equilibrium (special capped needles were used in order to avoid contamination from one phase with the other) and left to settle for 48 h. In this period, the complete separation of the two phases was achieved. Samples were taken by a heated syringe from the upper layer (FIL-rich phase). A series of LLE measurements were made by changing the temperature of the experiment. The phase diagram determination (both PFC and FIL rich side) was accomplished using a temperature controlled bath with a circulator heating (Lauda E200 and a cooler Raypa) capable of maintaining the temperature within  $\pm 0.01$  K.

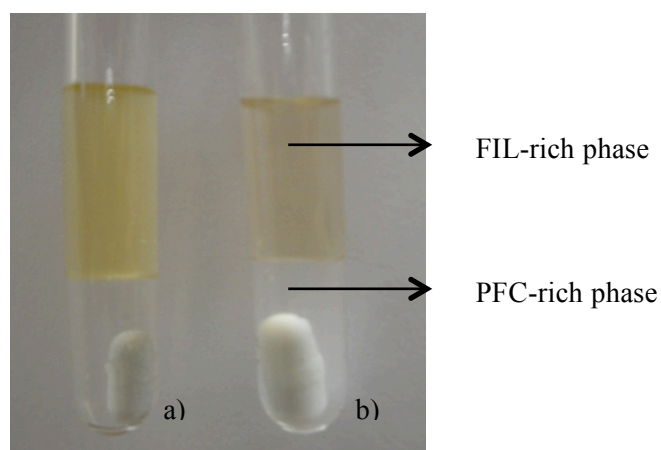


**Figure 3.1** – Binary mixtures for liquid-liquid equilibria: (a) perfluorodecalin + [EtMepy][(PFBu)SO<sub>3</sub>] and (b) perfluorooctane + [HexMeIm][(PFBu)SO<sub>3</sub>].

The solubility of fluorinated ionic liquids in PFC-rich phase was determined by synthetic method (visual method) because the value of the solubility is very small and no quantitative method (analytical method) can determine the tie-line composition. These liquid-liquid phase equilibrium measurements were carried out at a atmospheric pressure using a method based on the visual detection of the turbidity of the binary mixtures contained in 5 ml Pyrex glass cells equipped with magnetic stirrers. The initial solutions were prepared directly inside the 5ml Pyrex glass cells equipped with magnetic stirrers by syringing known amounts of each component, which were previously weighted using an analytical high-precision balance with a precision of  $\pm 10^{-5}$  g. The cell was initially immersed in a thermostatic bath and the sample was continuously stirred until two clear phases were observed. Then, the temperature was slowly raised until the last sign of turbidity disappeared. This temperature was taken as the temperature of the liquid-liquid phase transition. The temperature was measured using a platinum resistance thermometer

coupled to a Keithley 199 System DMM/Scanner. The overall temperature uncertainty of these visual determinations is obviously higher than that measured by the Pt100 and is estimated to be  $\pm 0.5$  K. The estimated uncertainty in the mixtures composition is of 0.0001 in mass fraction. Water + ethylene glycol mixture were used as the thermostatic fluids, depending on the temperature range.

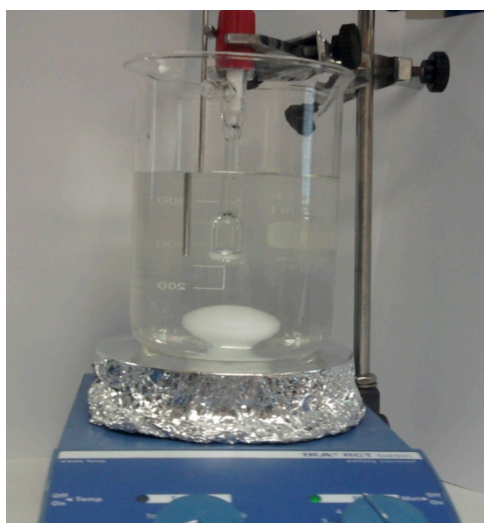


**Figure 3.2** – Experimental assembly used to measure solubility of fluorinated ionic liquid in PFC-rich.

The temperature was monitored using a four-wire platinum resistance Pt100 thermometer coupled to Keithley multimeter with an uncertainty of 0.01 K. This Pt100 thermometer was calibrated against high accuracy mercury thermometers (0.01K precision).

### **3.2.2.2 Analytical Method – Refractometry**

As mentioned before only the compositions of the perfluorocarbon in FIL-rich phase were determined by measuring the refractive index. For that purpose, an automatic refractometer ABBEMAT 500 Anton Paar with a resolution of  $\pm 10^{-6}$  and the uncertainty in the experimental measurements of  $\pm 4 \cdot 10^{-5}$  was used. Calibration curves (Appendix B) were made by measuring the refractive index of the samples with known composition at  $T = 343.15$  K. The samples were

prepared by filling glass vials with binary mixtures of FIL with perfluorocarbon of known composition, determined using a high-precision balance with a precision of  $\pm 10^{-5}$  g . The vials were closed with screw caps to ensure a secure seal and to prevent humidity. A sample was taken from the vial with a syringe through a silicone septum and was immediately put into the apparatus. The estimated uncertainty in the composition of the calibration curve is of  $\pm 10^{-4}$  in mole fraction and in the determination of the phase diagram 0.001 in mole fraction.

### **Method Validation**

In order to validate the quantitative method (refractometry) described above, binary mixtures of [BuMeIm][NTf<sub>2</sub>] + water were studied and compared with literature values [105]. The water used was double distilled, passed by a reverse osmosis system, and further treated with a Milli-Q Plus 185 water purification apparatus. In the water rich-phase, the phase composition was determined by the measurement of the refractive index and the application of the corresponding fitting polynomials. In order to provide a more complete work, and thus a better description of this system the IL rich-phase was also analyzed, and the phase composition was determined using a Metrohm 831 Karl Fisher coulometer (**Figure 2.1**). IL-rich phase samples of about 0.1 to 0.2 g were taken from the equilibrium vials using a glass syringe maintained in dry and warm conditions. The liquid-liquid phase diagram of water with [BuMeIm][NTf<sub>2</sub>] measure in this work is represented in **Figure 3.3** and compared with literature data [95]. A good agreement with literature [105] was achieved. The mole fraction solubility values determined using this quantitative method are reported in **Table 3.2**.



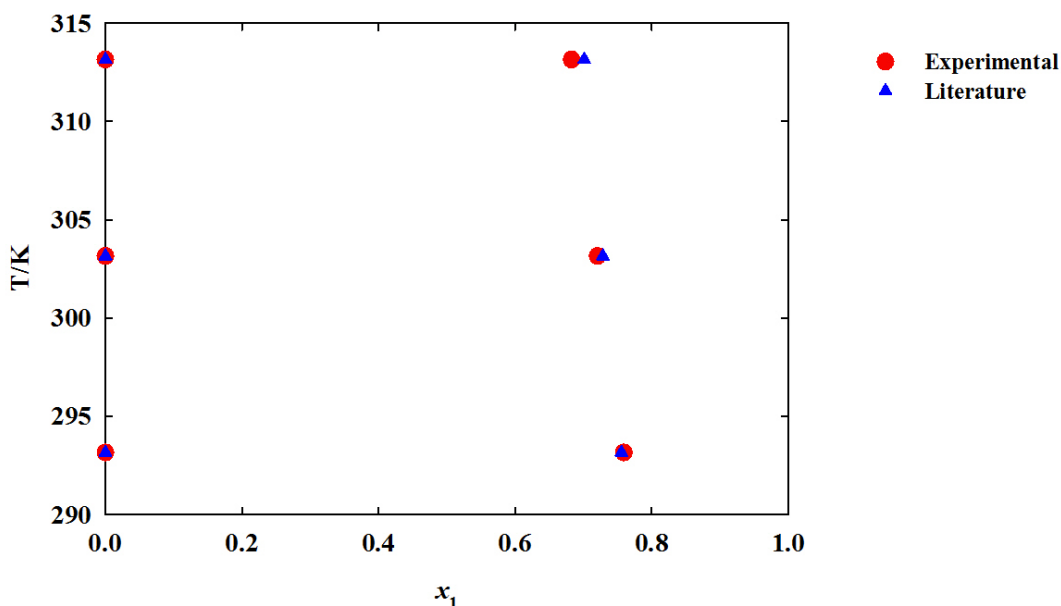


**Figure 3.3** - Liquid-liquid phase diagram for water (2) and [BuMeIm] [NTf<sub>2</sub>] (1) and comparison between values obtained and values from literature [105].

**Table 3.2** - Experimental liquid-liquid equilibria data for binary mixture [BuMeIm] [NTf<sub>2</sub>] + water as function of temperature and comparison with the values from the literature [105].

[BuMeIm] [NTf <sub>2</sub> ] (1) + Water (2)						
T/ K	Experimental	Literature	Error (%)	Experimental	Literature	Error(%)
	$x_1^{IL}$	$x_1^{IL}$		$x_2^{Water}$	$x_2^{Water}$	
293.15	0.7591	0.7557	0.321	0.99973	0.99971	0.002
303.15	0.7207	0.7285	0.764	0.99970	0.99968	0.001
313.15	0.6826	0.7011	1.486	0.99966	0.99961	0.004

IL = Ionic Liquid rich-phase

Water = Water rich-phase

### 3.3 Results and Discussion

In this section, the liquid-liquid phase equilibria will be presented for the following binary mixtures: perfluorodecalin + [NBu<sub>4</sub>][(PFOc)SO<sub>3</sub>], perfluorooctane + [NBu<sub>4</sub>][(PFOc)SO<sub>3</sub>], perfluorodecalin + [NBu<sub>4</sub>][(PFBu)SO<sub>3</sub>], perfluorooctane + [NBu<sub>4</sub>][(PFBu)SO<sub>3</sub>], perfluorodecalin + [HexMeIm][(PFBu)SO<sub>3</sub>], perfluorooctane + [HexMeIm][(PFBu)SO<sub>3</sub>], perfluorodecalin +

[OcMeIm][(PFBu)SO<sub>3</sub>], perfluorooctane + [OcMeIm][(PFBu)SO<sub>3</sub>] and perfluorodecalin + [EtMepy][(PFBu)SO<sub>3</sub>].

### 3.3.1 Liquid-Liquid Equilibria of PFCs and [NBu<sub>4</sub>][(PFOc)SO<sub>3</sub>]

Experimental data measured for perfluorodecalin and perfluorooctane with [NBu<sub>4</sub>][(PFOc)SO<sub>3</sub>] are presented in **Table 3.3**.

**Table 3.3** – Experimental liquid-liquid equilibria data for binary mixture perfluorocarbon with [NBu<sub>4</sub>][(PFOc)SO<sub>3</sub>].

Perfluorodecalin(1) + [NBu <sub>4</sub> ][(PFOc)SO <sub>3</sub> ](2)			Perfluorooctane(1) + [NBu <sub>4</sub> ][(PFOc)SO <sub>3</sub> ](2)		
T/ K	$x_2^{\text{PFC}^a}$	$x_2^{\text{FIL}}$	T/ K	$x_2^{\text{PFC}^a}$	$x_2^{\text{FIL}}$
308.15	–	0.8040	308.15	–	0.7529
313.15	–	0.7820	313.15	–	0.7462
318.15	–	0.7531	318.15	–	0.7344
323.15	–	0.7323	323.15	–	0.7301
328.15	–	0.7138	328.15	–	0.7244
333.15	–	0.6963	333.15	–	0.7181
338.15	–	0.6861	335.67	0.0005	–
343.15	–	0.6804	338.15	–	0.7114
344.90	0.0005	–	343.15	–	0.7100

PFC = Perfluorocarbon rich-phase

FIL = Fluorinated ionic liquid rich-phase

<sup>a</sup> only one value as was explained in the procedure

**Figure 3.4** illustrates the liquid-liquid equilibrium behaviour of binary mixture of the perfluorocarbons studied in this work with [NBu<sub>4</sub>][(PFOc)SO<sub>3</sub>]. The typical liquid-liquid equilibria behaviour of increasing miscibility with the temperature was observed, although the influence of the temperature is small. Another interesting point is that the solubility of the [NBu<sub>4</sub>][(PFOc)SO<sub>3</sub>] in PFC rich-phase is very close to  $x_2 = 0$  (pure perfluorocarbon) in both binary mixtures, while a larger solubility (and similar) of both PFC in [NBu<sub>4</sub>][(PFOc)SO<sub>3</sub>] was found. Nevertheless, perfluorooctane has larger solubility in FIL than perfluorodecalin until  $T = 323.15$  K. Above this temperature, the behaviour is reversed.

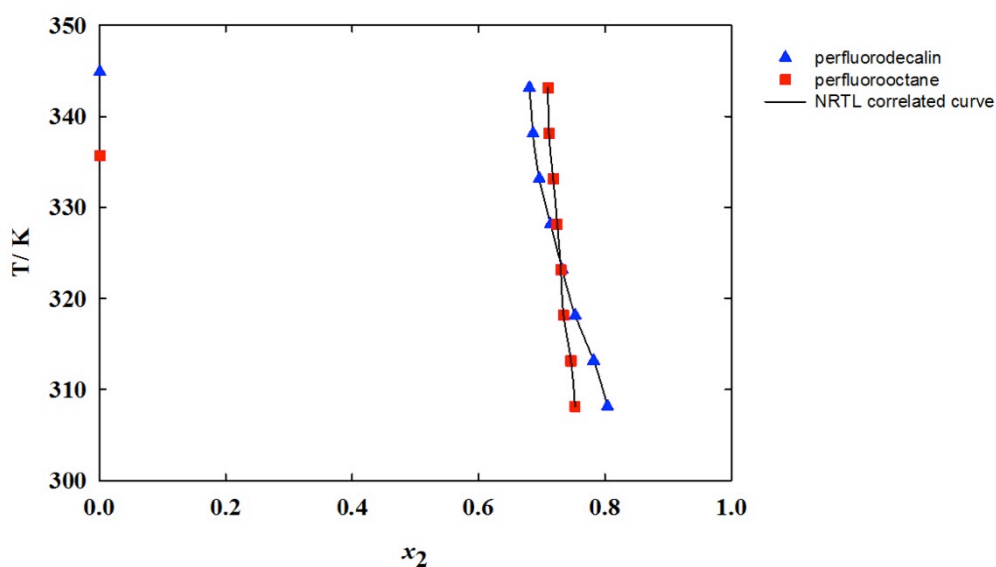


**Figure 3.4** - Liquid-liquid phase diagram for perfluorodecalin +  $[\text{NBu}_4][(\text{PFOc})\text{SO}_3]$  and for perfluorooctane +  $[\text{NBu}_4][(\text{PFOc})\text{SO}_3]$ .

### 3.3.2 Liquid-Liquid Equilibria of PFCs and $[\text{NBu}_4][(\text{PFBu})\text{SO}_3]$

Experimental data measured for perfluorodecalin and perfluorooctane with  $[\text{NBu}_4][(\text{PFBu})\text{SO}_3]$  and perfluorooctane with  $[\text{NBu}_4][(\text{PFBu})\text{SO}_3]$  are presented in **Table 3.4**.

**Table 3.4** – Experimental liquid-liquid equilibria data for binary mixture perfluorocarbon with  $[\text{NBu}_4][(\text{PFBu})\text{SO}_3]$ .

Perfluorodecalin(1) + $[\text{NBu}_4][(\text{PFBu})\text{SO}_3]$ (2)			Perfluorooctane(1) + $[\text{NBu}_4][(\text{PFBu})\text{SO}_3]$ (2)		
T/ K	$x_2^{\text{PFC a}}$	$x_2^{\text{FIL}}$	T/ K	$x_2^{\text{PFC a}}$	$x_2^{\text{FIL}}$
323.15	–	0.9207	325.65	–	0.9291
325.65	–	0.9142	328.15	–	0.9244
328.15	–	0.9120	333.15	–	0.9219
330.65	–	0.9094	336.75	0.0058	
333.15	–	0.9015	338.15	–	0.9138
338.15	–	0.8975	343.15	–	0.9034
343.15	–	0.8902	–	–	–
345.77	0.0003	–	–	–	–

PFC = Perfluorocarbon rich-phase

FIL = Fluorinated ionic liquid rich-phase

<sup>a</sup> only one value as was explained in the procedure

For the binary mixture perfluorooctane +  $[\text{NBu}_4][(\text{PFBu})\text{SO}_3]$ , only data from 333.15 K onwards were measured since  $[\text{NBu}_4][(\text{PFBu})\text{SO}_3]$  has a melting point of 327.13 K, according to **Table 2.2**. Also, the upper limit of the working temperature is determined by the high vapor pressure of perfluorocarbon.

**Figure 3.5** shows the phase behaviour in the binary mixtures perfluorocarbons with  $[\text{NBu}_4][(\text{PFBu})\text{SO}_3]$ . Again, the solubility of the fluorinated ionic liquid in PFC rich-phase is very close to  $x_2 = 0$ . In the FIL rich-phase, the behaviour of the solubilities are similar for both PFCs, for all the temperatures.

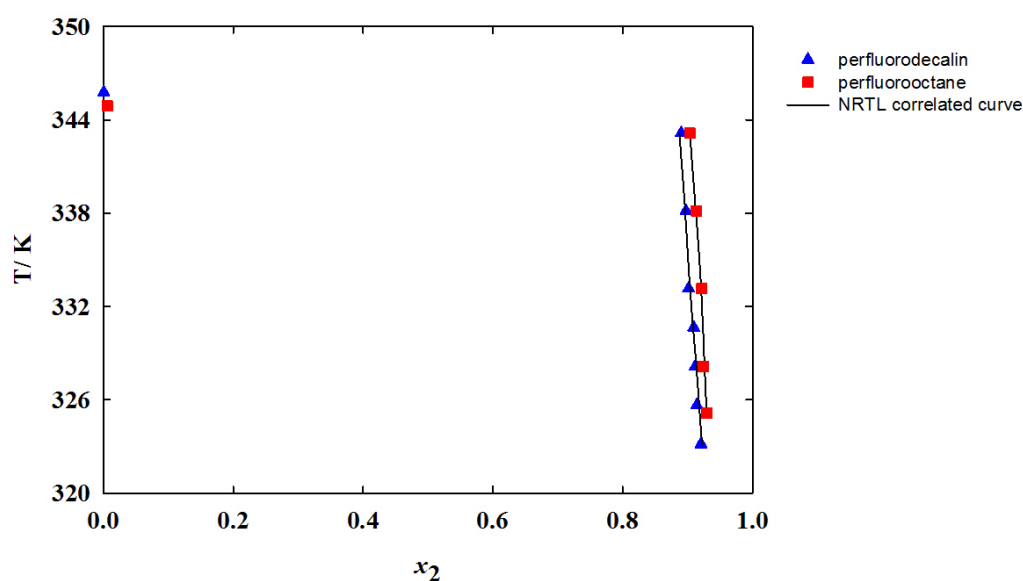


**Figure 3.5** - Liquid-liquid phase diagram for perfluorodecalin +  $[\text{NBu}_4][(\text{PFBu})\text{SO}_3]$  and for perfluorooctane +  $[\text{NBu}_4][(\text{PFBu})\text{SO}_3]$ .

### 3.3.3 Liquid-Liquid Equilibria diagram of PFCs and $[\text{HexMeIm}][(\text{PFBu})\text{SO}_3]$

Experimental data measured for perfluorodecalin and perfluorooctane with  $[\text{HexMeIm}][(\text{PFBu})\text{SO}_3]$  are presented in **Table 3.5**.

**Table 3.5** – Experimental liquid-liquid equilibria data for binary mixture perfluorocarbon with [HexMeIm][(PFBu)SO<sub>3</sub>].

Perfluorodecalin(1) + [HexMeIm][(PFBu)SO <sub>3</sub> ](2)			Perfluorooctane(1) + [HexMeIm][(PFBu)SO <sub>3</sub> ](2)		
T/ K	$x_2^{\text{PFC a}}$	$x_2^{\text{FIL}}$	T/ K	$x_2^{\text{PFC a}}$	$x_2^{\text{FIL}}$
298.15	–	0.9539	298.15	–	0.9510
303.15	–	0.9538	303.15	–	0.9485
308.15	–	0.9530	308.15	–	0.9465
313.15	–	0.9485	313.15	–	0.9460
318.15	–	0.9495	318.15	–	0.9451
323.15	–	0.9473	323.15	–	0.9416
328.15	–	0.9449	328.15	–	0.9407
333.15	–	0.9421	333.15	–	0.9408
338.15	–	0.9375	338.15	–	0.9376
341.87	0.0008	–	343.15	–	0.9361
343.15	–	0.9360	344.90	0.0008	–

PFC = Perfluorocarbon rich-phase

FIL = Fluorinated ionic liquid rich-phase

<sup>a</sup> only one value as was explained in the procedure

Experimental phase diagrams of LLE for the binary mixtures of both perfluorocarbons with [HexMeIm][(PFBu)SO<sub>3</sub>] are shown in **Figure 3.6**. The behaviour of the solubilities is extraordinarily similar for both PFCs at all temperatures. Again, the solubility of PFC in [HexMeIm][(PFBu)SO<sub>3</sub>] is several orders of magnitude higher than the solubility of [HexMeIm][(PFBu)SO<sub>3</sub>] in PFC.

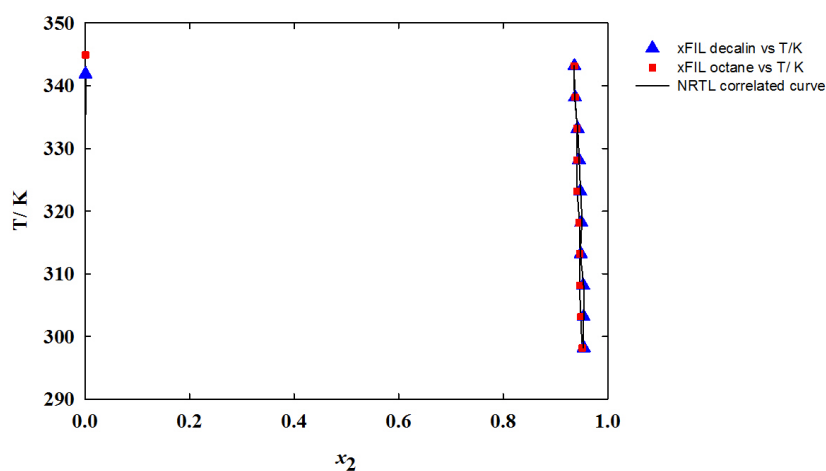


**Figure 3.6** - Liquid-liquid phase diagram for perfluorodecalin + [HexMeIm][(PFBu)SO<sub>3</sub>] and for perfluorooctane + [HexMeIm][(PFBu)SO<sub>3</sub>].

### 3.3.4 Liquid-Liquid Equilibria of PFCs and [OcMeIm][(PFBu)SO<sub>3</sub>]

Experimental data measured for perfluorodecalin and perfluorooctane with [OcMeIm][(PFBu)SO<sub>3</sub>] are presented in **Table 3.6**.

**Table 3.6** – Experimental liquid-liquid equilibria data for binary mixture perfluorocarbon with [OcMeIm][(PFBu)SO<sub>3</sub>].

Perfluorodecalin(1) + [OcMeIm][(PFBu)SO <sub>3</sub> ] (2)			Perfluorooctane(1) + [OcMeIm][(PFBu)SO <sub>3</sub> ] (2)		
T/ K	$x_2^{\text{PFC a}}$	$x_2^{\text{FIL}}$	T/ K	$x_2^{\text{PFC a}}$	$x_2^{\text{FIL}}$
298.15	–	0.9361	298.15	–	0.9085
303.15	–	0.9359	303.15	–	0.9053
308.15	–	0.9343	308.15	–	0.8985
313.15	–	0.9339	313.15	–	0.8962
318.15	–	0.9334	318.15	–	0.8910
323.15	–	0.9315	323.15	–	0.8886
328.15	–	0.9312	328.15	–	0.8863
329.02	0.0012	–	333.15	–	0.8858
333.15	–	0.9304	338.15	–	0.8779
338.15	–	0.9248	343.15	–	0.8745
343.15	–	0.9194	344.90	0.0008	–

PFC = Perfluorocarbon rich-phase

FIL = Fluorinated ionic liquid rich-phase

<sup>a</sup> only one value as was explained in the procedure

Experimental liquid-liquid equilibria data for binary mixtures perfluorocarbon with [OcMeIm][(PFBu)SO<sub>3</sub>] are showed in **Figure 3.7**. Again, the solubility of the [OcMeIm][(PFBu)SO<sub>3</sub>] in PFC rich-phase is very close to pure perfluorocarbon. In the FIL rich-phase, the solubility for perfluorooctane in fluorinated ionic liquid is higher than for perfluorodecalin.

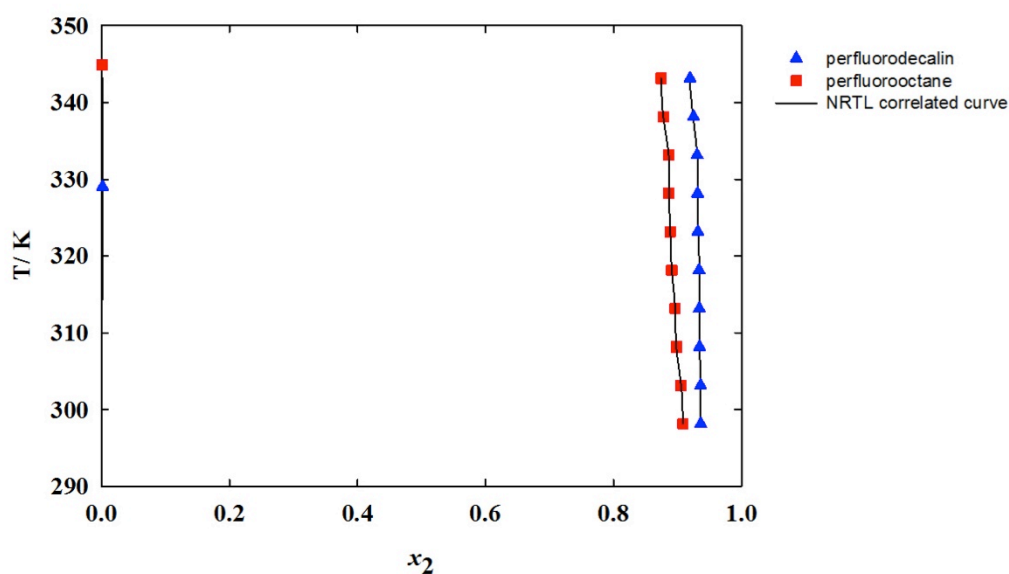


**Figure 3.7** - Liquid-liquid phase diagram for perfluorodecalin + [OcMeIm][(PFBu)SO<sub>3</sub>] and for perfluorooctane + [OcMeIm][(PFBu)SO<sub>3</sub>].

### 3.3.5 The Liquid-Liquid phase diagram of PFCs and [EtMepy][(PFBu)SO<sub>3</sub>]

The experimental data measured for [EtMepy][(PFBu)SO<sub>3</sub>] with perfluorodecalin are presented in **Table 3.7**. The equilibrium liquid-liquid for perfluorooctane with [EtMepy][(PFBu)SO<sub>3</sub>] is not presented here because no reliable data could be obtained for this systems, since 72 h were not enough for the equilibrium to be achieved.

**Table 3.7** – Experimental liquid-liquid equilibria data for binary mixture perfluorocarbon with [EtMepy][(PFBu)SO<sub>3</sub>].

Perfluorodecalin (1) + [EtMepy][(PFBu)SO <sub>3</sub> ] (2)		
T/ K	$x_2^{\text{PFC a}}$	$x_2^{\text{FIL}}$
293.15	–	0.9667
298.15	–	0.9638
303.15	–	0.9638
308.15	–	0.9622
313.15	–	0.9613
318.15	–	0.9609
323.15	–	0.9599
328.15	–	0.9591

332.69	0.0022	–
333.15	–	0.9584
338.15	–	0.9592
343.15	–	0.9584

PFC = Perfluorocarbon rich-phase

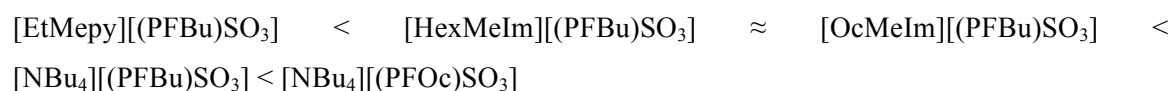
FIL = Fluorinated ionic liquid rich-phase

<sup>a</sup> only one value as was explained in the procedure

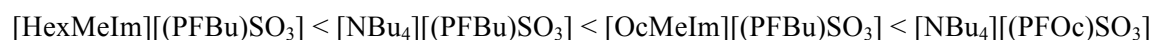
### 3.3.6 Comparisons of the Liquid-Liquid Phase Diagrams of Perfluorocarbons and FILs

All the liquid-liquid phase equilibria experimental data measured for perfluorodecalin and perfluorooctane with FILs are summarized and compared in **Figure 3.8**.

Comparing the experimental LLE data for the binary mixtures perfluorodecalin with fluorinated ionic liquids, it can be observed that the solubility of perfluorodecalin in FIL increases accordingly to the sequence:



The same comparison was carried out for the binary mixtures with perfluorooctane and the solubility of perfluorooctane in FIL increases accordingly to the sequence:



Taking into account the results obtained it can be concluded that:

In the case of perfluorodecalin: PFCs solubility increases from pyrrolidinium to imidazolium to the tetralkylammonium for FILs with the same anion,  $[(\text{PFBu})\text{SO}_3]^-$ ; and the increment of the alkyl chain length in the cation has no effect on the solubility.

In the case of perfluorooctane: the alkyl chain length of the cation influences its solubility in FILs.

For both PFCs was observed that for the same cation,  $[\text{NBu}_4]^+$ , an increase in the fluorinated chain of the anion, increases the PFC solubility.



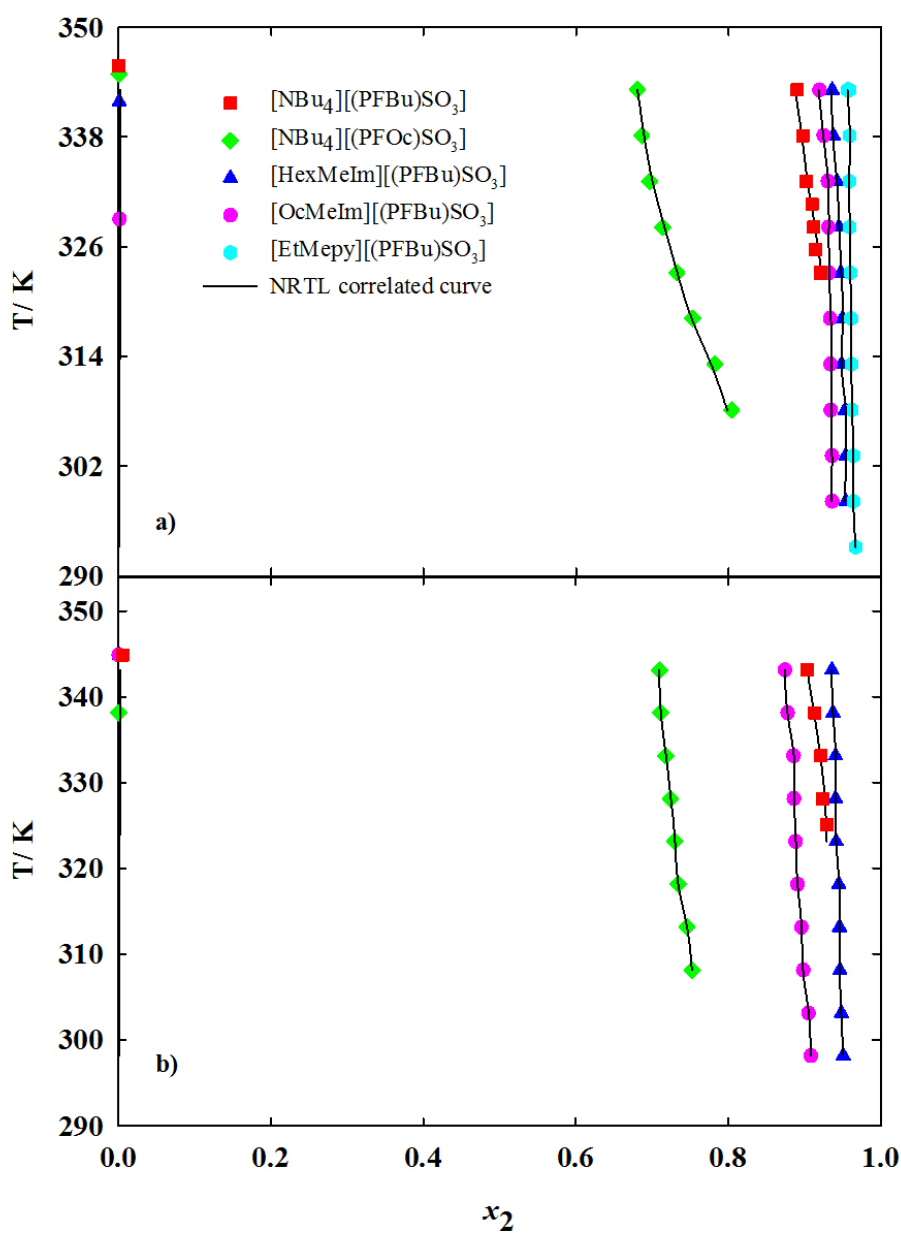


**Figure 3.8** - The liquid-liquid phase diagram of: a) perfluorodecalin and fluorinated ionic liquids and b) perfluorooctane and fluorinated ionic liquids.

### 3.3.7 Correlation of LLE

In this work, the NRTL (Non Random Two Liquid) equation [106] with temperature dependent interaction parameters was used to correlate the experimental binary LLE data. In general terms, the excess Gibbs energy for the binary mixtures of the correlative equation is expressed by the following equations:

$$\frac{\Delta G^E}{RT} = x_1 x_2 \left( \frac{\tau_{21} G_{21}}{x_1 + x_2 G_{21}} + \frac{\tau_{12} G_{12}}{x_2 + x_1 G_{12}} \right) \quad (3.3)$$

$$G_{12} = \exp(-\alpha_{12} \tau_{21}), \text{ where } \alpha_{12} = \alpha_{21} = \alpha \quad (3.4)$$

$$\tau_{12} = \frac{\Delta g_{12}}{RT} \text{ and } \tau_{21} = \frac{\Delta g_{21}}{RT} \quad (3.5)$$

$$\Delta g_{12} = a_{12} + b_{12} \cdot T \text{ and } \Delta g_{21} = a_{21} + b_{21} \cdot T \quad (3.6)$$

where  $x$  is the mole fraction,  $T$  is the temperature,  $\alpha$  is the non randomness parameter, and  $\tau_{12}$  and  $\tau_{21}$  are the interaction parameters. In this work, all parameters were optimized. The SOLVER function in Microsoft Excel was used to adjust these five parameters so that the objective function was minimized, providing the set of temperature-dependent adjustable parameters for the binary systems. The objective function is defined as follows:

$$\text{Objective function} = \sum_{i=1}^2 (x_i^{l,\text{exp}} - x_i^{l,\text{calc}})^2 \quad (3.7)$$

The calculated values of the equations are presented in **Table 3.8**. The standard deviation of the mole fraction and the temperature dependence of the correlative parameters are also listed in **Table 3.8**.

These deviations were calculated by applying the following expression for the binary mixtures:

$$\sigma = \left( \sum_{i=1}^2 \left( \frac{x_i^{l,\text{exp}} - x_i^{l,\text{calc}}}{x_i^{l,\text{exp}}} \right)^2 \right)^{0.5} \quad (3.8)$$

where  $x$  is the mole fraction and the subscripts  $i$  and  $l$  provide a designation for the component and the phase, respectively.

The fitting curves are shown in **Figures 3.5-3.11**. These figures show that the NRTL equation satisfactorily correlates LLE of the investigated binary mixtures.

**Table 3.8** – Parameters of the NRTL equations for the binary mixture.

PFC	$a_{12}$ (J mol <sup>-1</sup> )	$a_{21}$ (J mol <sup>-1</sup> )	$b_{12}$ (J mol <sup>-1</sup> K <sup>-1</sup> )	$b_{21}$ (J mol <sup>-1</sup> K <sup>-1</sup> )	$\alpha$	$\sigma$
<b>[NBu<sub>4</sub>][(PFOc)SO<sub>3</sub>]</b>						
Perfluorodecalin	24989.78	20999.93	1.57	- 43.93	0.30	2.64
Perfluorooctane	24989.78	20999.93	1.77	-44.75	0.30	2.65
<b>[NBu<sub>4</sub>][(PFBu)SO<sub>3</sub>]</b>						
Perfluorodecalin	24989.78	20999.88	-0.39	-50.05	0.22	1.75
Perfluorooctane	24989.78	20999.88	-0.39	-50.05	0.21	1.97
<b>[HexMeIm][(PFBu)SO<sub>3</sub>]</b>						
Perfluorodecalin	24989.82	20999.84	-22.77	-28.01	0.40	0.69
Perfluorooctane	24989.82	20999.83	-22.32	-29.48	0.40	0.47
<b>[OcMeIm][(PFBu)SO<sub>3</sub>]</b>						
Perfluorodecalin	24989.81	20999.83	-26.30	-33.32	0.39	2.58
Perfluorooctane	24989.81	20999.82	-25.06	-37.04	0.38	1.21
<b>[EtMepy][(PFBu)SO<sub>3</sub>]</b>						
Perfluorodecalin	24989.80	20999.85	-27.96	-27.10	0.42	0.20

### 3.3.8 Thermodynamic Functions

The change of the standard Gibbs energy is defined by:

$$\Delta G = \Delta H - T\Delta S \quad (3.9)$$

Where  $G$  represents the Gibbs energy,  $H$  the enthalpy and  $S$  the entropy.

The dissolution of liquid into another liquid is governed by thermodynamic energies involved, namely, standard molar Gibbs energy ( $\Delta_{\text{sol}}G_m^0$ ), standard molar enthalpy ( $\Delta_{\text{sol}}H_m^0$ ) and standard molar entropy ( $\Delta_{\text{sol}}S_m^0$ ) of solution. The thermodynamic functions describe the solvation process that is the process of attraction and association of molecules of a solvent with molecules of a solute. These thermodynamic functions can be obtained directly or from the temperature dependence of the experimental solute solubility values [107, 108]. These parameters picture the transference of one molecule of solute to a hypothetical dilute ideal solution where the mole fraction of the solvent is equal to one, and can be calculated according to the following equations:

$$\frac{\Delta_{\text{sol}}H_m^0(T)}{RT^2} = \left( \frac{\partial \ln(x_i)}{\partial T} \right)_p \quad (3.10)$$

$$\Delta_{\text{sol}}G_m^0(T) = \ln(x_i)_p \quad (3.11)$$

$$\Delta_{\text{sol}}S_m^0(T) = R \left( \frac{\partial \ln(x_i)}{\partial T} \cdot T + \ln x_i \right)_p \quad (3.12)$$

where  $x_i$  is the mole fraction solubility of the solute  $i$ ,  $R$  is the ideal gas constant, and  $T$  is the temperature at a constant pressure,  $p$ .

The conventional standard molar enthalpy, Gibbs energy and entropy of solution were determined for several temperatures, and are represented in **Table 3.9**. The values at 298.15 K were obtained using NRTL equation for the binary systems where the liquid-liquid equilibrium data has not been experimentally measured.

The molar enthalpies of solution of the studied PFCs in FILs, between 298.15 and 343.15 K, show that the solubilisation of the PFCs in FILs based on the ammonium cation,  $[\text{NBu}_4][(\text{PFOc})\text{SO}_3]$  and in  $[\text{NBu}_4][(\text{PFBu})\text{SO}_3]$ , is an endothermic process. However, in the case of  $[\text{HexMeIm}][(\text{PFBu})\text{SO}_3]$ ,  $[\text{OcMeIm}][(\text{PFBu})\text{SO}_3]$  and  $[\text{EtMepy}][(\text{PFBu})\text{SO}_3]$  the processes of solubilisation are exothermic. A decrease in the standard molar enthalpy of solution indicates that less energy is necessary to promote the dissolution of PFC in fluorinated ionic liquids. Through comparison between  $[\text{HexMeIm}][(\text{PFBu})\text{SO}_3]$  and  $[\text{OcMeIm}][(\text{PFBu})\text{SO}_3]$  is possible to see that the alkyl chain in imidazolium cation slightly influences the results. A negative enthalpy of solution means that the solute is less soluble at high temperatures.

**Table 3.9** – Thermodynamic conventional properties of solution of PFCs in FILs studied.

$T/ \text{K}$	$\Delta_{\text{sol}}G_m^0(T)$ ( $\text{kJ mol}^{-1}$ )	$\Delta_{\text{sol}}H_m^0(T)$ ( $\text{kJ mol}^{-1}$ )	$\Delta_{\text{sol}}S_m^0(T)$ ( $\text{J K}^{-1} \text{mol}^{-1}$ )	$T\Delta_{\text{sol}}S_m^0(T)$ ( $\text{kJ mol}^{-1}$ )
<b>Perfluorodecalin + [NBu<sub>4</sub>][(PFOc)SO<sub>3</sub>]</b>				
298.15	4.25	10.26	20.16	6.01
308.15	4.17	10.96	22.01	6.78
313.15	3.97	11.32	23.47	7.35
318.15	3.70	11.68	25.08	7.98
323.15	3.54	12.05	26.33	8.51
328.15	3.41	12.43	27.46	9.01
333.15	3.30	12.81	28.53	9.51
338.15	3.26	13.19	29.39	9.94
343.15	3.25	13.59	30.11	10.33
<b>Perfluorooctane + [NBu<sub>4</sub>][(PFOc)SO<sub>3</sub>]</b>				
298.15	3.70	3.93	0.78	6.56
308.15	3.58	4.20	2.02	7.38
313.15	3.57	4.34	2.46	7.75
318.15	3.51	4.48	3.06	8.17
323.15	3.52	4.62	3.41	8.53
328.15	3.52	4.77	3.81	8.91
333.15	3.51	4.91	4.22	9.30
338.15	3.49	5.06	4.63	9.70
343.15	3.53	5.21	4.89	10.06
<b>Perfluorodecalin + [NBu<sub>4</sub>][(PFBu)SO<sub>3</sub>]</b>				
298.15	8.27	16.34	27.07	8.25
323.15	6.81	18.93	37.49	12.12
325.65	6.86	19.22	37.95	12.36
328.15	6.63	19.52	39.26	12.88
330.65	6.60	19.81	39.96	13.21
333.15	6.42	20.12	41.11	13.70
338.15	6.40	20.72	42.35	14.32
343.15	6.30	21.34	43.83	15.04
<b>Perfluorooctane + [NBu<sub>4</sub>][(PFBu)SO<sub>3</sub>]</b>				
298.15	7.86	16.11	27.67	8.07

$T/ \text{K}$	$\Delta_{\text{sol}}G_m^0(T)$ ( $\text{kJ mol}^{-1}$ )	$\Delta_{\text{sol}}H_m^0(T)$ ( $\text{kJ mol}^{-1}$ )	$\Delta_{\text{sol}}S_m^0(T)$ ( $\text{J K}^{-1} \text{mol}^{-1}$ )	$T\Delta_{\text{sol}}S_m^0(T)$ ( $\text{kJ mol}^{-1}$ )
325.65	7.17	19.49	37.85	12.33
328.15	7.04	19.79	38.84	12.75
333.15	7.06	20.40	40.03	13.34
338.15	6.89	21.02	41.77	14.12
343.15	6.67	21.64	43.64	14.97
<b>Perfluorodecalin + [HexMeIm][(PFBu)SO<sub>3</sub>]</b>				
298.15	0.12	-0.39	-1.72	-0.51
303.15	0.12	-0.41	-1.74	-0.53
308.15	0.12	-0.42	-1.77	-0.55
313.15	0.14	-0.43	-1.80	-0.56
318.15	0.14	-0.45	-1.84	-0.59
323.15	0.15	-0.46	-1.88	-0.61
328.15	0.15	-0.48	-1.93	-0.63
333.15	0.17	-0.49	-1.97	-0.65
338.15	0.18	-0.51	-2.04	-0.68
343.15	0.19	-0.52	-2.07	-0.70
298.15	0.12	-0.39	-1.72	-0.51
303.15	0.12	-0.41	-1.74	-0.53
<b>Perfluorooctane + [HexMeIm][(PFBu)SO<sub>3</sub>]</b>				
298.15	0.12	-0.39	-1.71	-0.51
303.15	0.13	-0.40	-1.76	-0.53
308.15	0.14	-0.41	-1.79	-0.55
313.15	0.14	-0.43	-1.82	-0.57
318.15	0.15	-0.44	-1.85	-0.59
323.15	0.16	-0.45	-1.90	-0.62
328.15	0.17	-0.47	-1.93	-0.63
333.15	0.17	-0.48	-1.95	-0.65
338.15	0.18	-0.50	-2.00	-0.68
343.15	0.19	-0.51	-2.04	-0.70
<b>Perfluorodecalin + [OcMeIm][(PFBu)SO<sub>3</sub>]</b>				
298.15	0.16	-0.25	-1.38	-0.87
303.15	0.17	-0.26	-1.40	-0.90
308.15	0.17	-0.27	-1.43	-0.95

$T/ \text{K}$	$\Delta_{\text{sol}}G_m^0(T)$ ( $\text{kJ mol}^{-1}$ )	$\Delta_{\text{sol}}H_m^0(T)$ ( $\text{kJ mol}^{-1}$ )	$\Delta_{\text{sol}}S_m^0(T)$ ( $\text{J K}^{-1} \text{mol}^{-1}$ )	$T\Delta_{\text{sol}}S_m^0(T)$ ( $\text{kJ mol}^{-1}$ )
313.15	0.18	-0.27	-1.45	-0.98
318.15	0.18	-0.28	-1.46	-1.02
323.15	0.19	-0.29	-1.49	-1.06
328.15	0.19	-0.30	-1.51	-1.09
333.15	0.20	-0.31	-1.53	-1.12
338.15	0.22	-0.32	-1.60	-1.18
343.15	0.24	-0.33	-1.66	-1.22
298.15	0.16	-0.25	-1.38	-0.87
303.15	0.17	-0.26	-1.40	-0.90
<b>Perfluorooctane + [OcMeIm][(PFBu)SO<sub>3</sub>]</b>				
298.15	0.24	-0.63	-2.92	-0.87
303.15	0.25	-0.65	-2.98	-0.90
308.15	0.27	-0.67	-3.08	-0.95
313.15	0.29	-0.70	-3.14	-0.98
318.15	0.31	-0.72	-3.22	-1.02
323.15	0.32	-0.74	-3.28	-1.06
328.15	0.33	-0.77	-3.34	-1.09
333.15	0.34	-0.79	-3.38	-1.12
338.15	0.37	-0.81	-3.49	-1.18
343.15	0.38	-0.84	-3.55	-1.22
<b>Perfluorodecalin + [EtMepy][(PFBu)SO<sub>3</sub>]</b>				
293.15	0.08	-0.13	-0.74	-0.22
298.15	0.09	-0.14	-0.77	-0.23
303.15	0.09	-0.14	-0.78	-0.24
308.15	0.10	-0.15	-0.80	-0.25
313.15	0.10	-0.15	-0.81	-0.25
318.15	0.11	-0.16	-0.82	-0.26
323.15	0.11	-0.16	-0.84	-0.27
328.15	0.11	-0.17	-0.86	-0.28
333.15	0.12	-0.17	-0.87	-0.29
338.15	0.12	-0.18	-0.87	-0.29
343.15	0.12	-0.18	-0.88	-0.30

Furthermore, the standard molar enthalpy of solution,  $\Delta_{\text{sol}}H_m^0(T)$ , can be split into two contributions: the standard molar enthalpy of vaporization of the solute,  $\Delta_1^g H_m^0$ , and the standard molar enthalpy of solvation,  $\Delta_{\text{svt}}H_m^0(T)$  [107] as follows:

$$\Delta_{\text{sol}}H_m^0(T) = \Delta_{\text{svt}}H_m^0(T) + \Delta_1^g H_m^0 \quad (3.13)$$

According to the scale particle theory, solvation processes can be envisaged as taking place in two steps at the molecular level: 1. an adequate cavity is opened in the solvent; 2. the single solute molecule is then inserted and establishes specific interactions. The enthalpy of solvation can help explain why solvation occurs, and besides an amount related to the formation of the cavity, is determined by solute–solvent interactions only, whereas the enthalpy of solution is determined by the balance of solute–solvent and solute–solvent interactions [109].

The standard molar Gibbs free of solvation,  $\Delta_{\text{svt}}G_m^0(T)$ , can be derived for a temperature  $T$  using the hypothetical reference state in the gas phase and at the pressure  $p^0 = 10^5$  Pa.

$$\Delta_{\text{svt}}G_m^0(T) = \Delta_{\text{sol}}G_m^0(T) + RT \ln \left( \frac{p(s2,T)}{p^0} \right) \quad (3.14)$$

$$\Delta_{\text{svt}}S_m^0(T) = \frac{\Delta_{\text{svt}}H_m^0(T) - \Delta_{\text{svt}}G_m^0(T)}{T} \quad (3.15)$$

where  $p(s2,T)$  is the vapor pressure of the solute at 298.15 K and has a value of 833.26 Pa for perfluorodecalin and 5172.89 Pa for perfluorooctane [110, 111]. The standard molar enthalpy of vaporization ( $\Delta_1^g H_m^0$ ) for perfluorodecalin is 45.4 kJmol<sup>-1</sup> and for perfluorooctane is 41.13 kJmol<sup>-1</sup>, both at 298.15 K [112, 113].

The conventional standard molar enthalpy, Gibbs energy and entropy of solvation were determined for several temperatures, and are represented in **Table 3.10**. These low molar enthalpies of solution and solvation indicate that the enthalpic energetic balance involved in the dissolution and solvation, respectively, of PFC in FIL is favourable.



**Table 3.10** – Thermodynamic conventional properties of solvation of PFCs in FILs studied at 298.15 K.

PFC	$\Delta_{\text{svt}}G_m^0(T)$ (kJ mol <sup>-1</sup> )	$\Delta_{\text{svt}}H_m^0(T)$ (kJ mol <sup>-1</sup> )	$\Delta_{\text{svt}}S_m^0(T)$ (J K <sup>-1</sup> mol <sup>-1</sup> )	$T\Delta_{\text{svt}}S_m^0(T)$ (kJ mol <sup>-1</sup> )
<b>[NBu<sub>4</sub>][(PFOc)SO<sub>3</sub>]</b>				
Perfluorodecalin	-7.62	-35.14	-92.31	-27.52
Perfluorooctane	-3.64	-37.23	-112.64	-26.97
<b>[NBu<sub>4</sub>][(PFBu)SO<sub>3</sub>]</b>				
Perfluorodecalin	0.92	-24.82	-86.35	-25.28
Perfluorooctane	-4.01	-29.29	-84.80	-25.75
<b>[HexMeIm][(PFBu)SO<sub>3</sub>]</b>				
Perfluorodecalin	-11.75	-45.79	-114.18	-34.33
Perfluorooctane	-7.22	-41.55	-115.14	-34.33
<b>[OcMeIm][(PFBu)SO<sub>3</sub>]</b>				
Perfluorodecalin	-11.70	-45.65	-113.85	-34.69
Perfluorooctane	-7.10	-41.79	-116.34	-34.69
<b>[EtMepy][(PFBu)SO<sub>3</sub>]</b>				
Perfluorodecalin	-11.78	-45.54	-113.23	-33.76

The thermodynamics functions shown above deal with solvation at a macroscopic level while the solvation is a molecular process. Another approach to define a standard state could be based on statistical mechanical methods as proposed by Ben-Naim [107]. The changes that occur in the solute neighbourhood during the dissolution process at a constant temperature,  $T$ , and constant pressure,  $p$ , with the composition of the system unchanged are represented by the local standard Gibbs energy,  $\Delta_{\text{svt}}G_m^*(T)$ , the molar local standard enthalpy,  $\Delta_{\text{svt}}H_m^*(T)$ , and the molar local standard entropy,  $\Delta_{\text{svt}}S_m^*(T)$ , of solvation [107, 114]. These standard thermodynamic functions can be related to the conventional thermodynamic functions described in equations 3.13 to 3.15, using the following equations:

$$\Delta_{\text{svt}}G_m^*(T) = \Delta_{\text{svt}}G_m^0(T) - RT \ln \left( \frac{RT}{p^0 V_{j,m}} \right) \quad (3.16)$$

$$\Delta_{\text{svt}}H_m^*(T) = \Delta_{\text{svt}}H_m^0(T) - RT(T\alpha_j - 1) \quad (3.17)$$

$$\Delta_{\text{svt}}S_m^*(T) = \Delta_{\text{svt}}S_m^0(T) + R \ln \left( \frac{RT}{p^0 V_{j,m}} \right) - RT(T\alpha_j - 1) \quad (3.18)$$

where  $V_{j,m}$  is the molar volume of the solvent  $j$  and  $\alpha_j$  is the isobaric thermal expansibility of the solvent, derived from experimental density data. This coefficient is directly related to the temperature derivative of the density by way of the equation:

$$\alpha_j = - \left( \frac{\partial \ln(\rho)}{\partial T} \right)_p \quad (3.19)$$

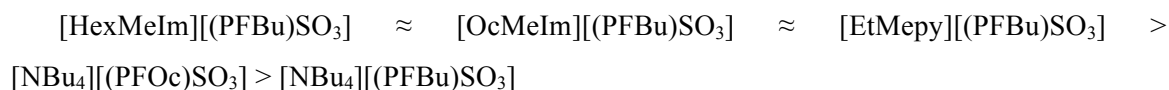
The Ben-Naim local standard Gibbs energy, enthalpy and entropy changes along with the molar volume and the thermal expansion coefficient of the liquids at 298.15 K are reported in **Table 3.11**. The values of molar volume are reported in **Table 2.5** and the thermal expansion coefficients were calculated from equation 2.1.

**Table 3.11** – Thermodynamic local standard properties of the solvation of PFCs in the FILs studied at 298.15 K.

PFC	$\frac{\alpha_j \text{ K}^{-1}}{V_m/\text{cm}^3 \cdot \text{mol}^{-1}}$	$\Delta_{\text{svt}}G_m^*$ (kJ mol <sup>-1</sup> )	$\Delta_{\text{svt}}H_m^*$ (kJ mol <sup>-1</sup> )	$\Delta_{\text{svt}}S_m^*$ (J K <sup>-1</sup> mol <sup>-1</sup> )	$T\Delta_{\text{svt}}S_m^*$ (kJ mol <sup>-1</sup> )
<b>[NBu<sub>4</sub>][(PFOc)SO<sub>3</sub>]</b>					
Perfluorodecalin	$7.547 \cdot 10^{-4}$	-17.00	-33.22	-54.39	-16.22
Perfluorooctane	562.93	-13.02	-35.30	-74.73	-15.67
<b>[NBu<sub>4</sub>][(PFBu)SO<sub>3</sub>]</b>					
Perfluorodecalin	$6.482 \cdot 10^{-4}$	-9.08	-22.82	-46.11	-13.28
Perfluorooctane	439.01	-14.01	-27.29	-44.55	-13.75
<b>[HexMeIm][(PFBu)SO<sub>3</sub>]</b>					
Perfluorodecalin	$6.840 \cdot 10^{-4}$	-22.42	-43.82	-71.78	-21.69
Perfluorooctane	335.06	-17.89	-39.57	-72.74	-21.69
<b>[OcMeIm][(PFBu)SO<sub>3</sub>]</b>					
Perfluorodecalin	$6.802 \cdot 10^{-4}$	-22.13	-43.67	-72.25	-22.28
Perfluorooctane	369.49	-17.53	-39.82	-74.74	-22.68
<b>[EtMepy][(PFBu)SO<sub>3</sub>]</b>					
Perfluorodecalin	$6.648 \cdot 10^{-4}$	-22.91	-43.55	-69.23	-20.64
	278.08				

The values reported show that under the Ben-Naim local standard conditions, the Gibbs free energy of solvation is always negative, thus the solvation process is spontaneous.

The Ben-Naim standard enthalpies of solvation show that the solvation is favourable because the contribution is mainly enthalpic, although there entropic contribution is still non negligible. From these values it can be concluded that the interactions between PFC and FILs exist and that they are the main contributors to the spontaneous solvation of these molecules. The following order was observed for the local standard molar enthalpies of solvation:



Based on the experimental standard molar or on the local standard enthalpies of solvation, it can be observed that the ammonium fluorinated ionic liquids lead to strong enthalpic interactions with the PFCs, while the imidazoliums and pyridiniums fluorinated ionic liquids show lower and similar values. The decrease of the molar enthalpy of solvation reflects the favourable solute – solvent interaction.

### **3.4 Conclusions**

The liquid-liquid equilibria for binary mixtures involving fluorinated ionic liquids with two different PFCs, perfluorodecalin and perfluorooctane, were determined experimentally from 293.15 to 343.15 K. The aim of this chapter is to select PFC + FIL binary mixtures with a high solubility so that these fluorinated ionic liquids can replace partially the PFCs used as oxygen therapeutics, thus enhancing the performance of PFCs artificial blood substitutes. The largest solubility of the studied PFCs in the FIL rich-phase was achieved when  $[\text{NBu}_4][(\text{PFOc})\text{SO}_3]$  was used. The solubility values for perfluorodecalin (0.68 in molar fraction) and perfluorooctane (0.71 in molar fraction) obtained, indicate that this fluorinated ionic liquid can be a good election for partially replacing the PFCs used in oxygen therapeutics.

The standard molar enthalpies of solution are temperature dependent and essentially independent of the alkyl chain length of the cation. The molar enthalpies of solution of the studied perfluorocarbons in FILs show that the solubilisation of the PFCs in ammonium fluorinated ionic liquids are endothermic processes and for other FILs the process of solubilisation is exothermic. The Ben-Naim standard enthalpies of solvation show the solvation is favourable because the enthalpic contributions are bigger than the entropic contributions.



## **4. Final Remarks**

---



---

## 4.1 Conclusions

This work is a part of a broader project FCT: PTDC/EQU-FTT/118800/2010 focused on the development of a new and improved generation of artificial blood substitutes containing fluorinated ionic liquids. The overall objective of this thesis was to evaluate the thermophysical properties of some FILs and their liquid-liquid phase equilibria of FILs with PFCs in order to evaluate the feasibility of partially replacing PFCs in the emulsions used as suitable oxygen carriers.

The first part of this thesis includes the study of thermophysical properties of the FILs in order to compare with those of the PFC used as oxygen therapeutics. Mapping the behaviour of thermodynamic and thermophysical properties, it can be concluded that [EtMepy][(PFBu)SO<sub>3</sub>] is a good selection because it has a viscosity and a density similar to that of PFC. However, [EtMepy][(PFBu)SO<sub>3</sub>] presents the lowest value of molar free volume, which might hinder the solubility of respiratory gases.

The second part of this thesis addresses the phase behaviour of the FILs with PFC. The feasibility of using FIL for replacing, totally or in part, the PFC present in the emulsions was evaluated through the study of the liquid-liquid equilibria of binary mixtures of five fluorinated ionic liquids with perfluorodecalin and perfluorooctane. The largest solubility of the studied PFCs in the used FILs was achieved when [NBu<sub>4</sub>][(PFOc)SO<sub>3</sub>] was used. The solubility values for perfluorodecalin and perfluorooctane obtained, indicate that this fluorinated ionic liquid can be a good election for partially replacing the PFCs used in oxygen therapeutics. Based on the analysis of the thermodynamic functions, it can be concluded that the solvation process is spontaneous, since the Gibbs free energy of solvation is always negative.

## 4.2 Future Work

As future work, it would be interesting to continue the study of new families of fluorinated ionic liquids with the aim to fine-tune the properties of fluorinated ionic liquids, which can possibly be used in the PFC-based emulsion.

On the other hand, the next natural step of this work will be the determination of the solubilities of fluorinated ionic liquids in water and the liquid-liquid equilibria of the ternary mixtures FIL + PFC + water. These studies have a particular interest either from the fundamental or from the application point of view, since these data are not available in the literature. Also, since there are no accurate thermodynamic models which can be confidently be used to predict

the properties or/and phase equilibria of fluorinated compounds these data can be a great help in understanding the phase behaviour of these mixtures so that new reliable models can be developed. Then the thermophysical and thermodynamic properties, of the most relevant binary mixtures of FIL + water or FIL + PFC and of the miscible ternary systems containing FIL + PFC + water will be measured in the miscible solubility range.

The final task will be formulation of emulsions and the evaluation of their stability with time and temperature. Besides, the oxygen and carbon dioxide solubility in FILs + water emulsions and FIL + PFC + water emulsions will be measured and compared with those PFC + water emulsions. The use of serum instead of pure water, that is the presence of salts, will also need to be addressed. This information will allow us to conclude about the effect of the addition of FILs in the currently used PFC based emulsions.



## **5. References**

---



1. Lowe, K.C., *Perfluorinated blood substitutes and artificial oxygen carriers*. Blood Reviews, 1999. **13**(3): p. 171-184.
2. Stollings, J.L. and L.J. Oyen, *Oxygen therapeutics: Oxygen delivery without blood*. Pharmacotherapy, 2006. **26**(10): p. 1453-1464.
3. Riess, J.G., *Oxygen carriers ("blood substitutes") - Raison d'Etire, chemistry, and some physiology*. Chemical Reviews, 2001. **101**(9): p. 2797-2919.
4. Chang, T.M.S., *Blood Substitutes: Principles, Methods, Products and Clinical Trials*. Vol. 2. 1998: Karger Landes Systems.
5. Faithfull, N.S., *Oxygen delivery from fluorocarbon emulsions - aspects of convective and diffusive transport.*, in *Blood Substitutes and Oxygen Carriers 1993*, M. Dekker: New York. p. 569-576.
6. Clark, L.C., et al., *Perfluorocarbons having a short dwell time in liver*. Science, 1973. **181**(4100): p. 680-682.
7. Okamoto, H., k. Yamanouchi, and T. Imagawa, *Persistence of fluorocarbons in circulating blood and organs*, in *Proceed 22nd Intercompany Conf1973*: Osaka, Japan.
8. Naito, R. and K. Yokoyoma, *Perfluorochemical blood substitutes. Technical Information Series n°5 and n°7*, in *Green Cross Corp*.1978: Osaka, Japan.
9. Kerins, D.M., *Role of the perfluorocarbon Fluosol - da in coronary angioplasty*. American Journal of the Medical Sciences, 1994. **307**(3): p. 218-221.
10. Lowe, K.C., *Perfluorochemicals in vascular medicine*. Vascular Medicine Review, 1994(5): p. 15-32.
11. Lowe, K.C., *Perfluorochemical respiratory gas carriers: applications in medicine and biotechnology*. Science Prog, 1997(80): p. 169-193.
12. Gervits, L.L., *Perfluorocarbon-based blood substitutes. Russian experience.*, in *Fluorine in Medicine in the 21st Century 1994*, Rapra: Shrewsbury. p. 197-205.
13. Sharma, S.K., K.C. Lowe, and S.S. Davis, *Novel compositions of emulsified perfluorochemicals for biological uses*. Biomaterials Artificial Cells and Artificial Organs, 1988. **16**(1-3): p. 447-450.
14. Smart, B.E., *Fluorine substituent effects (on bioactivity)*. Journal of Fluorine Chemistry, 2001. **109**(1): p. 3-11.
15. Dias, A.M.A., *Thermodynamic Properties of Blood Substitutes*, in *Departamento de Quimica2005*, Universidade de Aveiro.
16. Krafft, M.P., *Fluorocarbons and fluorinated amphiphiles in drug delivery and biomedical research*. Advanced Drug Delivery Reviews, 2001. **47**(2-3): p. 209-228.
17. Miller, J.H., J.M. Googe, and J.C. Hoskins, *Combined macular hole and cataract surgery*. American Journal of Ophthalmology, 1997. **123**(5): p. 705-707.
18. Cohn, S.M., *Blood substitutes in surgery*. Surgery, 2000. **127**(6): p. 599-602.

19. Rowinsky, E.K., *Novel radiation sensitizers targeting tissue hypoxia*. Oncology-New York, 1999. **13**(10): p. 61-70.
20. Porter, T.R., et al., *Non invasive identification of acute myocardial - ischemia and reperfusion with contrast ultrasound using intravenous perfluoropropane-exposed sonicated dextrose albumin* Journal of the American College of Cardiology, 1995. **26**(1): p. 33-40.
21. Leach, C.L., et al., *Partial liquid ventilation with perflubron in premature infants with severe respiratory distress syndrome*. New England Journal of Medicine, 1996. **335**(11): p. 761-767.
22. Eilenberg, S.S., V.M. Tartar, and R.F. Mattrey, *Reducing magnetic-susceptibility differences using liquid fluorocarbon pads (sat pad<sup>TM</sup>) - results with spectral presaturation of fat*. Artificial Cells Blood Substitutes and Immobilization Biotechnology, 1994. **22**(4): p. 1477-1483.
23. Mattrey, R.F., et al., *Perfluorooctylbromide - a liver spleen-specific and tumor-imaging ultrasound contrast material* Radiology, 1982. **145**(3): p. 759-762.
24. Zuck, T.F. and J.G. Riess, *Current status of injectable oxygen carriers*. Critical Reviews in Clinical Laboratory Sciences, 1994. **31**(4): p. 295-324.
25. Raveendran, P. and S.L. Wallen, *Cooperative C-H center dot center dot center dot O hydrogen bonding in CO(2)-Lewis base complexes: Implications for solvation in supercritical CO(2)*. Journal of the American Chemical Society, 2002. **124**(42): p. 12590-12599.
26. Horvath, I.T. and J. Rabai, *Facile catalyst separation without water-fluorous biphasic hydroformylation of olefins*. Science, 1994. **266**(5182): p. 72-75.
27. Wallington, T.J., et al., *The environmental-impact of CFC replacements - HFCS and HCFCS*. Environmental Science & Technology, 1994. **28**(7): p. A320-A326.
28. Elibol, M. and F. Mavituna, *A remedy to oxygen limitation problem in antibiotic production: addition of perfluorocarbon*. Biochemical Engineering Journal, 1999. **3**(1): p. 1-7.
29. Wasanasathian, A. and C.A. Peng, *Enhancement of microalgal growth by using perfluorocarbon as oxygen carrier*. Artificial Cells Blood Substitutes and Immobilization Biotechnology, 2001. **29**(1): p. 47-55.
30. Walden, P., *Molecular weights and electrical conductivity of several fused salts*. Bulletin de l'Académie Impériale des Sciences de St.-Petersbourg, 1914. **8**: p. 405-422.
31. Charles, G., *Cellulose solution*, U. Patent, Editor 1934.
32. Hurley, F.H., *Electrodeposition of Aluminium*, 1948.
33. T. P. Wier, F.H.H., 1948.
34. MacFarlane, D.R. and K.R. Seddon, *Ionic liquids - Progress on the fundamental issues*. Australian Journal of Chemistry, 2007. **60**(1): p. 3-5.

35. Seddon, K.R., *Room-temperature ionic liquids: Neoteric solvents for clean catalysis*. Kinetics and Catalysis, 1996. **37**(5): p. 693-697.
36. Seddon, K.R., *Ionic liquids for clean technology*. Journal of Chemical Technology and Biotechnology, 1997. **68**(4): p. 351-356.
37. Stegemann, H., et al., *Room-temperature molten polyiodides*. Electrochimica Acta, 1992. **37**(3): p. 379-383.
38. Bonhote, P., et al., *Hydrophobic, highly conductive ambient-temperature molten salts*. Inorganic Chemistry, 1996. **35**(5): p. 1168-1178.
39. Elaiwi, A., et al., *Hydrogen-bonding in imidazolium salts and its implications for ambient-temperature halogenoaluminate(III) ionic liquids*. Journal of the Chemical Society-Dalton Transactions, 1995(21): p. 3467-3472.
40. Jungnickel, C., et al., *Micelle formation of imidazolium ionic liquids in aqueous solution*. Colloids and Surfaces a-Physicochemical and Engineering Aspects, 2008. **316**(1-3): p. 278-284.
41. Earle, M.J., et al., *The distillation and volatility of ionic liquids*. Nature, 2006. **439**(7078): p. 831-834.
42. Rogers, R.D. and K.R. Seddon, *Ionic liquids - Solvents of the future?* Science, 2003. **302**(5646): p. 792-793.
43. Ranke, J., et al., *Design of sustainable chemical products - The example of ionic liquids*. Chemical Reviews, 2007. **107**(6): p. 2183-2206.
44. Welton, T., *Room-temperature ionic liquids. Solvents for synthesis and catalysis*. Chemical Reviews, 1999. **99**(8): p. 2071-2083.
45. Huddleston, J.G., et al., *Room temperature ionic liquids as novel media for 'clean' liquid-liquid extraction*. Chemical Communications, 1998(16): p. 1765-1766.
46. Visser, A.E., R.P. Swatloski, and R.D. Rogers, *pH-dependent partitioning in room temperature ionic liquids provides a link to traditional solvent extraction behavior*. Green Chemistry, 2000. **2**(1): p. 1-4.
47. Swatloski, R.P., et al., *Dissolution of cellulose with ionic liquids*. Journal of the American Chemical Society, 2002. **124**(18): p. 4974-4975.
48. Wilkes, J.S., *A short history of ionic liquids - from molten salts to neoteric solvents*. Green Chemistry, 2002. **4**(2): p. 73-80.
49. Forsyth, S.A., J.M. Pringle, and D.R. MacFarlane, *Ionic liquids - An overview*. Australian Journal of Chemistry, 2004. **57**(2): p. 113-119.
50. Anthony, J.L., E.J. Maginn, and J.F. Brennecke, *Solubilities and thermodynamic properties of gases in the ionic liquid 1-n-butyl-3-methylimidazolium hexafluorophosphate*. Journal of Physical Chemistry B, 2002. **106**(29): p. 7315-7320.
51. Tempel, D.J., et al., *Ionic liquids for storage and delivery of hazardous gases*. Abstracts of Papers of the American Chemical Society, 2006. **231**.

52. Almantariotis, D., et al., *Effect of Fluorination and Size of the Alkyl Side-Chain on the Solubility of Carbon Dioxide in 1-Alkyl-3-methylimidazolium Bis(trifluoromethylsulfonyl)amide Ionic Liquids*. Journal of Physical Chemistry B, 2010. **114**(10): p. 3608-3617.
53. Arvai, R., et al., *New aryl-containing fluorinated sulfonic acids and their ammonium salts, useful as electrolytes for fuel cells or ionic liquids*. Journal of Fluorine Chemistry, 2008. **129**(10): p. 1029-1035.
54. Bara, J.E., et al., *Gas separations in fluoroalkyl-functionalized room-temperature ionic liquids using supported liquid membranes*. Chemical Engineering Journal, 2009. **147**(1): p. 43-50.
55. Li, X.J., et al., *Fluorine-containing ionic liquids from N-alkylpyrrolidine and N-methylpiperidine and fluorinated acetylacetones: Low melting points and low viscosities*. European Journal of Inorganic Chemistry, 2008(21): p. 3353-3358.
56. Linder, T. and J. Sundermeyer, *Three novel anions based on pentafluorophenyl amine combined with two new synthetic strategies for the synthesis of highly lipophilic ionic liquids*. Chemical Communications, 2009(20): p. 2914-2916.
57. Skalicky, M., et al., *Synthesis of bis(polyfluoroalkylated)imidazolium salts as key intermediates for fluorous NHC ligands*. Journal of Fluorine Chemistry, 2009. **130**(10): p. 966-973.
58. Tindale, J.J., K.L. Mouland, and P.J. Ragogna, *Thiol appended, fluorinated phosphonium ionic liquids as covalent superhydrophobic coatings*. Journal of Molecular Liquids, 2010. **152**(1-3): p. 14-18.
59. Tsukada, Y., et al., *Preparation of novel hydrophobic fluorine-substituted-alkyl sulfate ionic liquids and application as an efficient reaction medium for lipase-catalyzed reaction*. Tetrahedron Letters, 2006. **47**(11): p. 1801-1804.
60. Xue, H. and J.M. Shreeve, *Ionic liquids with fluorine-containing cations*. European Journal of Inorganic Chemistry, 2005(13): p. 2573-2580.
61. Mezger, M., et al., *Molecular layering of fluorinated ionic liquids at a charged sapphire (0001) surface*. Science, 2008. **322**(5900): p. 424-428.
62. Celso, F., et al., *Study on the thermodynamic properties of highly fluorinated 1,2,4-oxadiazolopyridinium salts and their perspective applications as ionic liquid crystals*. Journal of Materials Chemistry, 2007. **17**: p. 1201-1208.
63. Tindale, J.J., et al., *Synthesis and characterization of fluorinated phosphonium ionic liquids*. Canadian Journal of Chemistry-Revue Canadienne De Chimie, 2007. **85**(10): p. 660-667.
64. Smith, G.D., et al., *A comparison of fluoroalkyl-derivatized imidazolium:TFPI and alkyl-derivatized imidazolium:TFPI ionic liquids: a molecular dynamics simulation study*. Physical Chemistry Chemical Physics, 2010. **12**(26): p. 7064-7076.
65. Tindale, J.J. and P.J. Ragogna, *Highly fluorinated phosphonium ionic liquids: novel media for the generation of superhydrophobic coatings*. Chemical Communications, 2009(14): p. 1831-1833.

- 
66. Ganapatibhotla, L.V.N.R., et al., *Ionic liquids with fluorinated block-oligomer tails: Influence of self-assembly on transport properties*. Journal of Materials Chemistry, 2011. **21**(48): p. 19275-19285.
  67. Shiflett, M.B. and A. Yokozeki, *Solubility and diffusivity of hydrofluorocarbons in room-temperature ionic liquids*. Aiche Journal, 2006. **52**(3): p. 1205-1219.
  68. Yoshida, Y. and G. Saito, *Ionic liquids based on diethylmethyl(2-methoxyethyl)ammonium cations and bis(perfluoroalkanesulfonyl)amide anions: influence of anion structure on liquid properties*. Physical Chemistry Chemical Physics, 2011. **13**(45): p. 20302-20310.
  69. Castiglione, F., et al., *Structural Organization and Transport Properties of Novel Pyrrolidinium-Based Ionic Liquids with Perfluoroalkyl Sulfonylimide Anions*. Journal of Physical Chemistry B, 2009. **113**(31): p. 10750-10759.
  70. Muldoon, M.J., et al., *Improving carbon dioxide solubility in ionic liquids*. Journal of Physical Chemistry B, 2007. **111**(30): p. 9001-9009.
  71. Dias, A.M.A., et al., *Vapor-liquid equilibrium of carbon dioxide-perfluoroalkane mixtures: Experimental data and SAFT modeling*. Industrial & Engineering Chemistry Research, 2006. **45**(7): p. 2341-2350.
  72. Merrigan, T.L., et al., *New fluorosurfactant ionic liquids function as surfactants in conventional room-temperature ionic liquids*. Chemical Communications, 2000(20): p. 2051-2052.
  73. Keipert, P.E., *Use of oxygent<sup>TM</sup>, a perfluorochemical-based oxygen carrier, as an alternative to intraoperative blood-transfusion*. Artificial Cells Blood Substitutes and Immobilization Biotechnology, 1995. **23**(3): p. 381-394.
  74. Deive, F.J., M.A. Rivas, and A. Rodriguez, *Thermophysical properties of two ionic liquids based on benzyl imidazolium cation*. Journal of Chemical Thermodynamics, 2011. **43**(3): p. 487-491.
  75. Grunert, A., *Artificial oxygen carriers - perfluorocarbons*. Infusionstherapie Und Transfusionsmedizin, 1994. **21**: p. 57-62.
  76. Kuznetsova, I.N., V.S. Yurchenko, and G.A. Kochetkova, *Physicochemical parameters of perfluorocarbon emulsions with different osmolarities*. Pharmaceutical Chemistry Journal, 2009. **43**(7): p. 408-414.
  77. Rizzo, S., et al., *Colored perfluorocarbon liquids as novel intraoperative tools*. Graefes Archive for Clinical and Experimental Ophthalmology, 2012. **250**(5): p. 653-659.
  78. Tariq, M., et al., *Densities and refractive indices of imidazolium- and phosphonium-based ionic liquids: Effect of temperature, alkyl chain length, and anion*. Journal of Chemical Thermodynamics, 2009. **41**(6): p. 790-798.
  79. Hamelin, J., T.K. Bose, and J. Thoen, *Dielectric-constant and the electric-conductivity near the consolute point of the critical binary-liquid mixture nitroethane-3-methylpentane*. Physical Review A, 1990. **42**(8): p. 4735-4742.
  80. Klug, O. and B.A. Lopatin, *New developments in conductimetric and oscillometric analysis*. Elsevier Science Publisher, 1988.

81. Santos, F.J.V., et al., *Electrical Conductivity and Viscosity of 1-Hexyl-3-methylimidazolium Bis(trifluorosulfonyl)imide, C(6)mim (CF<sub>3</sub>SO<sub>2</sub>)(<sub>2</sub>)N (CAS-RN# 382150-50-7)*. International Journal of Thermophysics, 2010. **31**(10): p. 1869-1879.
82. Widegren, J.A. and J.W. Magee, *Density, viscosity, speed of sound, and electrolytic conductivity for the ionic liquid 1-hexyl-3-methylimidazolium bis(trifluoromethylsulfonyl)imide and its mixtures with water*. Journal of Chemical and Engineering Data, 2007. **52**(6): p. 2331-2338.
83. Widegren, J.A., et al., *Electrolytic conductivity of four imidazolium-based room-temperature ionic liquids and the effect of a water impurity*. Journal of Chemical Thermodynamics, 2005. **37**(6): p. 569-575.
84. Riess, J.G. and M.P. Krafft, *Fluorinated materials for in vivo oxygen transport (blood substitutes), diagnosis and drug delivery*. Biomaterials, 1998. **19**(16): p. 1529-1539.
85. Zhou, L., et al., *Magnetic polarizability of hadrons from lattice QCD*. Nuclear Physics B- Proceedings Supplements, 2003. **119**: p. 272-274.
86. Moldover, M.R., *IUPAC Experimental Thermodynamics Vol. VI: Measurement Thermodynamic Properties of Single Phases*, Elsevier. p. 435-451.
87. Reichardt, C., *Solvents and Solvent Effects in Organic Chemistry*. 3 ed: Wiley.
88. Deetlefs, M., K.R. Seddon, and M. Shara, *Predicting physical properties of ionic liquids*. Physical Chemistry Chemical Physics, 2006. **8**(5): p. 642-649.
89. Iglesias-Otero, M.A., et al., *Density and refractive index in mixtures of ionic liquids and organic solvents: Correlations and predictions*. Journal of Chemical Thermodynamics, 2008. **40**(6): p. 949-956.
90. Dias, A.M.A., et al., *Densities and vapor pressures of highly fluorinated compounds*. Journal of Chemical and Engineering Data, 2005. **50**(4): p. 1328-1333.
91. Angell, C.A., N. Byrne, and J.P. Belieres, *Parallel developments in aprotic and protic ionic liquids: Physical chemistry and applications*. Accounts of Chemical Research, 2007. **40**(11): p. 1228-1236.
92. Postel, M., J.G. Riess, and J.G. Weers, *Fluorocarbon emulsions - the stability issue*. Artificial Cells Blood Substitutes and Immobilization Biotechnology, 1994. **22**(4): p. 991-1005.
93. Liu, H.J. and E. Maginn, *An MD Study of the Applicability of the Walden Rule and the Nernst-Einstein Model for Ionic Liquids*. Chemphyschem, 2012. **13**(7): p. 1701-1707.
94. Walden, P., *Organic solutions- and ionisation means. III. Chapter: Internal friction and its connection with conductivity*. Zeitschrift Fur Physikalische Chemie--Stoichiometrie Und Verwandtschaftslehre, 1906. **55**(2): p. 207-249.
95. Papaiconomou, N., et al., *The effect of position and length of alkyl substituents in pyridinium based ionic liquids on temperature dependent transport properties*. Electrochimica Acta, 2012. **70**: p. 124-130.



96. Harris, K.R., *Relations between the Fractional Stokes-Einstein and Nernst-Einstein Equations and Velocity Correlation Coefficients in Ionic Liquids and Molten Salts*. Journal of Physical Chemistry B, 2010. **114**(29): p. 9572-9577.
97. Miran, M.S., et al., *Physicochemical properties determined by Delta pK(a) for protic ionic liquids based on an organic super-strong base with various Bronsted acids*. Physical Chemistry Chemical Physics, 2012. **14**(15): p. 5178-5186.
98. Xu, W., E.I. Cooper, and C.A. Angell, *Ionic liquids: Ion mobilities, glass temperatures, and fragilities*. Journal of Physical Chemistry B, 2003. **107**(25): p. 6170-6178.
99. Ueno, K., H. Tokuda, and M. Watanabe, *Ionicity in ionic liquids: correlation with ionic structure and physicochemical properties*. Physical Chemistry Chemical Physics, 2010. **12**(8): p. 1649-1658.
100. Treybal, R.E., *Liquid extraction*. 2 ed1963, New York: McGraw-Hill.
101. Newsham, D.M.T., *Liquid-liquid equilibria*, in *Science and Practice of Liquid- Liquid Extraction*, J.D. Thornton, Editor 1992: Oxford. p. 1-39.
102. Smith, J.M., H.C. Van Ness, and M.M. Abbott, *Introduction to Chemical Engineering Thermodynamics*. 7 ed2005, New York: McGraw-Hill.
103. Hefter, G.T., *Liquid-Liquid Solubilities in The Experimental Determination of Solubilities*2003: John Wiley & Sons, Ltd.
104. Wilson, G.M., *Vapor-liquid equilibrium .11. new expression for excess free energy of mixing*. Journal of the American Chemical Society, 1964. **86**(2): p. 127-&.
105. Freire, M.G., et al., *Mutual solubilities of water and the C(n)mim Tf(2)N hydrophobic ionic liquids*. Journal of Physical Chemistry B, 2008. **112**(6): p. 1604-1610.
106. Pereiro, A.B. and A. Rodriguez, *Binary mixtures containing OMIM PF(6): density, speed of sound, refractive index and LLE with hexane, heptane and 2-propanol at several temperatures*. Physics and Chemistry of Liquids, 2008. **46**(2): p. 172-184.
107. Freire, M.G., et al., *Solubility of water in fluorocarbons: Experimental and COSMO-RS prediction results*. Journal of Chemical Thermodynamics, 2010. **42**(2): p. 213-219.
108. Adkins, C.J., *Equilibrium Thermodynamics*. 3 ed1968: Cambridge University Press.
109. Della Gatta, G., E. Badaea, and M. Saczuk, *Thermodynamics of solvation of some linear and branched aliphatic aldehydes in water and heptane*. Journal of Chemical Thermodynamics, 2010. **42**(10): p. 1204-1208.
110. Majer, V. and V. Svoboda, *Enthalpies of Vaporization of Organic Compounds: A Critical Review and Data Compilation*. Vol. 300. 1985, Oxford: Blackwell Scientific Publicati.
111. Zhogina, E.V., et al., *Standard enthalpies of the formation of cis-perfluorodecalins and trans-perfluorodecalins*. Zhurnal Fizicheskoi Khimii, 1987. **61**(11): p. 2890-2893.
112. Ermakov and Skripov, Russian Journal of Physical Chemistry, 1969. **43**: p. 726.

113. Varushchenko, R.M., et al., Russian Journal of Physical Chemistry, 1981. **55**(10): p. 1480 - 1483.
114. Ben-Naim, A., *On the evolution of the concept of solvation thermodynamics*. Journal of Solution Chemistry, 2001. **30**(5): p. 475-487.

# Appendix A

---



## A.1 [(EtPFHex)MeIm][PF<sub>6</sub>]

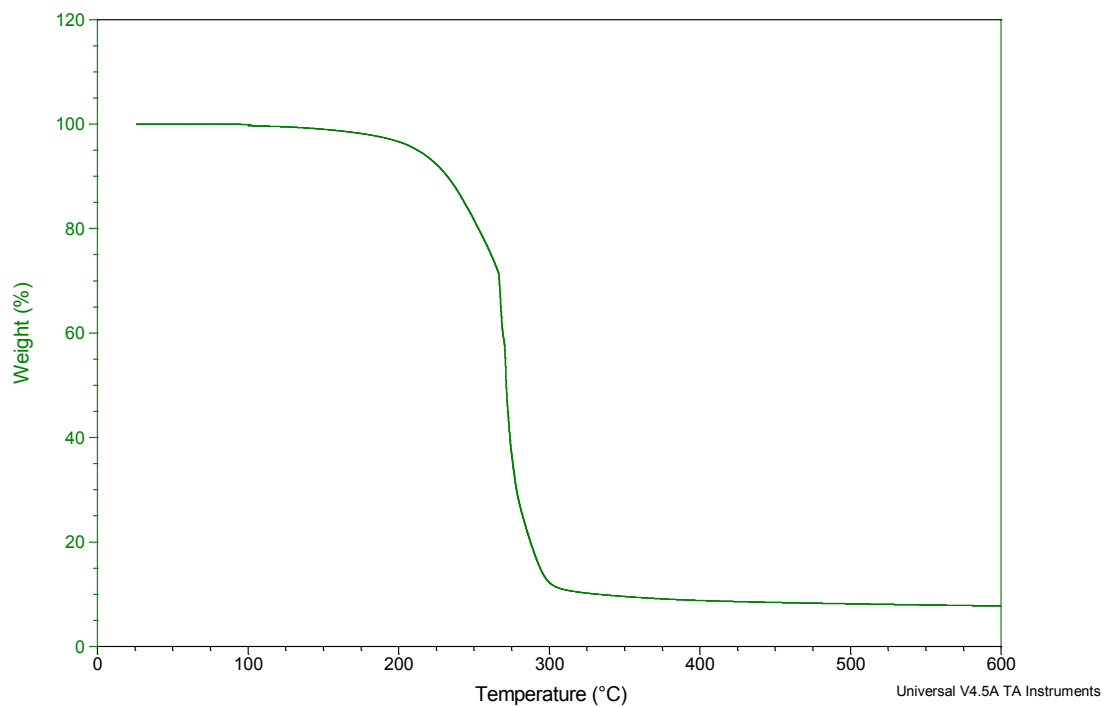


Figure A.1 – TGA curve for [(EtPFHex)MeIm][PF<sub>6</sub>].

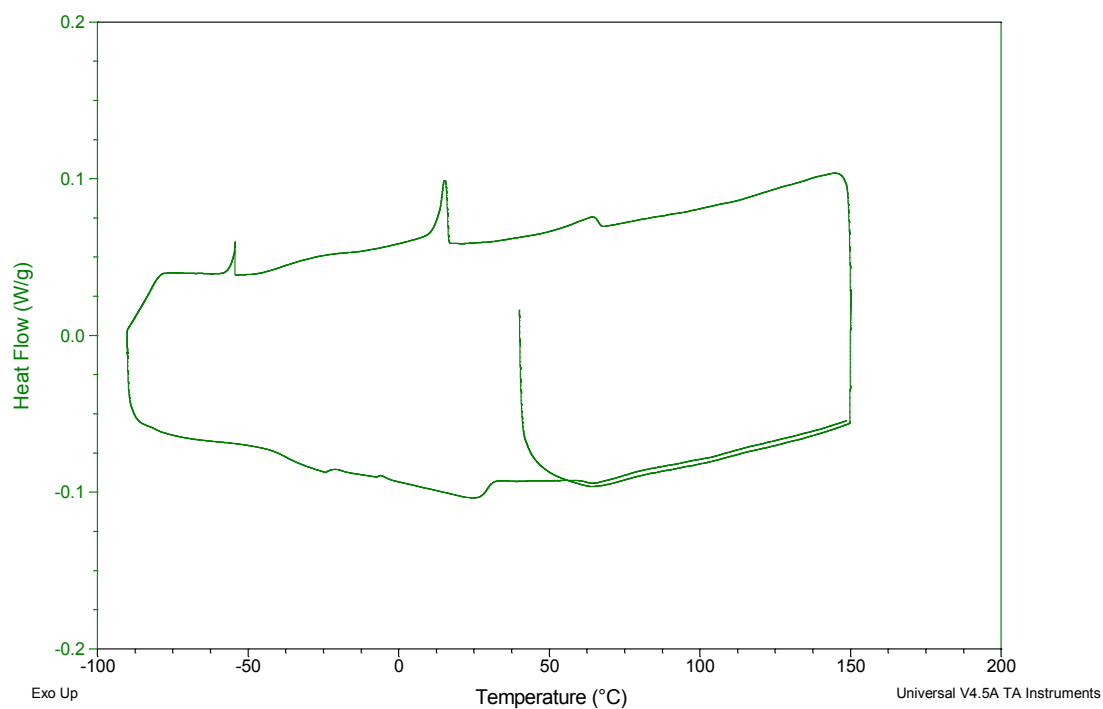


Figure A.2 – DSC curve for [(EtPFHex)MeIm][PF<sub>6</sub>].

## A.2 [(EtPFHex)BuIm][PF<sub>6</sub>]

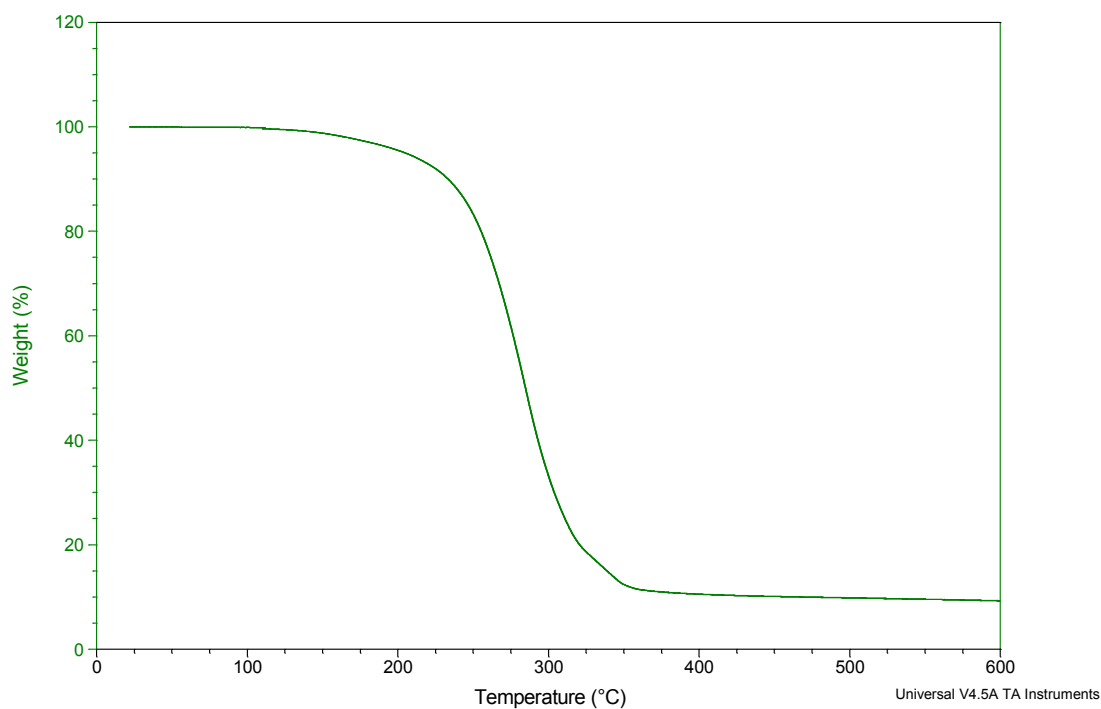


Figure A.3 – TGA curve for [(EtPFHex)BuIm][PF<sub>6</sub>].

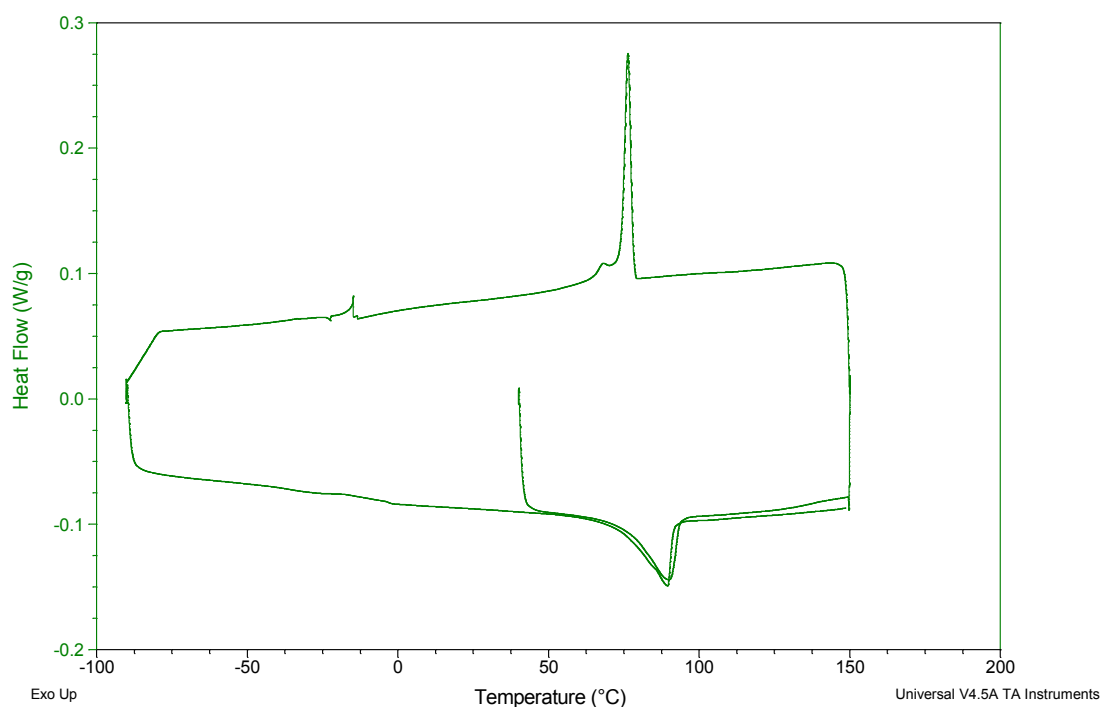


Figure A.4 – DSC curve for [(EtPFHex)BuIm][PF<sub>6</sub>].

### A.3 [NBu<sub>4</sub>][(PFOc)SO<sub>3</sub>]

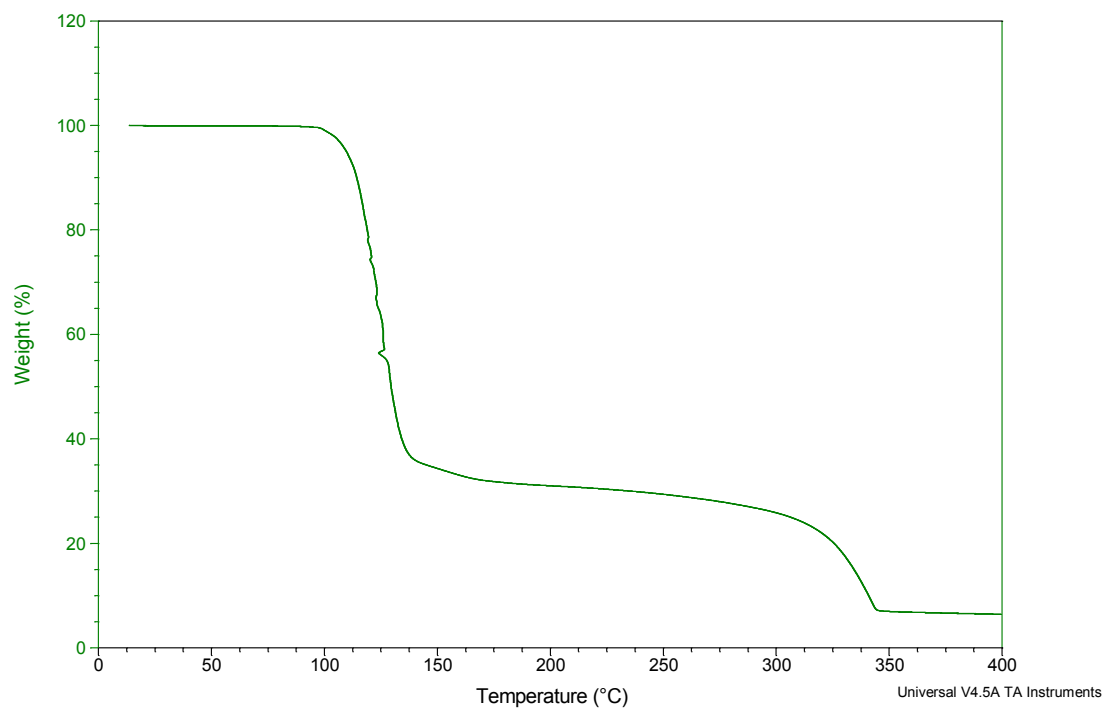


Figure A.5 – TGA curve for [NBu<sub>4</sub>][(PFOc)SO<sub>3</sub>].

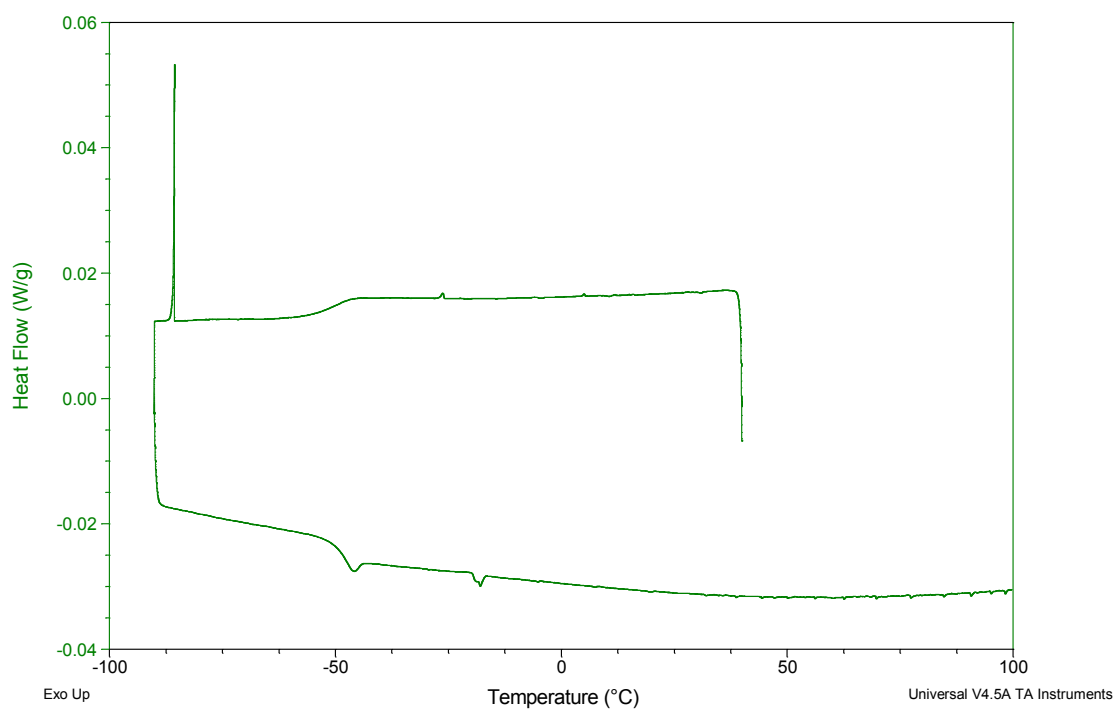


Figure A.6 – DSC curve for [NBu<sub>4</sub>][(PFOc)SO<sub>3</sub>].

## A.4 [NBu<sub>4</sub>][(PFBu)SO<sub>3</sub>]

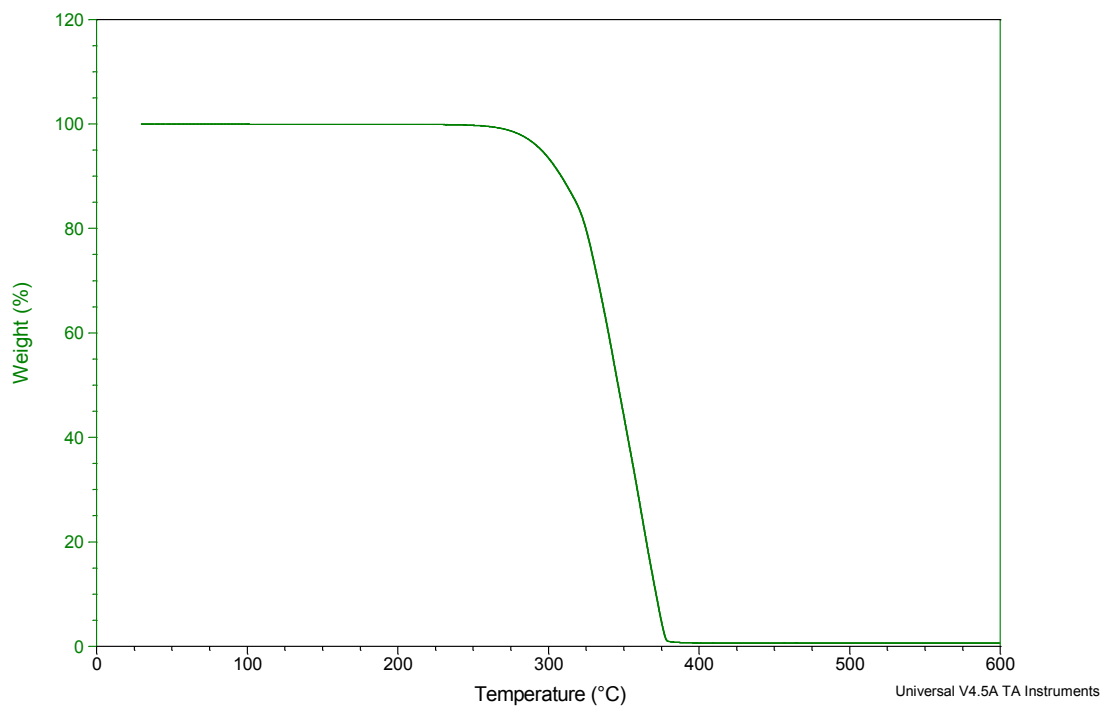


Figure A.7 – TGA curve for [NBu<sub>4</sub>][(PFBu)SO<sub>3</sub>].

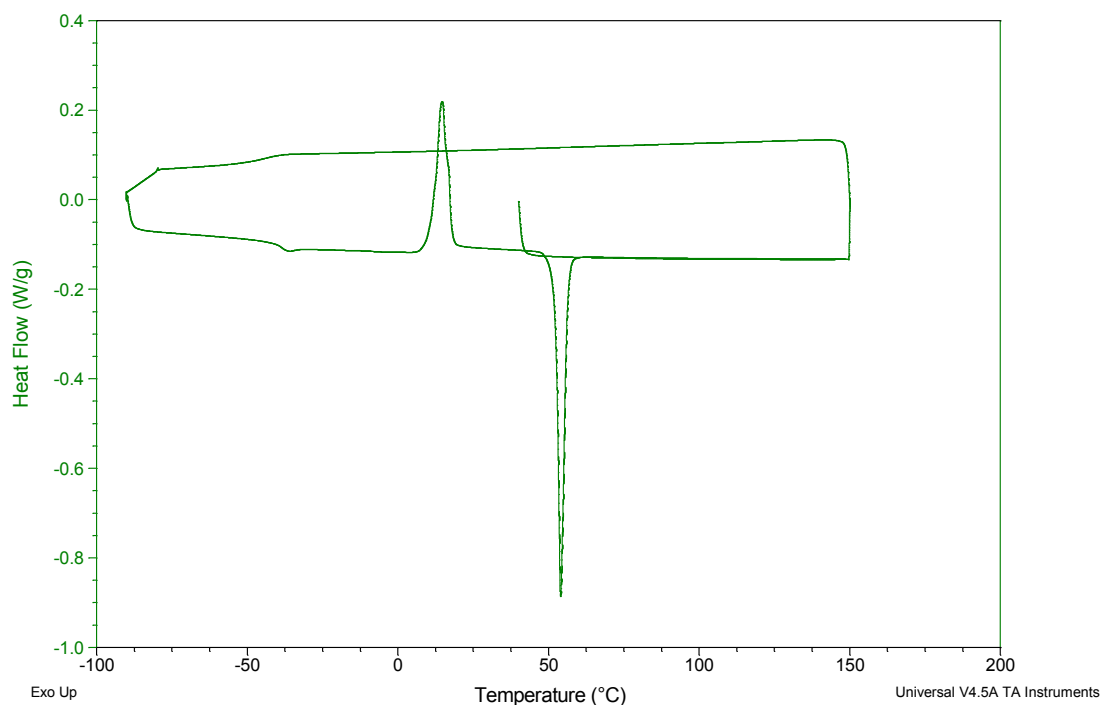


Figure A.8 – DSC curve for [NBu<sub>4</sub>][(PFBu)SO<sub>3</sub>].



## A.5 [HexMeIm][(PFBu)SO<sub>3</sub>]

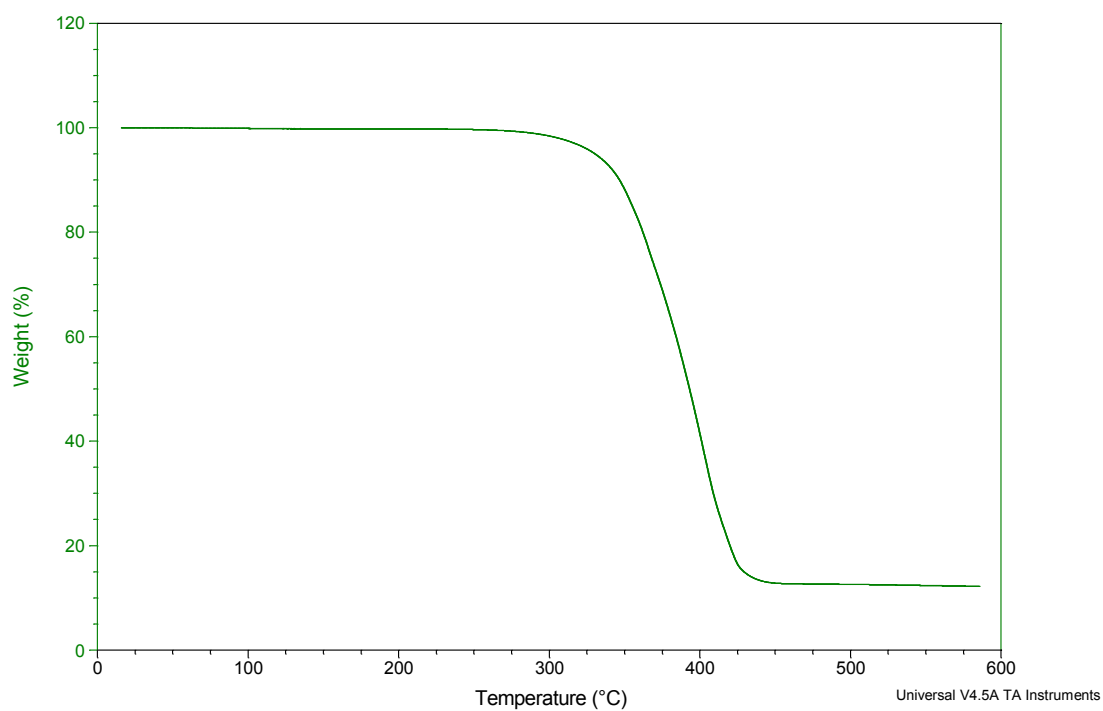


Figure A.9 – TGA curve for [HexMeIm][(PFBu)SO<sub>3</sub>].

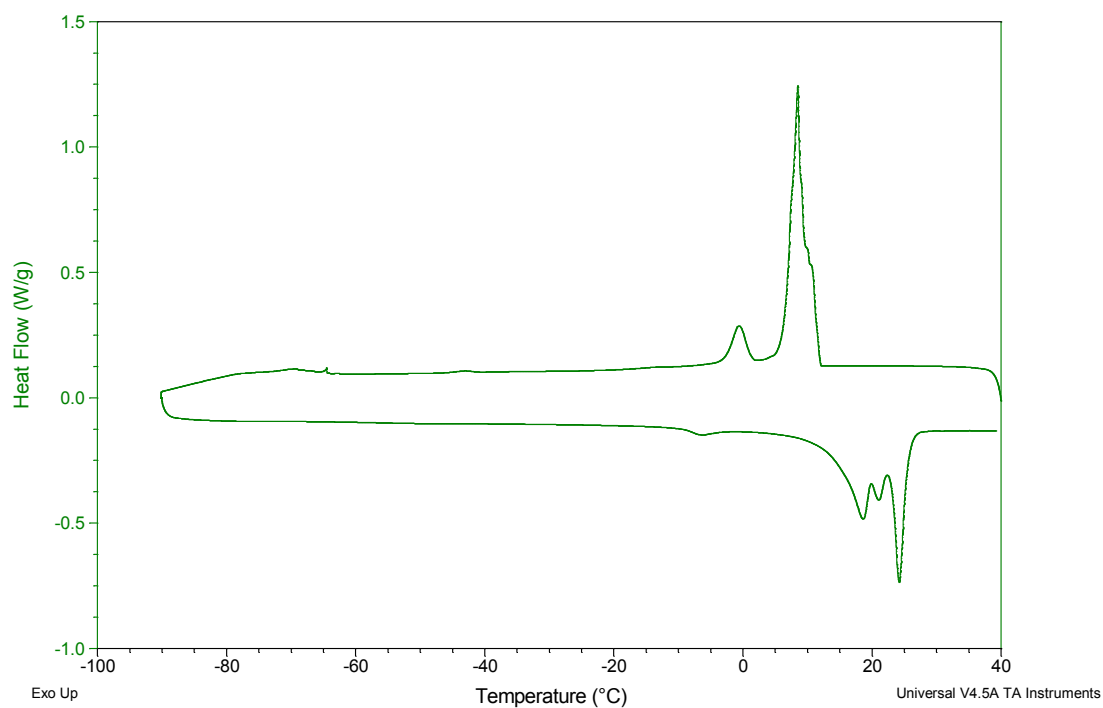


Figure A.10 – DSC curve for [HexMeIm][(PFBu)SO<sub>3</sub>].

## A.6 [OcMeIm][(PFBu)SO<sub>3</sub>]

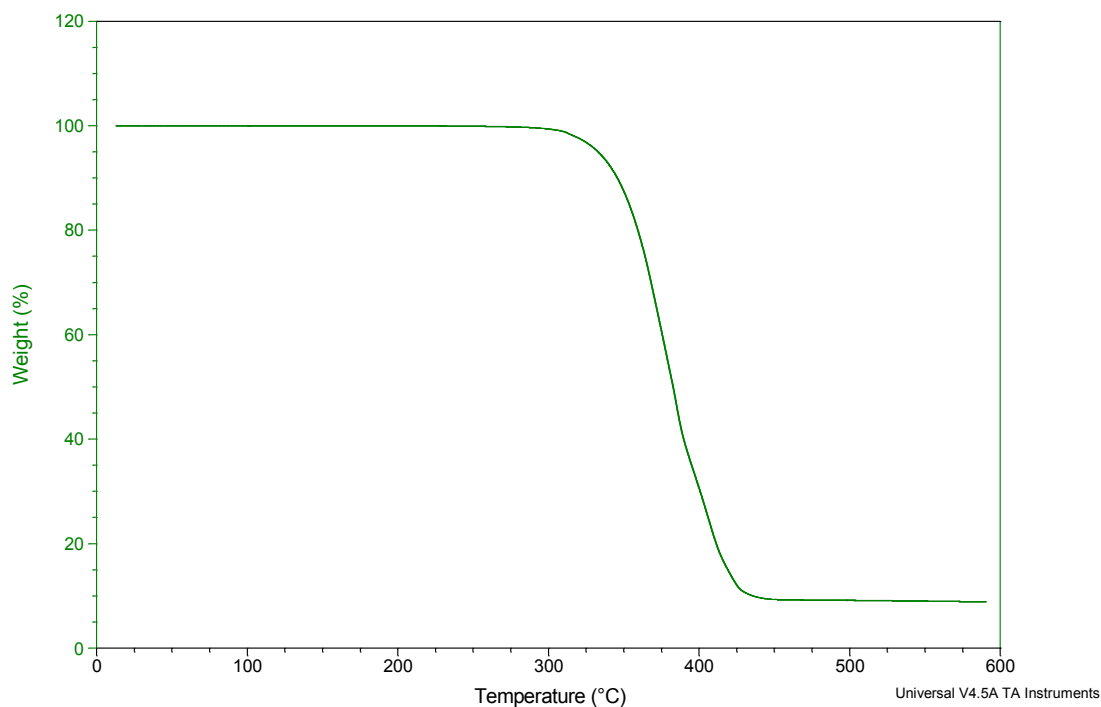


Figure A.11 – TGA curve for [OcMeIm][(PFBu)SO<sub>3</sub>].

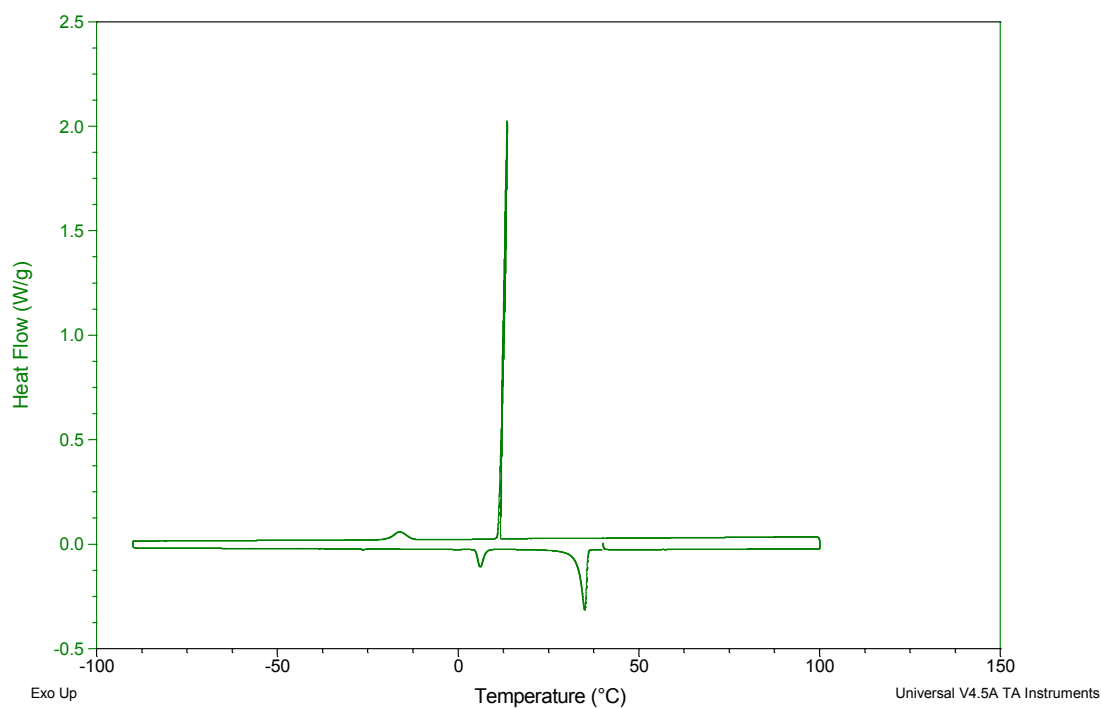


Figure A.12 – DSC curve for [OcMeIm][(PFBu)SO<sub>3</sub>].

## A.7 [EtMepy][(PFBu)SO<sub>3</sub>]

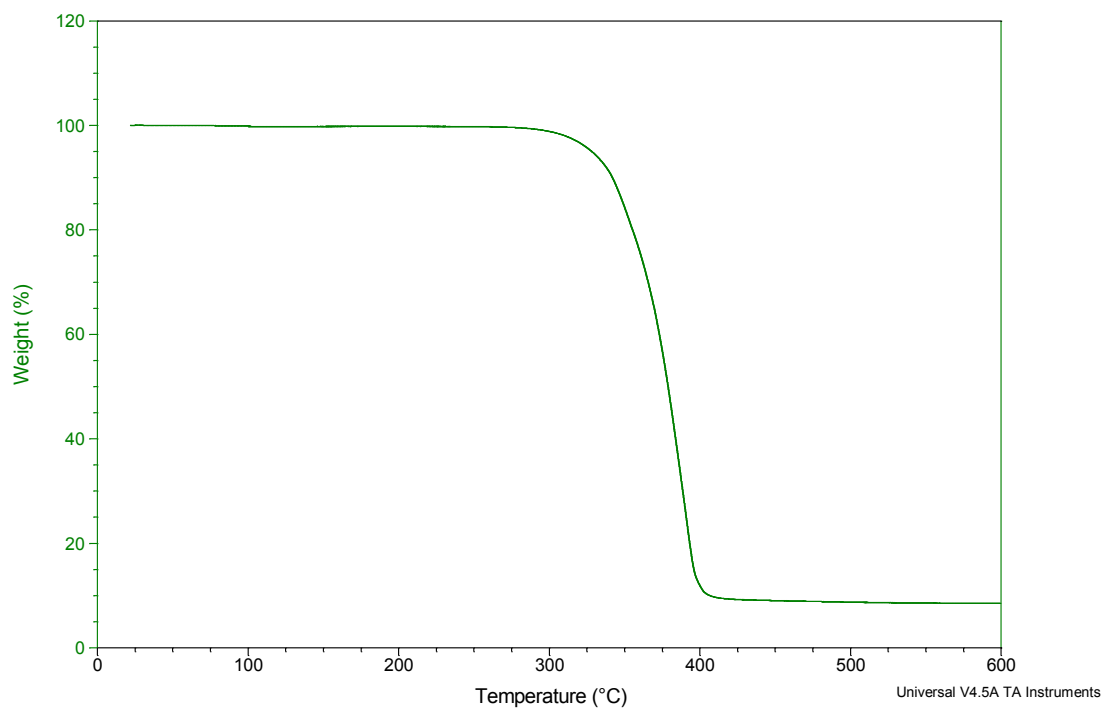


Figure A.13 – TGA curve for [EtMepy][(PFBu)SO<sub>3</sub>].

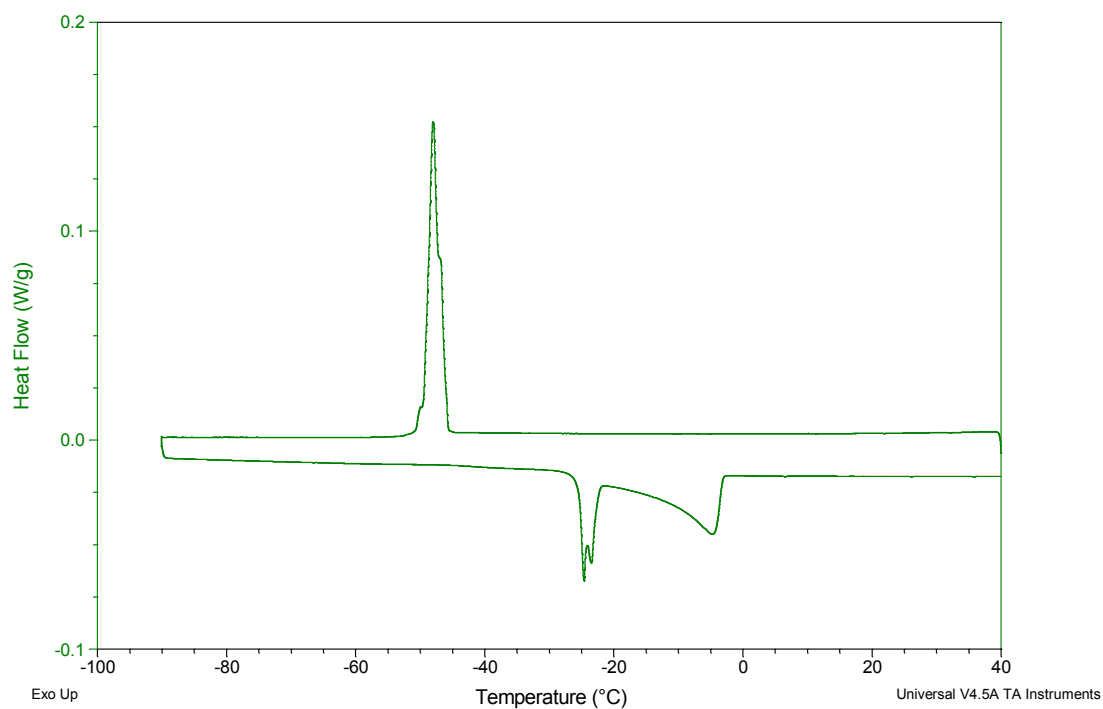


Figure A.14 – DSC curve for [EtMepy][(PFBu)SO<sub>3</sub>].

## A.8 [BuMepyr][PFBuSO<sub>3</sub>]

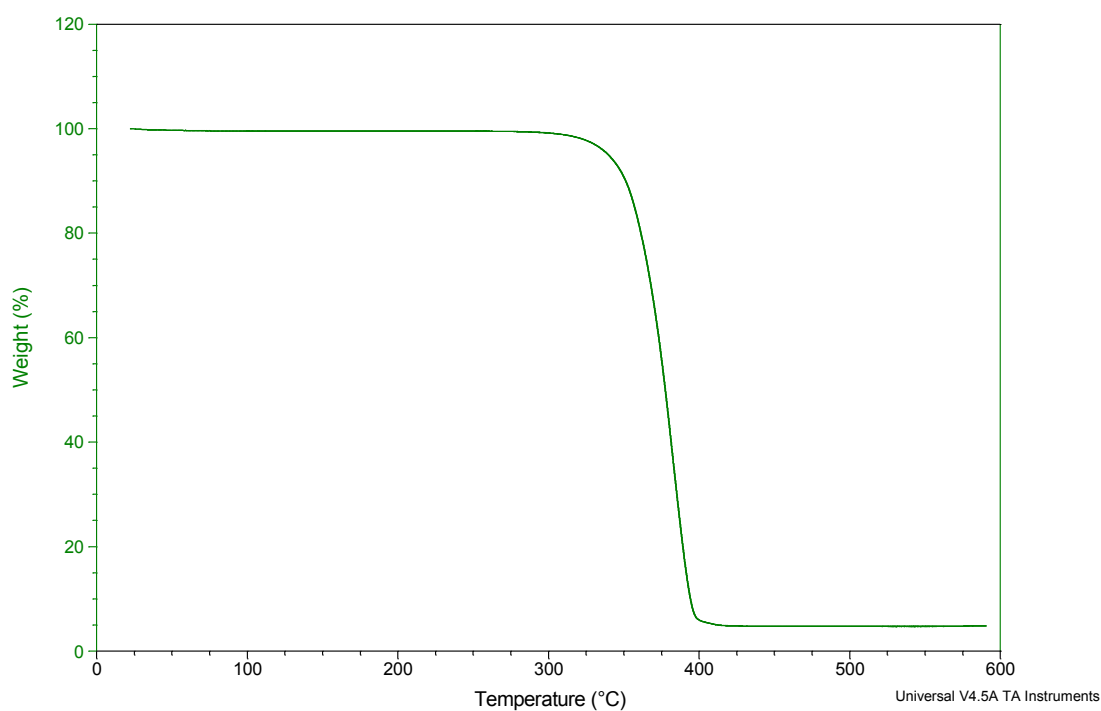


Figure A.15 – TGA curve for [BuMepyr][PFBuSO<sub>3</sub>].

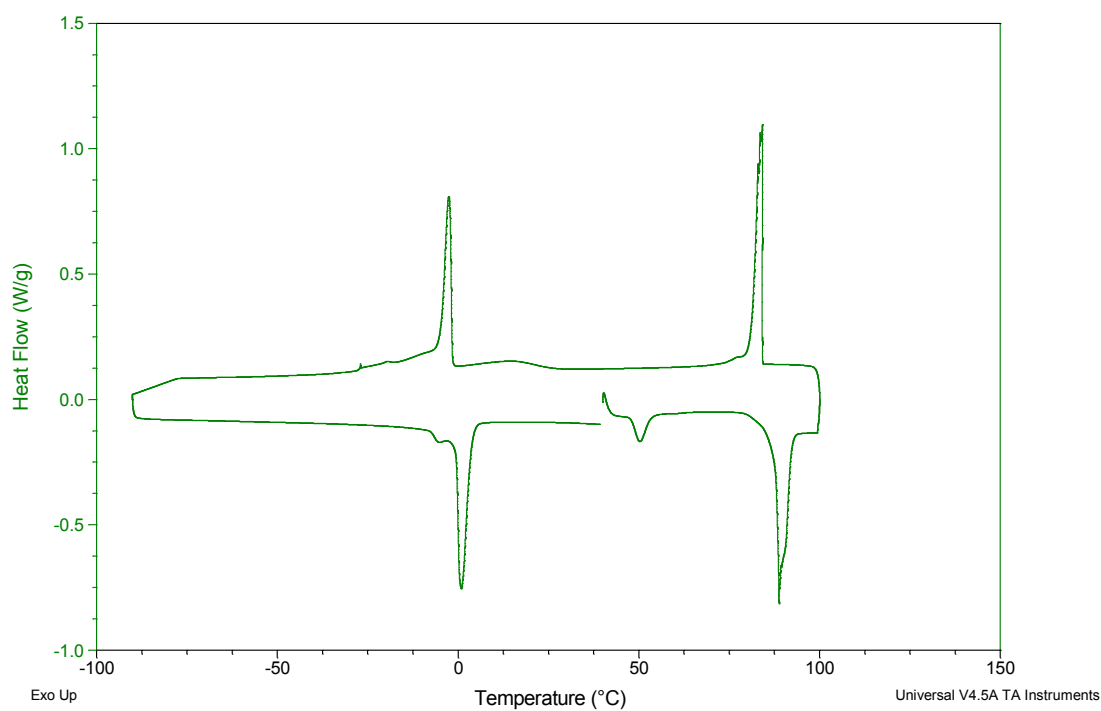


Figure A.16 – DSC curve for [BuMepyr][PFBuSO<sub>3</sub>].

## **Appendix B**

---



## B.1 Calibration curve for Perfluorodecalin and [NBu<sub>4</sub>][(PFOc)SO<sub>3</sub>]

In order to determine the amount of perfluorodecalin in [NBu<sub>4</sub>][(PFOc)SO<sub>3</sub>] phase, a calibration curve was used. For this purpose, solutions of different known concentrations of perfluorodecalin were prepared in FIL. **Table B.1** presents the concentration of the prepared solutions and the refractive index obtained. **Figure B.1** presents the linear function obtained and respective slope and correlation coefficient.

**Table B.1** – Refractive index as function of [NBu<sub>4</sub>][(PFOc)SO<sub>3</sub>] molar fraction for binary mixture [NBu<sub>4</sub>][(PFOc)SO<sub>3</sub>] + perfluorodecalin.

$x_{\text{FIL}}$	$n_{\text{D}}$
1.0000	1.382800
0.9649	1.381426
0.9353	1.380291
0.9073	1.379659
0.8773	1.377788
0.8472	1.376384
0.8172	1.374936
0.6990	1.369410

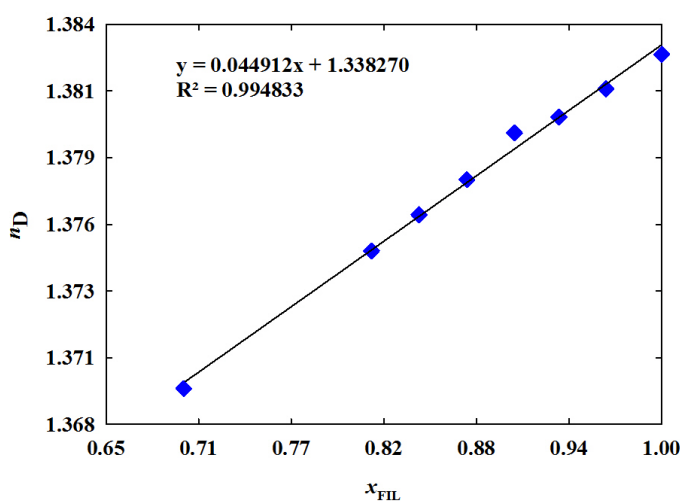


**Figure B.1** – Calibration curve for perfluorodecalin and [NBu<sub>4</sub>][(PFOc)SO<sub>3</sub>].

## B.2 Calibration curve for Perfluorooctane and $[\text{NBu}_4][(\text{PFOc})\text{SO}_3]$

In order to determine the amount of perfluorooctane in  $[\text{NBu}_4][(\text{PFOc})\text{SO}_3]$  phase, a calibration curve was used. For this purpose, solutions of different known concentrations of perfluorooctane were prepared in FIL. **Table B.2** presents the concentration of the prepared solutions and the refractive index obtained. **Figure B.2** presents the linear function obtained and respective slope and correlation coefficient.

**Table B.2** – Refractive index as function of  $[\text{NBu}_4][(\text{PFOc})\text{SO}_3]$  molar fraction for binary mixture  $[\text{NBu}_4][(\text{PFOc})\text{SO}_3]$  + perfluorooctane.

$x_{\text{FIL}}$	$n_{\text{D}}$
1.0000	1.382800
0.9640	1.381487
0.9310	1.379574
0.9003	1.377764
0.7823	1.372527
0.8567	1.375694
0.7158	1.367727

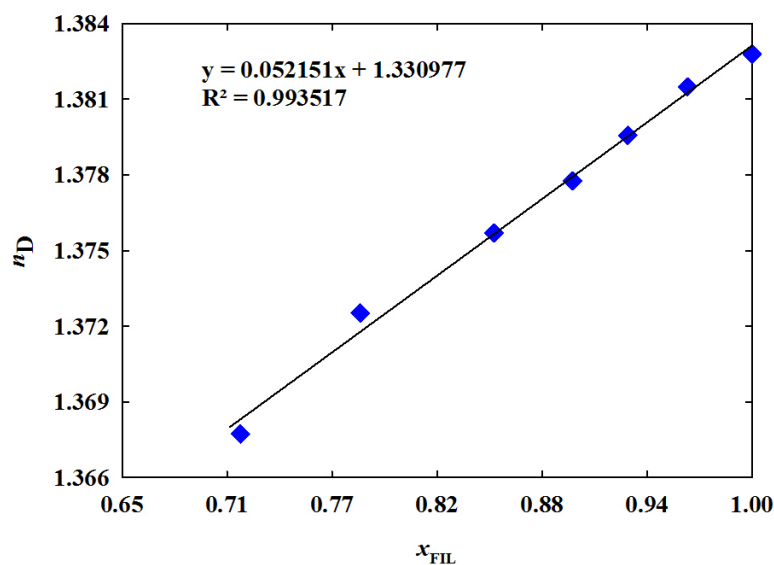


**Figure B.2** - Calibration curve for perfluorooctane and  $[\text{NBu}_4][(\text{PFOc})\text{SO}_3]$ .



### B.3 Calibration curve for Perfluorodecalin and [NBu<sub>4</sub>][(PFBu)SO<sub>3</sub>]

In order to determine the amount of perfluorodecalin in [NBu<sub>4</sub>][(PFBu)SO<sub>3</sub>] phase, a calibration curve was used. For this purpose, solutions of different known concentrations of perfluorodecalin were prepared in FIL. **Table B.3** presents the concentration of the prepared solutions and the refractive index obtained. **Figure B.3** presents the linear function obtained and respective slope and correlation coefficient.

**Table B.3** – Refractive index as function of [NBu<sub>4</sub>][(PFBu)SO<sub>3</sub>] molar fraction for binary mixture [NBu<sub>4</sub>][(PFBu)SO<sub>3</sub>] + perfluorodecalin.

$x_{\text{FIL}}$	$n_{\text{D}}$
1.0000	1.403054
0.9877	1.402483
0.9764	1.401813
0.9377	1.399959
0.9132	1.399181
0.8950	1.398460

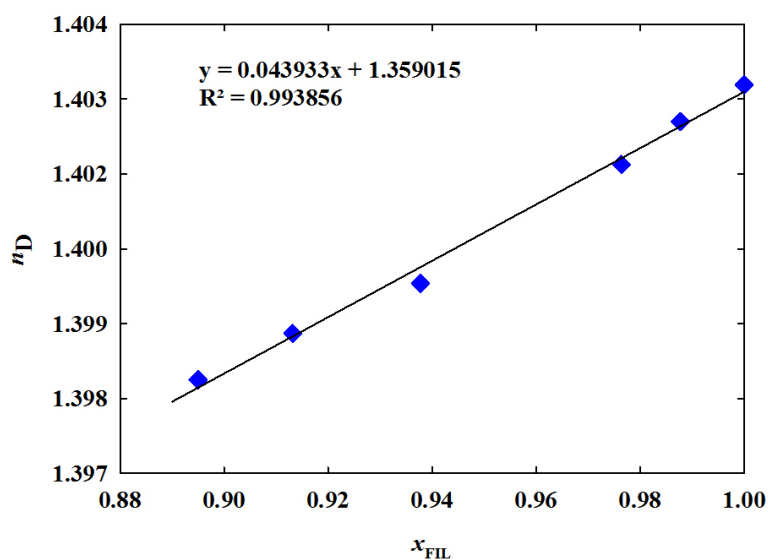


**Figure B.3** - Calibration curve for perfluorodecalin and [NBu<sub>4</sub>][(PFBu)SO<sub>3</sub>].

## B.4 Calibration curve for Perfluorooctane and $[\text{NBu}_4][(\text{PFBu})\text{SO}_3]$

In order to determine the amount of perfluorooctane in  $[\text{NBu}_4][(\text{PFBu})\text{SO}_3]$  phase, a calibration curve was used. For this purpose, solutions of different known concentrations of perfluorooctane were prepared in FIL. **Table B.4** presents the concentration of the prepared solutions and the refractive index obtained. **Figure B.4** presents the linear function obtained and respective slope and correlation coefficient.

**Table B.4** – Refractive index as function of  $[\text{NBu}_4][(\text{PFBu})\text{SO}_3]$  molar fraction for binary mixture  $[\text{NBu}_4][(\text{PFBu})\text{SO}_3]$  + perfluorooctane.

$x_{\text{FIL}}$	$n_{\text{D}}$
1.0000	1.403054
0.9787	1.402079
0.9647	1.401473
0.9542	1.401165
0.9431	1.400788
0.9309	1.400459
0.8998	1.399042

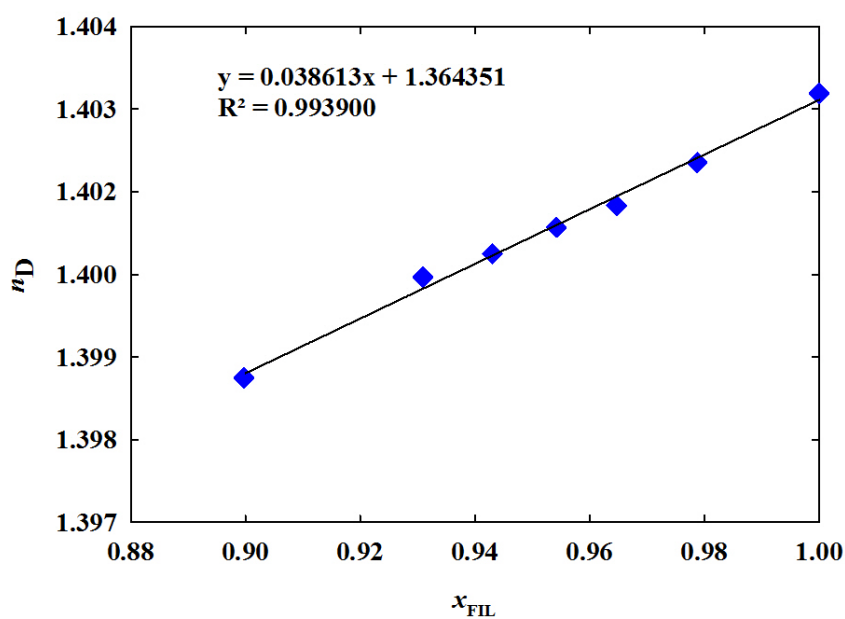


**Figure B.4** - Calibration curve for perfluorooctane and  $[\text{NBu}_4][(\text{PFBu})\text{SO}_3]$ .

## B.5 Calibration curve for Perfluorodecalin and [HexMeIm][(PFBu)SO<sub>3</sub>]

In order to determine the amount of perfluorodecalin in [HexMeIm][(PFBu)SO<sub>3</sub>] phase, a calibration curve was used. For this purpose, solutions of different known concentrations of perfluorodecalin were prepared in FIL. **Table B.5** presents the concentration of the prepared solutions and the refractive index obtained. **Figure B.5** presents the linear function obtained and respective slope and correlation coefficient.

**Table B.5** – Refractive index as function of [HexMeIm][(PFBu)SO<sub>3</sub>] molar fraction for binary mixture [HexMeIm][(PFBu)SO<sub>3</sub>] + perfluorodecalin.

$x_{\text{FIL}}$	$n_{\text{D}}$
1.0000	1.395954
0.9914	1.395487
0.9794	1.394729
0.9701	1.393931
0.9613	1.393391
0.9527	1.392775

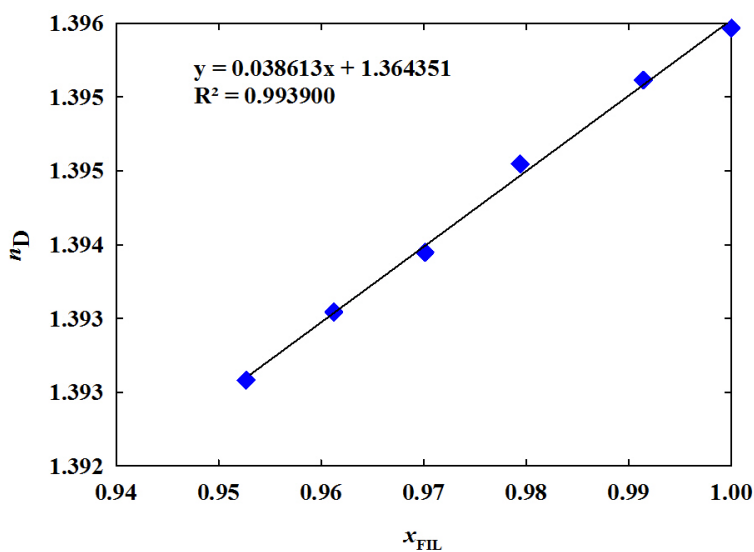


**Figure B.5** - Calibration curve for perfluorodecalin and [HexMeIm][(PFBu)SO<sub>3</sub>].

## B.6 Calibration curve for Perfluorooctane and [HexMeIm][(PFBu)SO<sub>3</sub>]

In order to determine the amount of perfluorooctane in [HexMeIm][(PFBu)SO<sub>3</sub>] phase, a calibration curve was used. For this purpose, solutions of different known concentrations of perfluorooctane were prepared in FIL. **Table B.6** presents the concentration of the prepared solutions and the refractive index obtained. **Figure B.6** presents the linear function obtained and respective slope and correlation coefficient.

**Table B.6** – Refractive index as function of [HexMeIm][(PFBu)SO<sub>3</sub>] molar fraction for binary mixture [HexMeIm][(PFBu)SO<sub>3</sub>] + perfluorooctane.

$x_{FIL}$	$n_D$
1.0000	1.395954
0.9864	1.395451
0.9690	1.394607
0.9573	1.394065
0.9462	1.393626
0.9349	1.393259

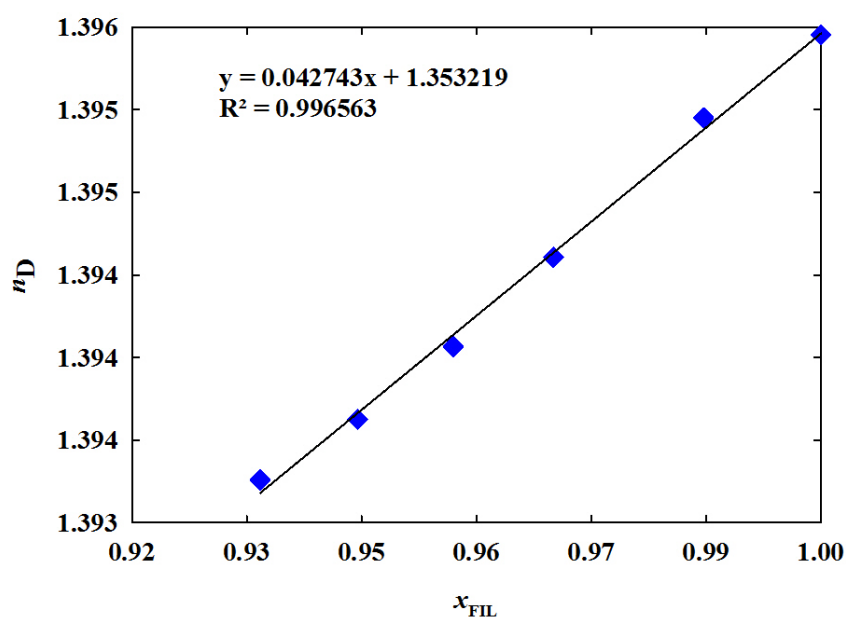


**Figure B.6** - Calibration curve for perfluorooctane and [HexMeIm][(PFBu)SO<sub>3</sub>].

## B.7 Calibration curve for Perfluorodecalin and [OcMeIm][(PFBu)SO<sub>3</sub>]

In order to determine the amount of perfluorodecalin in [OcMeIm][(PFBu)SO<sub>3</sub>] phase, a calibration curve was used. For this purpose, solutions of different known concentrations of perfluorodecalin were prepared in FIL. **Table B.7** presents the concentration of the prepared solutions and the refractive index obtained. **Figure B.7** presents the linear function obtained and respective slope and correlation coefficient.

**Table B.7** – Refractive index as function of [OcMeIm][(PFBu)SO<sub>3</sub>] molar fraction for binary mixture [OcMeIm][(PFBu)SO<sub>3</sub>] + perfluorodecalin.

$x_{\text{FIL}}$	$n_{\text{D}}$
1.000	1.400076
0.9829	1.399332
0.9728	1.398825
0.9659	1.398034
0.9526	1.397405
0.9302	1.396136
0.9154	1.395646
0.9040	1.395031

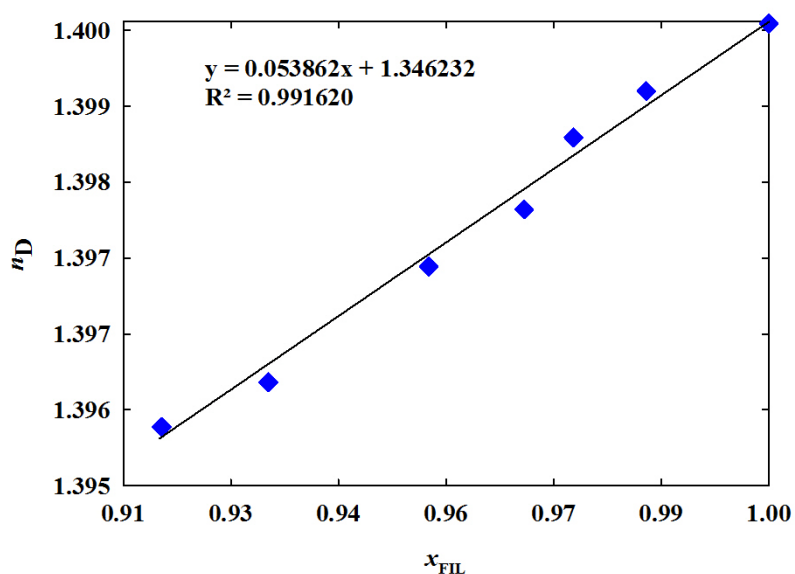


**Figure B.7** - Calibration curve for perfluorodecalin and [OcMeIm][(PFBu)SO<sub>3</sub>].

## B.8 Calibration curve for Perfluorooctane and [OcMeIm][(PFBu)SO<sub>3</sub>]

In order to determine the amount of perfluorooctane in [OcMeIm][(PFBu)SO<sub>3</sub>] phase, a calibration curve was used. For this purpose, solutions of different known concentrations of perfluorooctane were prepared in FIL. **Table B.8** presents the concentration of the prepared solutions and the refractive index obtained. **Figure B.8** presents the linear function obtained and respective slope and correlation coefficient.

**Table B.8** - Refractive index as function of [OcMeIm][(PFBu)SO<sub>3</sub>] molar fraction for binary mixture [OcMeIm][(PFBu)SO<sub>3</sub>] + perfluorooctane.

$x_{\text{FIL}}$	$n_{\text{D}}$
1.0000	1.400076
0.9757	1.399563
0.9120	1.398680
0.8786	1.398348
0.8307	1.397504
0.8112	1.397298

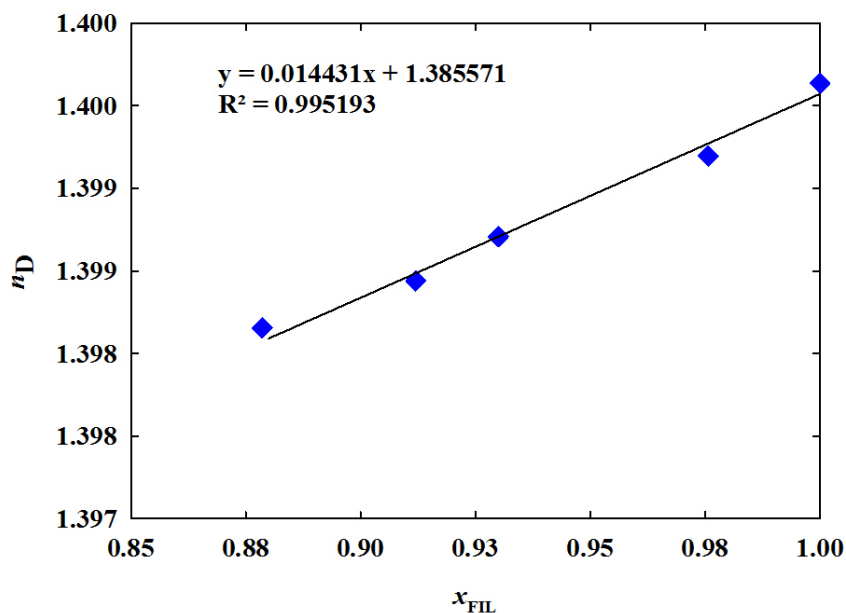


**Figure B.8** - Calibration curve for perfluorooctane and [OcMeIm][(PFBu)SO<sub>3</sub>].

## B.9 Calibration curve for Perfluorodecalin and [EtMepy][(PFBu)SO<sub>3</sub>]

In order to determine the amount of perfluorooctane in [EtMepy][(PFBu)SO<sub>3</sub>] phase, a calibration curve was used. For this purpose, solutions of different known concentrations of perfluorodecalin were prepared in FIL. **Table B.9** presents the concentration of the prepared solutions and the refractive index obtained. **Figure B.9** presents the linear function obtained and respective slope and correlation coefficient.

**Table B.9** – Refractive index as function of [EtMepy][(PFBu)SO<sub>3</sub>] molar fraction for binary mixture [EtMepy][(PFBu)SO<sub>3</sub>] + perfluorodecalin.

$x_{\text{FIL}}$	$n_{\text{D}}$
1.0000	1.406419
0.9951	1.405526
0.9857	1.407133
0.9844	1.405111
0.9773	1.405023
0.9752	1.405491
0.9732	1.406212
0.9693	1.405722

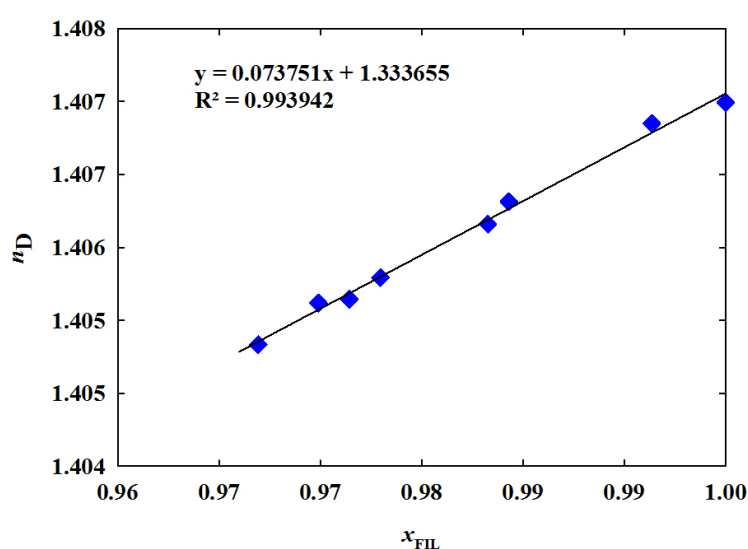


**Figure B.9** - Calibration curve for perfluorodecalin and [EtMepy][(PFBu)SO<sub>3</sub>].

